Final Report on UGC- MRP

F.No.- 43-519/2014(SR), dated 29.12.2015.

Entitled

Study of Structural and Physical Properties of $R_2T_{17-x}M_x$ (R = rare earth element; T = Fe, Co; M = Al, Ga, Si, Cr, Mn) System

By

Dr. Sanjoy Mukherjee
Associate Professor
Department of Physics
The University of Burdwan
Purba Bardhaman, West Bengal
PIN -713104

December, 2018

Annexure - III

UNIVERSITY GRANTS COMMISSION
BAHADUR SHAH ZAFAR MARG
NEW DELHI – 110 002

STATEMENT OF EXPENDITURE IN RESPECT OF MAJOR RESEARCH PROJECT

1. Name of Principal Investigator — Dr. Sanjoy Mukherjee
2. Deptt. of Principal Investigator — Department of Physics
   University/College — The University of Burdwan
3. UGC approval Letter No. and Date — F.No.- 43-519/2014(SR), dated 29.12.2015.
4. Title of the Research Project — **Study of Structural and Physical Properties of $R_2T_{17-x}M_x$ (R = rare earth element; T = Fe, Co; M = Al, Ga, Si, Cr, Mn) System**
5. Effective date of starting the project — 01.07.2015
6. a. Period of Expenditure: From — 01.07.2015 to 30.06.2018
   b. Details of Expenditure

S.No.	Item	Amount Approved (Rs.)	Grant released (1st installment) (Rs.)	Expenditure Incurred (Rs.)	Balance (Rs.)
i.	Books & Journals	0.00	0.00	0.00	0.00
ii.	Equipment	6,00,000.00	6,00,000.00	5,39,491.00	60,509.00
iii.	Contingency	1,00,000.00	90,000.00	44,338.00	45,662.00
iv.	Field Work/Travel (Give details in the proforma at Annexure- IV).	30,000.00	27,000.00	*30,000.00	-3,000.00
v.	Hiring Services	0.00	0.00	0.00	0.00
vi.	Chemicals & Glassware	1,00,000.00	90,000.00	49,276.00	40724.00
vii.	Overhead	80,000.00	80,000.00	80,000.00	0.00
viii.	Any other items (Please specify)	0.00	0.00	0.00	0.00

*Including committed expenditure of Rs. 3,000.00

Continued

c . Staff

Date of Appointment 31.05.16.

S.No	Items	Amount Approved (Rs.)	Grant released (1st installment) (Rs.)	Expenditure incurred (Rs.)	Balance
1.	Honorarium to P.I Retired Teachers) @ Rs. 18,000/-	Not Applicable			
2.	**Project fellow:** **NET/GATE qualified** Rs. 16,000/- p.m. for initial 2 years and Rs. 18,000/- p.m. for the third year.	3,50,452.00 HRA – 40,052.00	3,15,407.00 HRA – 36,047.00	*3,50,452.00 *HRA – 35,045.00 Total = 3,85,497.00	-35,045.00 HRA – 1,002.00

***Including committed expenditure of Rs. 35,045.00 (Fellowship) and Rs. 3,504.00 (HRA)**

1. It is certified that the appointment(s) have been made in accordance with the terms and conditions laid down by the Commission.

2. If as a result of check or audit objection some irregularly is noticed at later date, action will be taken to refund, adjust or regularize the objected amounts.

3. Payment @ revised rates shall be made with arrears on the availability of additional funds.

4. It is certified that out of the grant of Rs. **12,38,454.00** (10,95,000.00 + 1,43,454.00) (**Rupees Twelve Lakh, Thirty Eight Thousand, Four Hundred, Fifty Four only**) received from the University Grants Commission under the scheme of support for Major Research Project entitled **"Study of Structural and Physical Properties of $R_2T_{17-x}M_x$ (R = rare earth element; T = Fe, Co; M = Al, Ga, Si, Cr, Mn) System"** vide UGC letter No. **F. No. -43-519/2014 (SR) dated 29th December, 2015 and dated 26th October, 2017**, an amount of **Rs. 11,28,602.00** (including committed expenditure of Rs. 41,549.00) has been **utilized** for the purpose for which it was sanctioned and in accordance with the terms and conditions laid down by the University Grants Commission, **leaving an unspent balance of Rs. 1,09,852.00.**

Note: It may be noted that in accordance with the sanction letter dated 29th December, 2015, the amount approved for the project fellow was Rs. 6,00,000.00, and the grant released as first installment had been Rs. 3,00,000.00. Such sanction letter

Continued

provides a fellow qualified in GATE/NET/GPAT a fellowship of Rs. 16,000.00 pm for the first two years and Rs. 18,000.00 pm for the third (final) year. Accordingly, the student Shovan Dan (qualified in GATE) had been appointed with a stipend of Rs. 16,000.00 pm, and he joined this project on 31.05.2016. However, unfortunately, in the grant being released as second installment vide letter dated 26th October, 2017, the allocation was found to be revised as Rs. 14,000.00 pm for the first two years and Rs. 16,000.00 pm for the third (final) year.

Our expenditure (shown above) towards fellowship has been calculated considering Rs. 14,000.00 pm for the period 31.05.2016 to 30.05.2018, and Rs. 16,000.00 pm for the period 31.05.2018 to 30.06.2018. An added amount of 10% HRA has also been provided. The calculated expenditure amounts to Rs. 3,90,504.00.

The total expenditure including HRA (10%) towards fellowship should be Rs. 4,42,839.00 if one calculates considering Rs. 16,000.00 pm for the period 31.05.2016 to 30.05.2018, and Rs. 18,000.00 pm for the period 31.05.2018 to 30.06.2018.

Thus, the deficit amount for the project fellow appears as Rs. 52,335.00. **I would like to request you to be kind enough to permit us for realizing the deficit amount from the available balance amount of the project.**

Sanjoy Mukherjee

PRINCIPLE INVESTIGATOR

ASSOCIATE PROFESSOR
DEPT. OF PHYSICS
UNIVERSITY OF BURDWAN

19-11-18

FINANCE OFFICER

FINANCE OFFICER
THE UNIVERSITY OF BURDWAN
BURDWAN, WEST BENGAL

3/12/18

REGISTRAR

REGISTRAR (Officiating)
THE UNIVERSITY OF BURDWAN
BURDWAN-713104

1-11-18

STATUTORY AUDITOR

JADAB KUMAR RAY
M. No. 53411
BURDWAN
Chartered Accountants

Annexure – IV

UNIVERSITY GRANTS COMMISSION
BAHADUR SHAH ZAFAR MARG
NEW DELHI – 110 002

STATEMENT OF EXPENDITURE INCURRED ON FIELD WORK DURING THE PERIOD 01.07.2015 - 30.06.2018

Name of the Principal Investigator: Dr. Sanjoy Mukherjee.

Name of the Place Visited	Duration of the Visit		Mode of Journey	Expenditure Incurred (Rs.)
Hyderabad	**From** 27.1.2017.	**To** 06.02.17.	Rail/Taxi	15,000.00
Saha Institute of Nuclear Physics Kolkata	Several times during the period 01.07.2015 – 30.06.2018.		Rail/Bus	15,000.00

Certified that the above expenditure is in accordance with the UGC norms for Major Research Projects.

Sanjoy Mukherjee.
PRINCIPAL INVESTIGATOR
ASSOCIATE PROFESSOR
DEPT. OF PHYSICS
UNIVERSITY OF BURDWAN

19-11-18
FINANCE OFFICER
FINANCE OFFICER
THE UNIVERSITY OF BURDWAN
BURDWAN, WEST BENGAL

REGISTRAR
REGISTRAR (Officiating)
THE UNIVERSITY OF BURDWAN
BURDWAN-713104

1-11-18
STATUTORY AUDITOR
JADAB KUMAR ROY
BURDWAN
53411
Chartered Accountants

Annexure – V

UNIVERSITY GRANTS COMMISSION
BAHADUR SHAH ZAFAR MARG
NEW DELHI – 110 002

Utilization Certificate

1. Certified that out of the grant of Rs. **12,38,454.00** (10,95,000.00 + 1,43,454.00) (**Rupees Twelve Lakh, Thirty Eight Thousand, Four Hundred, Fifty Four only**) received from the University Grants Commission under the scheme of support for Major Research Project entitled **"Study of Structural and Physical Properties of $R_2T_{17-x}M_x$ (R = rare earth element; T = Fe, Co; M = Al, Ga, Si, Cr, Mn) System"** vide UGC letter No. **F. No. -43-519/2014 (SR) dated 29th December, 2015 and dated 26th October, 2017,** an amount of **Rs. 11,28,602.00** (including committed expenditure of Rs. 41,549.00) has been **utilized** for the purpose for which it was sanctioned and in accordance with the terms and conditions laid down by the University Grants Commission, **leaving an unspent balance of Rs. 1,09,852.00.**

Sanjoy Mukherjee.

SIGNATURE OF THE PRINCIPAL INVESTIGATOR

ASSOCIATE PROFESSOR
DEPT. OF PHYSICS
UNIVERSITY OF BURDWAN

9-11-18

FINANCE OFFICER

FINANCE OFFICER
THE UNIVERSITY OF BURDWAN
BURDWAN, WEST BENGAL

REGISTRAR

REGISTRAR (Officiating)
THE UNIVERSITY OF BURDWAN
BURDWAN-713104

1-11-18

STAUTORY AUDITOR

JADAB KUMAR RAY
BURDWAN
53411
Chartered Accountants

Month-wise detailed statement of expenditure towards salary and HRA of project fellow

Name of the Project Fellow: Shovan Dan, **Date of Joining**: 31.05.2016

Month-wise Fellowship Paid to the Project Fellow from 31.05.2016 to 30.05.2018

Period	Salary per month	HRA per month	Amount of salary paid	HRA paid	Total amount paid
May, 2016 (For one day)	14,000.00	1,400.00	452.00	45.00	497.00
June, 2016 – June 2018	14,000.00	1,400.00	3,50,000.00	35,000.00	3,69,600.00
Total			**3,50,452.00**	**35,045.00**	**3,85,497.00**

Sanjoy Mukherjee
PRINCIPAL INVESTIGATOR
ASSOCIATE PROFESSOR
DEPT. OF PHYSICS
UNIVERSITY OF BURDWAN

FINANCE OFFICER
FINANCE OFFICER
THE UNIVERSITY OF BURDWAN
BURDWAN, WEST BENGAL

REGISTRAR
REGISTRAR (Officiating)
THE UNIVERSITY OF BURDWAN
BURDWAN-713104

Annexure – IX

UNIVERSITY GRANTS COMMISSION
BAHADUR SHAH ZAFAR MARG
NEW DELHI – 110 002

PROFORMA FOR SUBMISSION OF INFORMATION AT THE TIME OF SENDING THE FINAL REPORT OF THE WORK DONE ON THE PROJECT

1.Title of the project	Study of Structural and Physical Properties of $R_2T_{17-x}M_x$ (R = rare earth element; T = Fe, Co; M = Al, Ga, Si, Cr, Mn) System
2. Name and address of the principal investigator	Department of Physics, The University of Burdwan, Golapbag, Purba Bardhaman, West Bengal, Pin – 713 104
3. Name and address of the institution	The University of Burdwan, Rajbati, Purba Bardhaman, West Bengal, Pin – 713 104
4. UGC approval letter number and date	**F.No.- 43-519/2014(SR), dated 29.12.2015.**
5. Date of Implementation	01.07.2015
6. Tenure of the project	01.07.2015 - 30.06.2018
7. Total grant allocated	**Rs. 13,00,504.00**
8. Total grant received	**Rs. 12,38,454.00**
9. Final expenditure	**Rs. 11,28,602.00**
10. Title of the Project	Study of Structural and Physical Properties of $R_2T_{17-x}M_x$ (R = rare earth element; T = Fe, Co; M = Al, Ga, Si, Cr, Mn) System
11. Objectives of the project	See Annexure A
12. Whether objectives were achieved	See Annexure B
13. Achievements from the project	See Annexure C
14. Summary of the findings (500 words)	See Annexure D
15. Contribution to the society	See Annexure E
16. Whether any Ph.D. enrolled/produced out of the project	Yes, Mr. Shovan Dan has been enrolled for Ph.D. and will submit his thesis soon.
17. No. of publications out of the project	**4 (Int. Journal, published - 3, submitted - 1), List enclosed**

Sanjoy Mukherjee
PRINCIPAL INVESTIGATOR
ASSOCIATE PROFESSOR
DEPT OF PHYSICS
UNIVERSITY OF BURDWAN

3/12/18
REGISTRAR
REGISTRAR (Officiating)
THE UNIVERSITY OF BURDWAN
BURDWAN-713104

Publications and Presentations

International Journals:

1. Zero thermal expansion with high Curie temperature in $Ho_2Fe_{16}Cr$ alloy, Shovan Dan, S. Mukherjee, Chandan Mazumdar and R. Ranganathan, ***RSC Adv.*, 2016, 6, 94809.**

2. Thermal expansion properties of $Ho_2Fe_{16.5}Cr_{0.5}$, Shovan Dan, S. Mukherjee, Chandan Mazumdar and R. Ranganathan, ***J. Phys. Chem. Solids*, 2018, 115, 92**

3. Temperature Dependent Magnetic Behavior of $Ho_2Fe_{17-X}Cr_x$ (x = 0.5, 1, 2), S. Mukherjee, **International Journal Of Engineering Sciences & Research Technology, 2018, 7(2), 642.**

4. Effect of Si substitution in ferromagnetic Pr_2Fe_{17}: a magnetocaloric material with zero thermal expansion operative at high temperature, Shovan Dan, S. Mukherjee, Chandan Mazumdar and R. Ranganathan, submitted to **Physical Chemistry Chemical Physics.**

International Conferences:

5. "Study of thermal Expansion Behaviour of $Ho_2Fe_{17-x}Cr_x$Compounds, Oral Presentation by Dr. S. Mukherjee at International Conference On Magnetic Materials and Applications, VIT University, Hyderabad, India, 2-4 December, 2015.

6. Magnetovolume Effect Induced Zero Thermal Expansion in $Er_2Fe_{16.5}Cr_{0.5}$, Poster presentation by Shovan Dan at International Conference of Magnetism, Sanfransisco, USA, 15-20th July, 2018 **(Best Poster Awarded)**

National conferences:

7. "Zero Thermal Expansion in Cr doped R_2Fe_{17} (R = Ho, Ce) compounds", Oral Presentation by Dr. S. Mukherjee at National Thematic Workshop on Recent Advances in Materials Sciences, Organized by UGC-DAE Consortium for Scientific Research, Kolkata Centre and the Department of Physics, The University of Burdwan, 08-09 March, 2016.

8. Near Zero Thermal Expansion in $Ho_2Fe_{16.5}Cr_{0.5}$, Poster presentation by Shovan Dan at International Conference On Magnetic Materials and Applications, Hyderababad, India. 1-3rd February, 2017.

9. "Towards Zero Thermal Expansion: A New Approach", Oral Presentation by Dr. S. Mukherjee at A National Conference on Condensed Matter Physics: CMDAYS 2018, Organized by the Department of Physics, The University of Burdwan, 29-31 August, 2018.

Sanjoy Mukherjee.

Annexure A

Objective of the Project

In search of permanent magnet materials, a lot of work has been done on the substitution of non-magnetic elements (Al, Ga, Si) as well as magnetic elements (Cr, Mn) at the T-site of R_2T_{17} compounds to look into its effect on T_C, M_S, and coercivity. However, apart from this very practical view point, there exist a few fundamental points which have not been sufficiently explored in the past. The magneto-crystalline anisotropy and the associated thermo-magnetic irreversibility is such a point. The said substitution on the T-site, changes the relative strength of the uniaxial anisotropy of the R sublattice relative to the anisotropy of the T-sublattice as a function of temperature. This may sometimes cause spin reorientation and give rise to interesting magnetic behavior. We propose to undertake a detailed magnetic study as a function of temperature, magnetic field and time, on$R_2T_{17-x}M_x$ (T = Fe, Co; M = Ga, Al, Si, Cr, Mn) system to have a clear understanding of the complex magnetic behavior of this system.

We also propose to undertake a detailed study on the structural properties, *viz.*, lattice parameters and volume of $R_2T_{17-x}M_x$ (T = Fe, Co; M = Ga, Al, Si, Cr, Mn) system as a function of temperature, as the magneto-volume effects play a major role in this system below T_C. Such study will help us to find new materials with negative thermal expansion (NTE) coefficients, and to have a clear understanding of the related physics. Such study is important both from fundamental as well as practical point of view.

Sanjoy Mukherjee

Annexure B

Whether objectives were achieved

Our objectives were fully achieved. The proposal of our project on $R_2T_{17-x}M_x$ (R = rare earth element, T = Fe, Co; M = Ga, Al, Si, Cr, Mn) system had two main parts. Firstly, we proposed to undertake a detailed magnetic study as a function of temperature, magnetic field and time, to have a clear understanding of the complex magnetic behavior of this system. Secondly, we proposed to undertake a detailed study on the structural properties, *viz.*, lattice parameters and volume as a function of temperature, as the magneto-volume effects play a major role in this system below T_C. The intention behind such study was to find new materials with negative thermal expansion (NTE) coefficients, and to have a clear understanding of the related physics.

In our work, we have studied in detail the magnetic properties of our five series of samples namely, (1) $Ho_2Fe_{17-x}Cr_x$, $x = 0, 0.5, 1, 2$; (2) $Ce_2Fe_{17-x}Cr_x$, $x = 0, 0.5, 1$; (3) $Dy_2Fe_{17-x}Cr_x$, $x = 0, 0.5, 1, 2$; (4) $Er_2Fe_{17-x}Cr_x$, $x = 0, 0.5, 1, 2$, (5) $Pr_2Fe_{16}Si$. The important parameters: Curie temperature (T_C), Saturation Magnetization (M_S) and Coercivity (H_C) are as follows:

Sample Name	T_C (K)	M_S (μ_B/f.u)	H_c (Oe)
Ho_2Fe_{17}	326	23.5	175
$Ho_2Fe_{16.5}Cr_{0.5}$	390	11.84	330
$Ho_2Fe_{16}Cr$	415	16.4	720
$Ho_2Fe_{15}Cr_2$	402	10.8	2300
Dy_2Fe_{17}	355	17.16	128
$Dy_2Fe_{16.5}Cr_{0.5}$	430	-------	-----
$Dy_2Fe_{16}Cr$	456	-------	------
$Dy_2Fe_{15}Cr_2$	423	6.46	2500
Er_2Fe_{17}	304	25.57	90
$Er_2Fe_{16.5}Cr_{0.5}$	413	19.36	300
$Er_2Fe_{16}Cr$	420	20.12	450
$Er_2Fe_{15}Cr_2$	393	7.57	2000
Ce_2Fe_{17}	110	29.60	~ 0
$Ce_2Fe_{16.5}Cr_{0.5}$	230	27.93	~ 0
$Ce_2Fe_{16}Cr$	230	35.63	~ 0
$Pr_2Fe_{16}Si$	390	35	500

Sanjoy Mukherjee.

We have also studied the thermal expansion properties of the said compounds in detail. The results are as follows.

Sample	PTE	NTE	ZTE
$Ho_2Fe_{17-x}Cr_x$			
$x = 0$	>336 K	< 250 K	---------
$x = 0.5$	> 250 K	201-300 K	13-200 K
$x = 1$	> 300 K	330-425 K	13-330 K
$x = 2$	>13 K	----------	----------
$Dy_2Fe_{17-x}Cr_x$			
$x = 0$	>215 K	----------	13 – 215 K
$x = 0.5$	>430 K	----------	13- 300 K
$x = 1$	>430 K	----------	13 - 400 K
$x = 2$	>430 K	330-430 K	0 – 220 K
$Er_2Fe_{17-x}Cr_x$			
$x = 0$	>370 K	13 – 370 K	----------
$x = 0.5$	>400 K	300-400 K	13-300 K
$x = 1$	>400 K	----------	13-350 K
$x = 2$	> 13 K	----------	----------
$Ce_2Fe_{17-x}Cr_x$			
$x = 0$	> 250 K	Below 100 K , strong NTE	-----
$x = 0.5$	> 300 K	200-280 K	13-185 K
$x = 1$	> 300 K	160-280 K	13-160 K
$Pr_2Fe_{16}Si$	> 250 K	----------	200-340

Sanjoy Mukherjee

Annexure C

Achievements from the project

- We had prepared five series of $R_2Fe_{17-x}M_x$ (x = Cr and Si) compounds for R = rare earth element = Ho, Ce, Dy, Er, Pr.
- The samples had been characterized by X-ray diffraction (XRD) analysis. All the samples form in single phase.
- We have studied the thermal expansion properties of the prepared samples.
- We have studied the magnetic properties of the prepared samples.
- We have studied the magnetocloric effect in a few interesting samples.

The details of our work done is as follows.

1. Sample Preparation

a) Name of the samples prepared:

In the proposed $R_2T_{17-x}M_x$ (T = Fe, Co; M = Ga, Al, Si, Cr, Mn) system we have prepared the following samples:

(1) $Ho_2Fe_{17-x}Cr_x$, $x = 0, 0.5, 1, 2$; (2) $Ce_2Fe_{17-x}Cr_x$, $x = 0, 0.5, 1$; (3) $Dy_2Fe_{17-x}Cr_x$, $x = 0, 0.5, 1$; (4) $Er_2Fe_{17-x}Cr_x$, $x = 0, 0.5, 1, 2$; (5) $Pr_2Fe_{16}Si$.

b) Method of preparation of samples:

The above mentioned polycrystalline compounds were prepared by the method of arc-melting (in an argon atmosphere) with at least 99.9% pure starting materials. The ingots were re-melted five to six times flipping each time after melting to ensure homogeneity. The samples were annealed in a vacuum sealed quartz tube at 1173 K for 7 days, followed by quenching in ice water.

2. Characterization of samples

Method: The room temperature XRD patterns of the samples were taken using CuK_α radiation in TTRAX III diffractometer (M/S Rigaku Corp., Japan). The XRD patterns at different temperatures (13 – 515 K) were recorded using the same instrument, with a very low scan speed (0.01° steps, and 0.4° min^{-1} rate) for a better statistical average. This is necessary in our case as our sample contains more than 85% Fe and the CuK_α radiation is in the absorption edge of Fe.

Sanjoy Mukherjee.

Confirmation of single phase samples: The analysis of room temperature XRD patterns, shown in Fig. 1 of the prepared samples confirm that the samples form in single phase. The patterns were refined with FullProf software package. The lattice parameters, crystal structure, space group and other structural details are tabulated in Table 1.

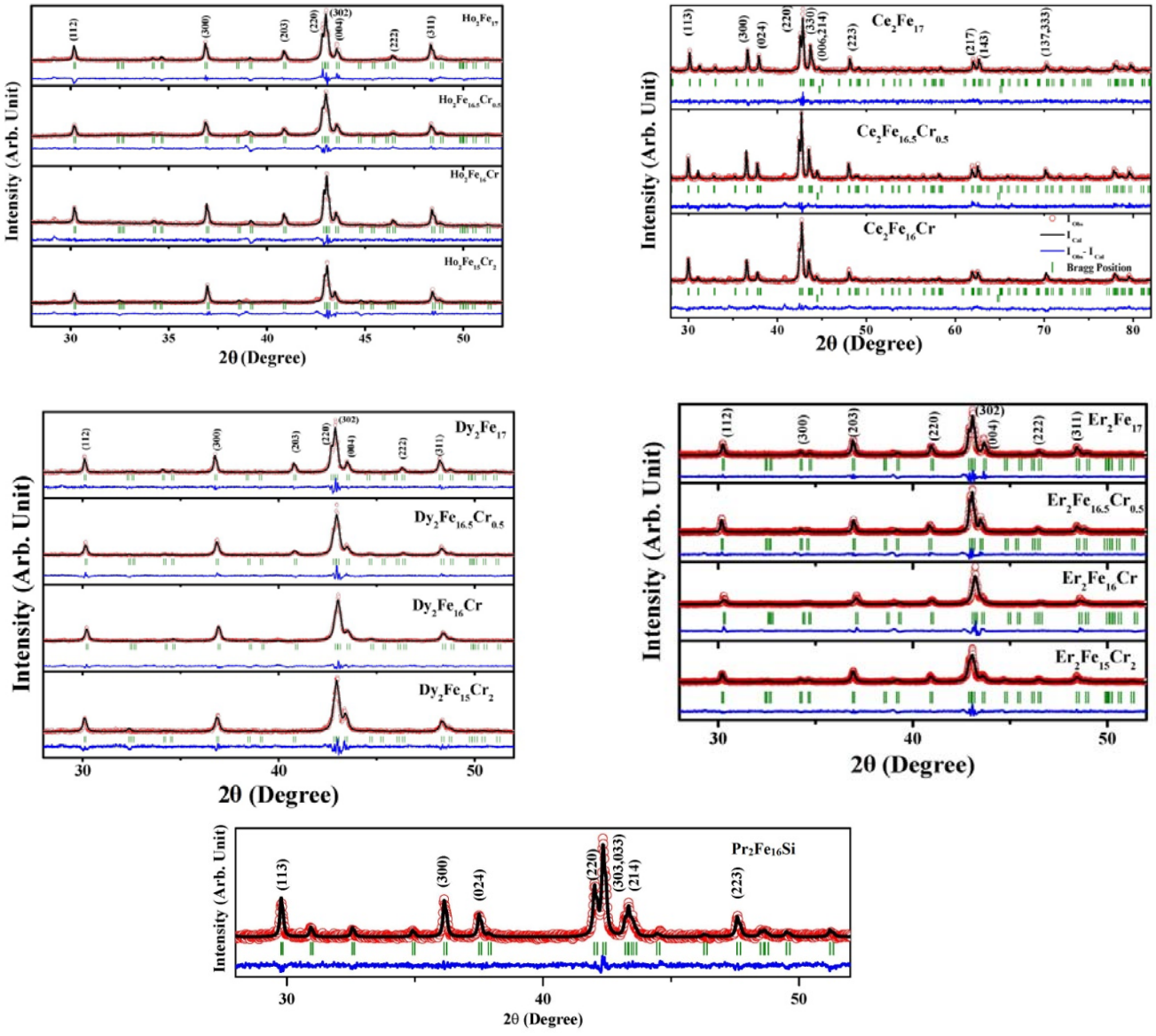

Fig.1. The experimental data points, theoretically estimated lines, the difference between them and the Bragg positions of all the samples are represented respectively by red circles, black line, blue line and olive horizontal bars. Bragg peak positions are also index at the top of all XRD patterns.

Table 1 - Structural details of all prepared samples

Sample name	Structure type	Space group	*a* (Å)	*c* (Å)	*v*(Å^3)
Ho_2Fe_{17}	Th_2Ni_{17} (Hexagonal)	$P6_3/mmc$ (#194)	8.435(9)	8.301(4)	511.62(3)
$Ho_2Fe_{16.5}Cr_{0.5}$			8.438(5)	8.305(0)	512.16(2)
$Ho_2Fe_{16}Cr$			8.424(6)	8.310(5)	510.80(9)
$Ho_2Fe_{15}Cr_2$			8.418(9)	8.324(2)	510.96(6)
Dy_2Fe_{17}			8.461(4)	8.312(8)	515.42(7)
$Dy_2Fe_{16.5}Cr_{0.5}$			8.449(7)	8.321(0)	514.51(0)
$Dy_2Fe_{16}Cr$			8.442(7)	8.325(3)	513.92(4)
$Dy_2Fe_{15}Cr_2$			8.429(9)	8.322(5)	512.20(1)
Er_2Fe_{17}*			8.430(3)	8.288(2)	510.13(2)
$Er_2Fe_{16.5}Cr_{0.5}$			8.422(7)	8.295(0)	509.62(4)
$Er_2Fe_{16}Cr$			8.412(6)	8.311(2)	509.40(0)
$Er_2Fe_{15}Cr_2$			8.401(3)	8.318(3)	508.46(8)
Ce_2Fe_{17}	Th_2Zn_{17} (Rhombohedral)	$R\bar{3}m$ (#166)	8.485(7)	12.405(8)	773.62(6)
$Ce_2Fe_{16.5}Cr_{0.5}$			8.478(9)	12.413(0)	772.83(9)
$Ce_2Fe_{16}Cr$			8.470(6)	12.422(5)	771.92(2)
$Pr_2Fe_{16}Si$			8.563(7)	12.469(0)	791.94(5)

3. Results and Discussion

(a) Study of Thermal Expansion

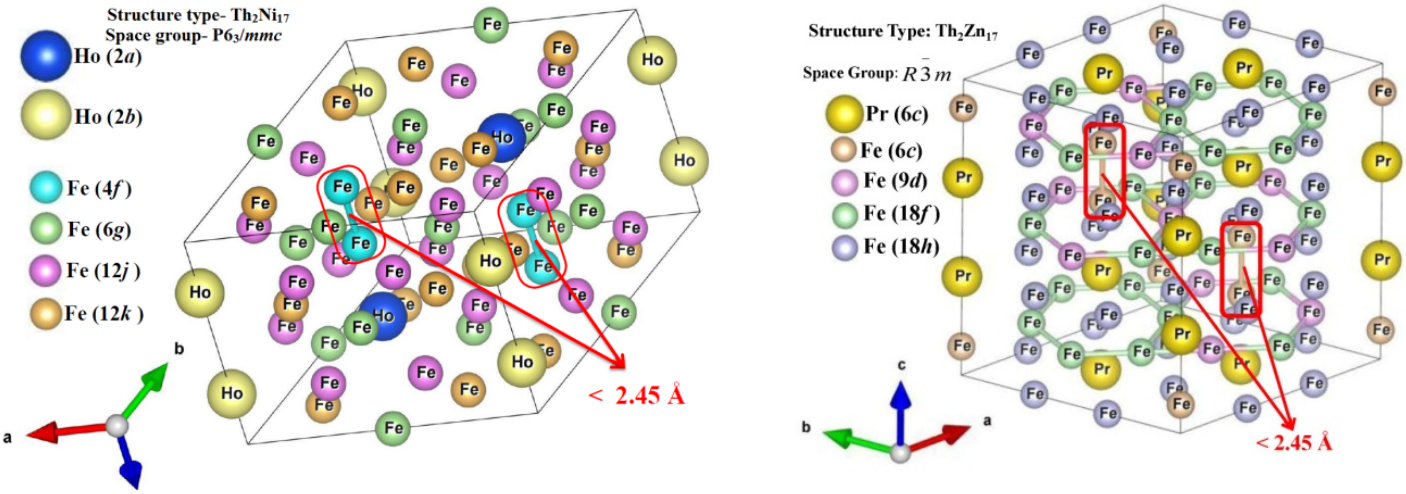

Fig. 2. Schematic crystal structure of hexagonal Th_2Ni_{17} type and rhombohedral Th_2Zn_{17} type structure.

R_2Fe_{17} (R = rare earth) compounds crystallize with a hexagonal Th_2Ni_{17} type structure (rhombohedral Th_2Zn_{17} type structure) for heavy rare earths (for light rare earths). The crystallographic sites for the Fe atoms are 4*f* (6*c*), 6*g* (9*d*), 12*j* (18*f*) and 12*k* (18*h*) sites, whereas, the rare earth atoms occupy 2*a* and 2*b* positions for hexagonal systems and 6*c* site for rhombohedral one [1-3].

As an example, we have shown *a*, *c*, *v* of the sample $Ho_2Fe_{16.5}Cr_{0.5}$ in Fig. 3. The temperature dependence of the spontaneous linear magnetostrictive deformation in the basal plane, $\lambda_a = (a_m - a_p) / a_p$, that along the *c*-axis $\lambda_c = (c_p - c_p)/ c_p$, and the spontaneous volume magnetostrictive deformation $\omega_S = (v_m - v_p)/ v_p$ are important parameters for identifying the strength and the nature of magnetoelastic coupling. a_m, c_m, *and* v_m are the experimentally measured values of *a*, *c* and *v*, whereas a_p, c_p, *and* v_p are the corresponding values obtained by extrapolation from the paramagnetic state using the Grüneisen relation [1],

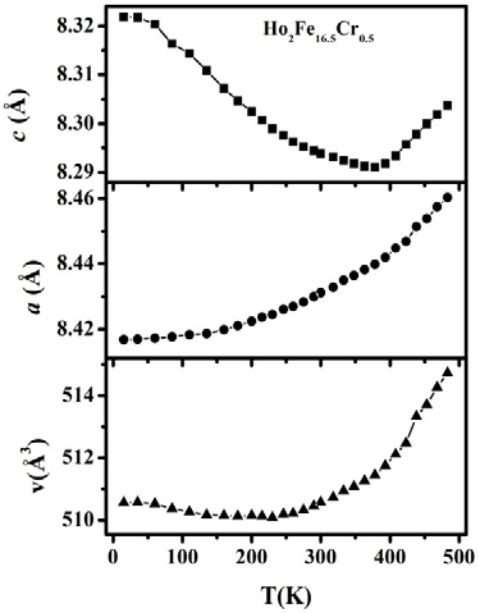

Fig. 3. Lattice parameters *a*, *c* and unit cell volume *v* of the sample $Ho_2Fe_{16.5}Cr_{0.5}$

$$\alpha = \frac{1}{v}\frac{\gamma\, C_v}{\kappa}, \qquad C_v(T) = \frac{R\left(\frac{T}{\theta_D}\right)^3 \int_0^{\frac{\theta_D}{T}} x^4 e^x}{(e^x-1)^2} dx$$

where θ_D is the Debye temperature and *R* is the molar gas constant.

The parameters a_m, c_m, and v_m along with a_p, c_p, and v_p are presented in Fig. 4 for the compound $Ho_2Fe_{16.5}Cr_{0.5}$. λ_a, λ_c and ω_S have been plotted as a function of temperature in Fig. 5. The value of θ_D has been taken as 400 K, estimated earlier for R_2Fe_{17} compounds other than Y_2Fe_{17} [4].

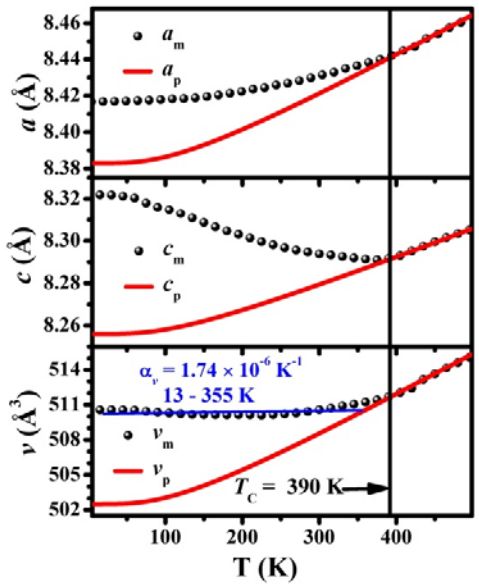

Fig. 4. The parameters a_m, c_m, and v_m along with a_p, c_p, and v_p for $Ho_2Fe_{16.5}Cr_{0.5}$

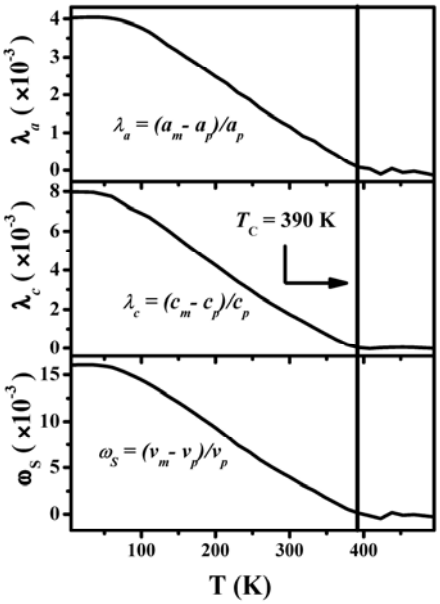

Fig. 5. λ_a, λ_c and ω_S for $Ho_2Fe_{16.5}Cr_{0.5}$

Our interest to study the thermal expansion behavior of $R_2Fe_{17-x}M_x$ (M = Cr/Si) stems from the fact that the parent compound shows negative thermal expansion (NTE). [2,5] The origin of NTE lies in the magnetovolume effect (MVE). In fact, a large amount of magnetic energy is stored along the Fe–Fe distance between the atoms at 4*f* (6*c*) sites of R_2Fe_{17} compounds.[6] This magnetic energy can be reduced by increasing the said distance, which is dependent only on the lattice parameter *c*. Finally, a compromise is obtained between the magnetic energy and the elastic energy by increasing the lattice volume for the magnetic state at a lower temperature. We aim to search for materials with near zero thermal expansion (ZTE), having high T_C for using as permanent magnetic materials. The Cr/Si- substitution at the Fe site can weaken the NTE behavior by reducing the MVE. The anomalous thermal expansion behavior of $Ho_2Fe_{17-x}Cr_x$ (x = 0.5, 1, 2) compounds have been shown in Fig. 6. Unit cell volume (v) as a function of temperature of $Dy_2Fe_{17-x}Cr_x$ and $Er_2Fe_{17-x}Cr_x$ (x = 0, 0.5, 1, 2) compounds are shown in Fig. 7. Fig. 8. shows the same for $CeFe_{17-x}Cr_x$ compounds. Fig.9. shows the temperature dependent a, c and v for the compound $Pr_2Fe_{16}Si$.

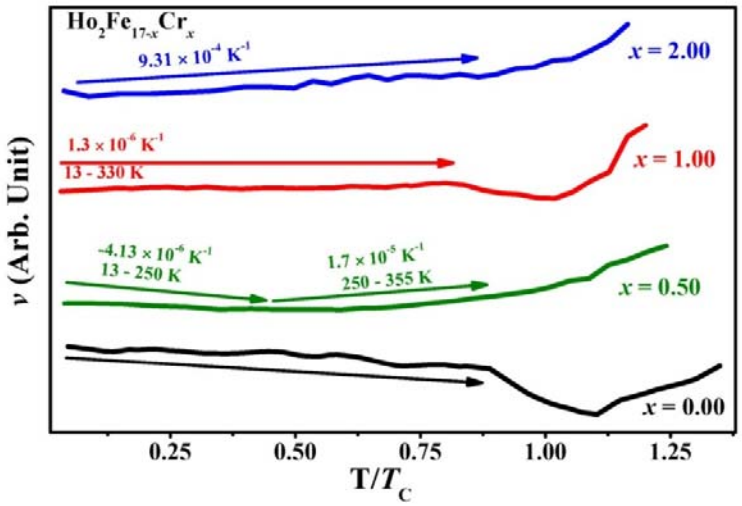

Fig. 6. Unit cell volume (v) as a function of temperature of $Ho_2Fe_{17-x}Cr_x$ (x = 0, 0.5, 1, 2) compounds.

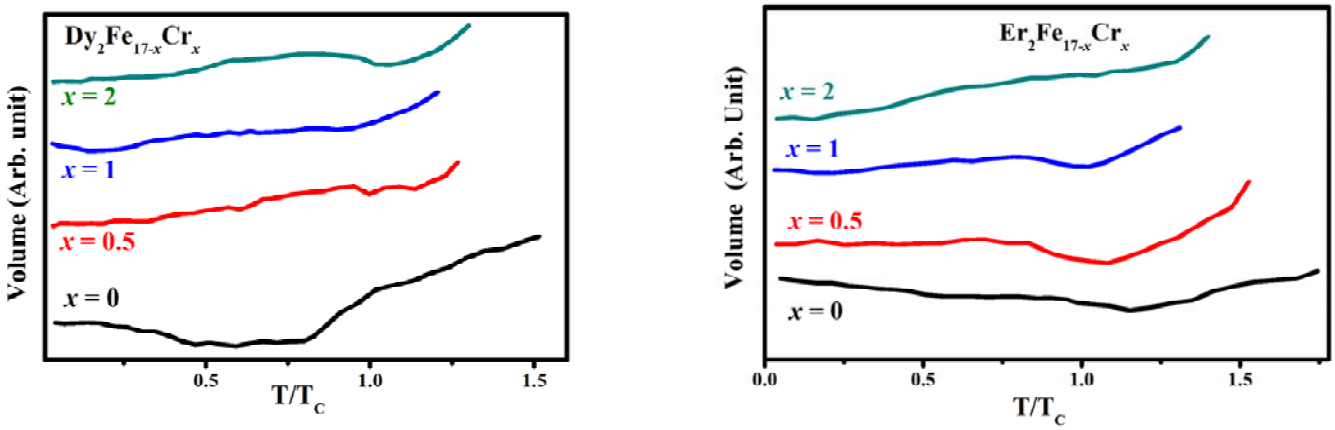

Fig. 7. Unit cell volume (v) as a function of temperature of $Dy_2Fe_{17-x}Cr_x$ and $Er_2Fe_{17-x}Cr_x$ (x = 0, 0.5, 1, 2) compounds.

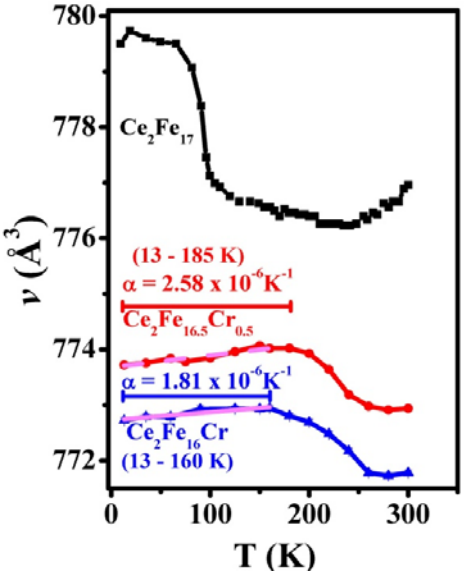

Fig. 8. Unit cell volume (v) as a function of temperature of $Ce_2Fe_{17-x}Cr_x$ (x = 0, 0.5, 1) compounds.

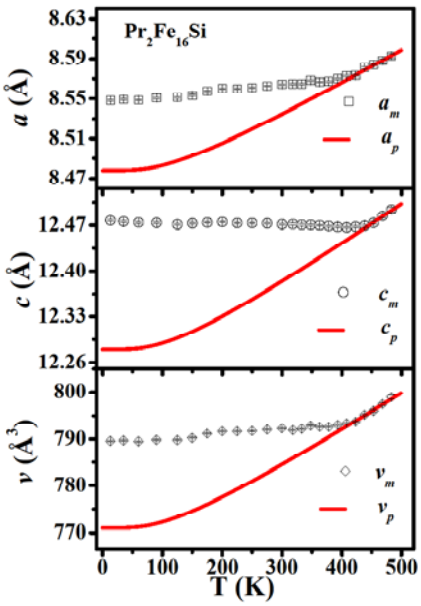

Fig. 9. Variation of lattice parameters and unit cell volume with temperature for $Pr_2Fe_{16}Si$

Table 2- Thermal Expansion Properties

Sample	PTE	NTE	ZTE
$Ho_2Fe_{17-x}Cr_x$			
$x = 0$	>336 K	< 250 K	---------
$x = 0.5$	> 250 K	201-300 K	13-200 K
$x = 1$	> 300 K	330-425 K	13-330 K
$x = 2$	>13 K	----------	----------
$Dy_2Fe_{17-x}Cr_x$			
$x = 0$	>215 K	----------	13 – 215 K
$x = 0.5$	>430 K	----------	13- 300 K
$x = 1$	>430 K	----------	13 - 400 K
$x = 2$	>430 K	330-430 K	0 – 220 K
$Er_2Fe_{17-x}Cr_x$			
$x = 0$	>370 K	13 – 370 K	----------
$x = 0.5$	>400 K	300-400 K	13-300 K
$x = 1$	>400 K	----------	13-350 K
$x = 2$	> 13 K	----------	----------
$Ce_2Fe_{17-x}Cr_x$			
$x = 0$	> 250 K	Below 100 K , strong NTE	-----
$x = 0.5$	> 300 K	200-280 K	13-185 K
$x = 1$	> 300 K	160-280 K	13-160 K
$Pr_2Fe_{16}Si$	> 250 K	----------	200-340 K

(a) Study of Magnetic Properties:

The magnetism in R_2Fe_{17} system can be explained by the interaction between two sub-lattices: rare earth sub-lattice and iron sub-lattice. Rare-earth atoms couple ferromagnetically to each other in the rare-earth sub-lattice. The coupling between the two sub-lattices depends upon the choice of the rare-earth atom. For example they couple ferromagnetically in compounds like $Pr_2Fe_{17,}$ ferrimagnetically in $Ho_2Fe_{17,}$ $Er_2Fe_{17,}$ Dy_2Fe_{17}, whereas the coupling is helimagnetic for Ce_2Fe_{17}.[2,5] Our prepared samples are Cr-substituted and Si-substituted R_2Fe_{17} compounds. Due to the antiferromagnetic (AFM) interaction between Fe atoms at 4*f* (6*c*) sites of the parent compound, these particular dumbbell pair contains a large amount of magnetic energy. Magnetically weaker Cr/Si atoms prefer to substitute Fe atoms at 4*f* (6*c*) sites. This reduces the magnetic stress generated along that bond. Total magnetic interaction strength at the iron sub-lattice is the numerical sum of total AFM strength 4*f* (6*c*) - 4*f* (6*c*) interaction and total FM strength between the Fe atoms placed other than 4*f* (6*c*) site. As small substitution of Cr prefers 4*f* (6*c*) site only, it reduces the total AFM interaction strength, and enhances the overall FM strength. Hence it increases the T_C. So a small fractional substitution of Cr/Si atoms for the Fe atoms enhances the T_C of the compounds. For higher concentrations of Cr/Si, T_C reduces. There,

Cr/Si atoms start populating sites other than 4*f* (6*c*) sites, and thereby, decreases the overall FM strength. T_C, H_C, M_S for all the prepared compounds are tabulated in Table 2. The Curie temperature (T_C) of the prepared samples has been determined from the magnetization (M) curve as a function of temperature (T). The saturation magnetization (M_S) and the coercivity (H_C) of each sample have been determined at different temperatures from the plot of M versus magnetic field (H). As an example we show M-T curve at H = 0.05 Tesla, and M-H curve at T = 5 K for $Ho_2Fe_{17-x}Cr_x$ (x = 0, 1, 2) in Fig. 10. (a) and (b).

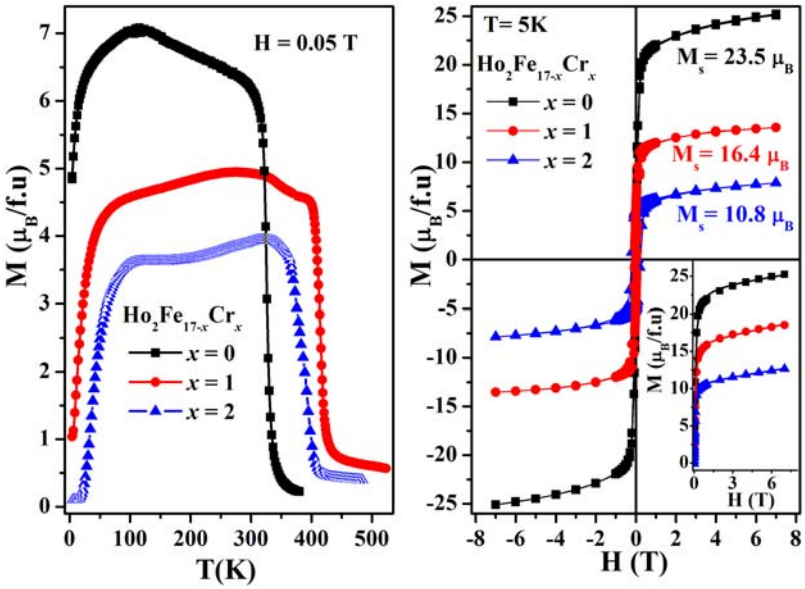

Fig. 10. (a) M versus T at H = 0.05 Tesla, (b) M versus H at T = 5 K for $Ho_2Fe_{17-x}Cr_x$ (x = 0, 1, 2)

Table 3 - T_C, M_S and H_c of all the prepared compounds.

Sample Name	T_C (K)	M_S (μ_B/f.u)	H_c (Oe)
Ho_2Fe_{17}	326	23.5	175
$Ho_2Fe_{16.5}Cr_{0.5}$	390	11.84	330
$Ho_2Fe_{16}Cr$	415	16.4	720
$Ho_2Fe_{15}Cr_2$	402	10.8	2300
Dy_2Fe_{17}	355	17.16	128
$Dy_2Fe_{16.5}Cr_{0.5}$	430	-------	-----
$Dy_2Fe_{16}Cr$	456	-------	------
$Dy_2Fe_{15}Cr_2$	423	6.46	2500
Er_2Fe_{17}	304	25.57	90
$Er_2Fe_{16.5}Cr_{0.5}$	413	19.36	300
$Er_2Fe_{16}Cr$	420	20.12	450
$Er_2Fe_{15}Cr_2$	393	7.57	2000
Ce_2Fe_{17}	110	29.60	~ 0
$Ce_2Fe_{16.5}Cr_{0.5}$	230	27.93	~ 0
$Ce_2Fe_{16}Cr$	230	35.63	~ 0
$Pr_2Fe_{16}Si$	390	35	500

(b) **Study of Magnetocaloric Effect**:

The magnetocaloric effect (MCE) is defined as the heating or cooling (*i.e.,* the temperature change) of a magnetic material due to the application of a magnetic field. When the magnetic field is applied adiabatically in a reversible process, the magnetic entropy decreases, but as the total entropy does not change, *i.e.*, S (T_0, H_0) = S (T_1, H_1), then the temperature increases. The adiabatic temperature change, $\Delta T_{ad} = T_1 - T_0$, is a measure of the MCE in the material. On the other hand, if the magnetic field is applied isothermally, the total entropy decreases due to the decrease in the magnetic contribution, and the entropy change in the process is defined as ΔS_M = S (T_0, H_0) − S (T_0, H_1). The isothermal magnetic entropy change, ΔS_M, is also a characteristic value of the MCE. The isothermal magnetic entropy change $|\Delta S_M|$ due to a change of the applied magnetic field from an initial value H = 0 to a final value H is obtained by numerical approximation of the Maxwell relation ΔS_M (T, H) = S_M (T, H) - S_M (T, 0) = $\int_0^H (\frac{\partial M(T',H')}{\partial T'})_{T=T'}$ dH', where T is the temperature at which each M (H) curve is measured.

For $Pr_2Fe_{16}Si$, isothermal M (H) data collected for H = 0 - 1.5 T, in a temperature region T = 360 - 450 K, centered around T_C = 390 K (in steps of 5 K) (Fig. 11). ΔS_M (T,H) have been estimated from our M(H) data by replacing the partial derivative $\frac{\partial M}{\partial T}$ by $\frac{\Delta M}{\Delta T}$, the ratio of finite differences, and finally integrating by numerical approximation. $|\Delta S_M|$ (T, H) have been shown in fig. 11.

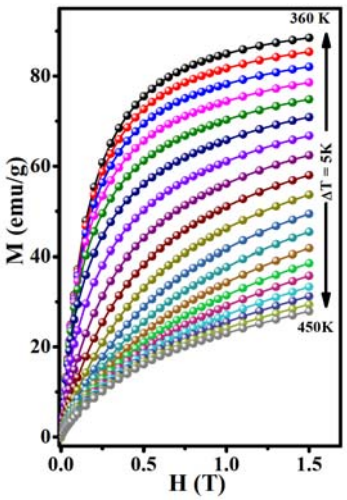

Fig. 11. M versus H at T = 360 - 450 K for $Pr_2Fe_{16}Si$.

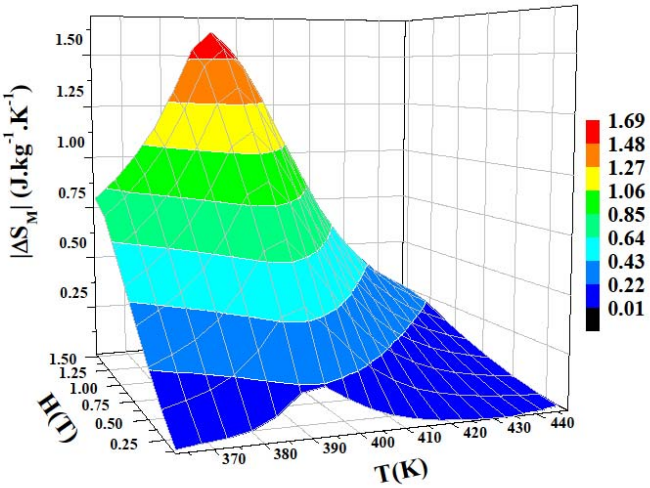

Fig. 12. $|\Delta S_M|$ (T, H) for $Pr_2Fe_{16}Si$.

ΔS_M reaches its maximum value $|\Delta S_M|^{max}$ = 1.61 J.kg^{-1}K^{-1}, around T_C = 390 K, whereas for the parent compound Pr_2Fe_{17}, for the field sweep of 1 T, $|\Delta S_M|^{max}$ is 2 J.kg^{-1}K^{-1}at T = 286 K (T_C of the parent compound)[7]. Since Si substitution increases the T_C, the operating temperature, namely, the one corresponds to $|\Delta S_M|^{max}$ is higher for $Pr_2Fe_{16}Si$ compared to the parent compound. This is a practical advantage. However, the associated disadvantage lies in lowering the value of $|\Delta S_M|^{max}$ due to reduction in average magnetic moment of Fe atoms. For $Pr_2Fe_{16}Si$, the operating temperature is really high and $|\Delta S_M|^{max}$ is moderate for ΔH = 1.5 T. Relative cooling power (RCP) for a particular H, defined as the product of $|\Delta S_M|^{max}$ and δT_{FWHM} (full width at half-maxima of ΔS_M versus T curve), gives a measure of both the working temperature range and the cooling efficiency. This is an important parameter for magnetocaloric materials. RCP for $Pr_2Fe_{16}Si$ is high (87 J.kg^{-1}).

We have also studied the MCE for the samples $Ce_2Fe_{17-x}Cr_x$ (x = 0.5, 1). For observing MCE, the field dependence of the magnetization isotherms, M (H), at several temperatures in the vicinity of the magnetic phase transitions are drawn for $Ce_2Fe_{16.5}Cr_{0.5}$ and $Ce_2Fe_{16}Cr$ (Fig. 13.). The maximal value of the peak entropy change $-\Delta S_M$ is quite larger for the compositions x = 0.5 and 1 than the parent compound, at T ~ 245K close to the Néel temperature. A 3-D plot of $-\Delta S_M$ as a function of T and H of the two compounds has been plotted in Fig. 14.

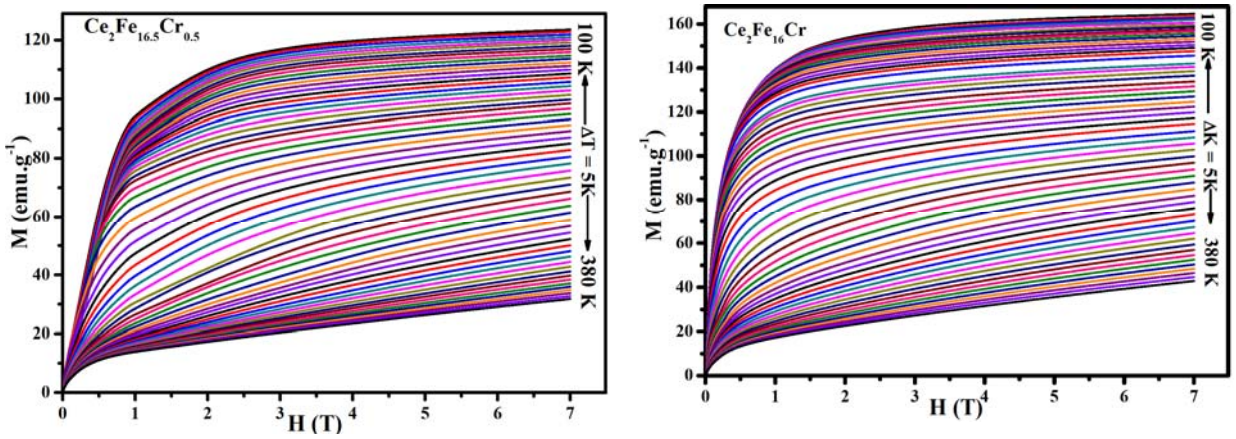

Fig. 13. M versus H of $Ce_2Fe_{16.5}Cr_{0.5}$ and $Ce_2Fe_{16}Cr$ at different temperatures.

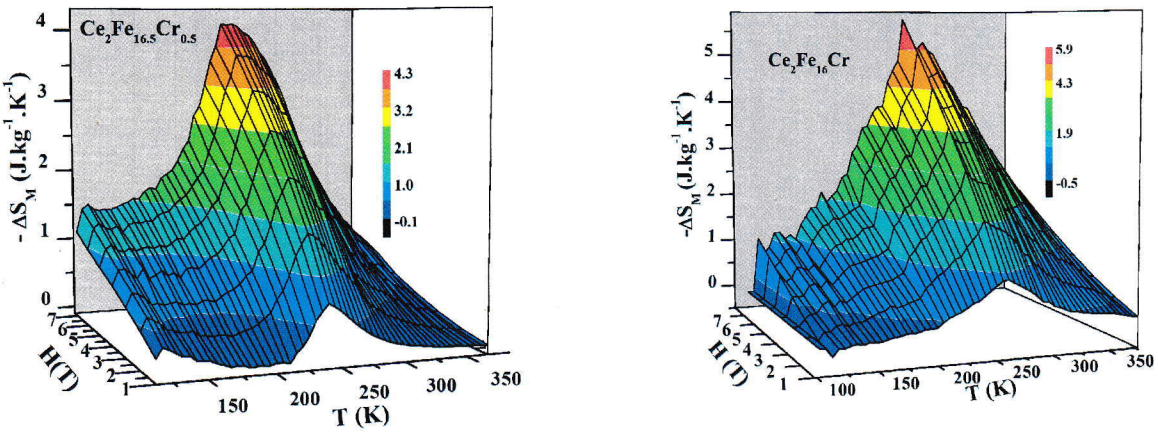

Fig. 14. A 3-D plot of $-\Delta S_M$ as a function of temperature (T) and magnetic field (H) of the compounds $Ce_2Fe_{16.5}Cr_{0.5}$ and $Ce_2Fe_{16}Cr$.

References

1. Y. Hao, X. Zhang, B. Wang, Y. Yuang and F. Wang, *J. Appl. Phys*., 2010, **108**, 023915.

2. P. A. -Alonso, P. Gorria, J.A. Blanco, J.S. -Marcos, G.J. Cuello, I.P. -Orench, J.A.R -Velamazán, G. Garbarino, I.de Pedro, J.R. Fernández, and J.L.S. Llamazares, *Phys. Rev. B*, 2012, 86,184411.

3. J. L. Wang, S. J. Campbell, O. Tegus, C. Marquina and M. R. Ibarra, *Phys. Rev. B: Condens. Matter Mater. Phys.*, 2007, **75**, 174423.

4. A.V. Andreev, A. V. Deryagin, S. M. Zadvorkin, N. V. Kudrevatykh, R. H. Levitin, V. N. Moskalev, Y. F. Popov and R. Y. Yumaguzhin, *Fizika Magnitnykh Materialov*, *Physics of Magnetic Materials*, ed. D. D. Mishin, Kalinin University, Kalinin, USSR, 1985, p. 21, in Russian.

5. P. A. Alanso, Doctoral Thesis, University of Oviedo, Spain, 2011.

6. D. Givord, R. Lemaire, W. J. James, J.-M. Moreau and J. S. Shah, *IEEE Trans. Magn*., 1971, **7**, 657–659.

7. P. Gorria, P. Alvarez, J.S. Marcos, J.L.S. Llamazares, M.J. Pérez, and J.A. Blanco, *Acta Mater.*, 2009, **57**, 1724-1733.

Sanjoy Mukherjee

Annexure D

Summary of the findings

- Chromium (Cr) and Silicon (Si) substitution in R_2Fe_{17} compounds (R = Ho, Ce, Er, Dy) increases the Curie temperature (T_C) and decreases the saturation magnetization (M_S).

- As indicated by the previous research workers the system $R_2Fe_{17-x}Cr_x$ is not suitable for permanent magnetic material.

- R_2Fe_{17} compounds show negative thermal expansion (NTE) behavior in certain temperature range depending upon the choice of R.

- Judicious substitution in Fe site by Cr/Si can give zero thermal expansion (ZTE) materials.

- **$Ho_2Fe_{16}Cr$ and $Er_2Fe_{16}Cr$ have been found as ZTE materials operating in the temperature range from very low to above room temperature.**

- **The study of magnetocaloric effect (MCE) establishes that, for $Pr_2Fe_{16}Si$, the operating temperature is really high (286 K), $|\Delta S_M|^{max}$ (2 $J.kg^{-1}K^{-1}$) is moderate for ΔH = 1.5 T, and the relative cooling power (RCP) is high (87 $J.kg^{-1}$).**

Sanjoy Mukherjee.

Annexure E

Contribution to the society

The study of this project appears to be very important and its outcome appears to be commendable. Zero thermal expansion (ZTE) materials are very rare and precious. As a result of our study, we could find that **$Ho_2Fe_{16}Cr$ and $Er_2Fe_{16}Cr$ behave as ZTE materials operating in the temperature range from very low to above room temperature. The materials are magnetic also. Hence, these materials can be used as ZTE magnetic materials.** On the other hand, **the study of magnetocaloric effect (MCE) establishes that, for $Pr_2Fe_{16}Si$, the operating temperature is really high (286 K), $|\Delta S_M|^{max}$ (2 $J.kg^{-1}K^{-1}$) is moderate for ΔH = 1.5 T, and the relative cooling power (RCP) is high (87 $J.kg^{-1}$). This might have a future for using as a refrigerant material.**

Sanjoy Mukherjee

RSC Advances

PAPER

Cite this: *RSC Adv.*, 2016, **6**, 94809

Zero thermal expansion with high Curie temperature in $Ho_2Fe_{16}Cr$ alloy

Shovan Dan,[a] S. Mukherjee,*[a] Chandan Mazumdar[b] and R. Ranganathan[b]

Received 10th August 2016
Accepted 23rd September 2016

DOI: 10.1039/c6ra20216k

www.rsc.org/advances

We report the observation of zero thermal expansion with a high Curie temperature in a $Ho_2Fe_{16}Cr$ alloy. Among the $R_2Fe_{17-x}Cr_x$ (R = rare earth elements) series of alloys, $Ho_2Fe_{16}Cr$ shows not only enhancement of the Curie temperature (T_C) to 415 K in comparison with the parent compound Ho_2Fe_{17} (330 K), but also shows zero thermal expansion (ZTE) in the wide temperature range 13–330 K due to reduction of the magneto-volume effect. We believe that such a single component ZTE magnetic material with a T_C higher than room temperature is of practical importance.

1 Introduction

Recently, ZTE materials with a very low coefficient of thermal expansion (α) have attracted considerable interest as a particular class of functional materials.[1–6] These materials appear to be of immense practical importance to improve the performance of various electronic and optical devices. Several materials: YbGaGe,[1] $Fe[Co(CN)_6]$,[2] $In(HfMg)_{0.5}Mo_3O_{12}$,[3] $0.8PbTiO_3$–$0.2Bi(Ni_{0.5}Ti_{0.5})O_3$,[4] antiperovskite manganese nitride Mn_3AN (A = Cu/Sn, Zn/Sn),[5] $(Al_{0.3}(HfMg)_{0.85})(WO_4)_3$,[6] Invar alloys,[7,8] $Sc_{0.05}Ga_{0.05}Fe_{0.1}F_3$,[9] $La(Fe,Si)_{13}$,[10] $La(Fe,Al)_{13}$,[11] carbon doped $La(Fe,Si)_{13}$ (ref. 12) *etc.* have been identified as ZTE materials, in different ranges of temperature.

Materials showing negative thermal expansion (NTE) play a key role in producing ZTE materials.[13,14] In general, to achieve ZTE materials, attempts have been made to form composites by dispersing particles of a NTE material like ZrW_2O_8 into an isotropic matrix of positive thermal expansion (PTE) material like copper (Cu) or aluminium (Al).[13,15,16] ZTE composites have also been synthesized using antiperovskite NTE materials like $Mn_3Cu_{0.5}A_{0.5}N$ (A = Ni, Sn),[17] $Mn_3Zn_{0.5}Sn_{0.5}N$[18] and Cu by optimizing their mass ratios. $LaFe_{10.5}Co_{1.0}Si_{1.5}$/Cu[19] has been recently found to show a tailoring thermal expansion property. In such composites, the NTE material is used to compensate for the thermal expansion of the matrix of PTE material to obtain a desired low α. However, the actual values of α do not match the desired values, as the effects of the interfaces could not be estimated in advance accurately.[13] Among the composites, α as low as 3.5×10^{-6} K^{-1} in the range of $T = 320$–355 K, has been obtained in the case of a metal matrix composite $Mn_3Cu_{0.5}Sn_{0.5}N_{1-\delta}$/AC8A.[13] In composites, the large difference in α between the matrix and the compensator causes a stress at the interfaces or grain boundaries, and thereby, may degrade the composite functionalities by forming micro-cracks.[13] Therefore, as a functional material, a single-component ZTE material[13] will be more effective than a composite one.

A single component ZTE material can be formed as a solid solution of a PTE material and a NTE material. $In(HfMg)_{0.5}Mo_3O_{12}$ [3] is such a solid solution of a PTE material $HfMgMo_3O_{12}$ and a NTE material $In_2Mo_3O_{12}$. It shows ZTE in the temperature range 500–900 K with an average linear intrinsic $\alpha = -0.4 \times 10^{-6}$ K^{-1}, and an average bulk $\alpha = 0.4 \times 10^{-6}$ K^{-1}. A similar single-phase ceramic material, $(Al_{2x}(HfMg)_{1-x})(WO_4)_3$,[6] formed by combining a NTE material $(HfMg)(WO_4)_3$ and a PTE material $Al_2(WO_4)_3$, behaves like a ZTE material for $x = 0.15$, between room temperature and 800 °C.

A single component ZTE material can also be achieved by lowering the NTE coefficient of a NTE material, by weakening the inherent mechanism responsible for NTE. The underlying mechanism responsible for the observed NTE in different reported materials is not unique; rather, they are widely different.[13,20] For example, a flexible network causes NTE in ZrW_2O_8,[21] $LiAlSiO_4$,[22] $Cd(CN)_2$,[23] ReO_3,[24] siliceous faujasite,[25] metal nitroprussides,[26] $HfScMo_2VO_{12}$ (ref. 27) *etc.* whereas atomic radius contraction is responsible for NTE in $Bi_{0.95}La_{0.05}NiO_3$.[28] The site anisotropy results in NTE in $GdPd_3B_{0.25}C_{0.75}$,[29] and tetragonality introduces NTE in $PbTiO_3$.[4] The magneto-volume effect (MVE) causes NTE in different magnetic materials like Invar alloys,[30,31] YMn_2,[32] pure[33] and substituted R_2Fe_{17} (R = rare earth element) compounds,[34–36] manganese antiperovskites.[37] A ZTE multiferroic compound $0.8PbTiO_3$–$0.2Bi(Ni_{0.5}Ti_{0.5})O_3$ (ref. 4) with $\alpha = 0.4 \times 10^{-7}$ K^{-1} between room temperature and 500 °C has been achieved by weakening the tetragonality of the parent compound $PbTiO_3$, by using the dopant $Bi(Ni_{0.5}Ti_{0.5})O_3$. A similar study has also been done on Nd/Sm substituted $0.5PbTiO_3$–$0.5BiFeO_3$.[38] Optimization of the heat treatment and the chemical composition lowers the NTE

[a]*Department of Physics, The University of Burdwan, Burdwan-713104, India. E-mail: sanseb68@yahoo.co.in*

[b]*Condensed Matter Physics Division, Saha Institute of Nuclear Physics, 1/AF, Bidhannagar, Kolkata-700064, India*

coefficient of antiperovskite Mn_3AN(A = Cu/Sn, Zn/Sn).[5] ZTE can be achieved by weakening the MVE in magnetic materials showing NTE. R_2Fe_{17} compounds are such magnetic materials, where on increasing the temperature, the lattice parameter c decreases faster than the lattice parameter a due to MVE, and thereby, results in NTE.

R_2Fe_{17} compounds with a hexagonal Th_2Ni_{17} structure for heavy rare earths (rhombohedral Th_2Zn_{17} structure for light rare earths) show NTE due to MVE. Cr-substitution in R_2Fe_{17} compounds can weaken the NTE behavior as well as increase T_C.[34–36] Thus, the study of Cr-substitution in R_2Fe_{17} compounds is important in searching for ZTE magnetic materials with a high T_C, although previous studies in Cr-substituted R_2Fe_{17} compounds (R = Tb, Tm, Gd) do not show the existence of ZTE in their studied range of temperature. Such studies are restricted only in a temperature range above room temperature. $Tm_2Fe_{17-x}Cr_x$ ($x > 0$) shows NTE near the T_C (around 430 K) with a minimum NTE coefficient of volume expansion, $\alpha_v = -9.15 \times 10^{-6}$ K^{-1} for the $x = 0.5$ compound.[36] $Tb_2Fe_{16}Cr$ possesses a minimum value of $\alpha_v = -5.28 \times 10^{-6}$ K^{-1} in the temperature range 292–511 K,[35] whereas $Gd_2Fe_{16}Cr$ has minimum $\alpha_v = -7.03 \times 10^{-6}$ K^{-1} in the temperature range 294–454 K.[34] Possessing a lower NTE coefficient[33] and having T_C (330 K) higher than the room temperature among the R_2Fe_{17} compounds, Ho_2Fe_{17} may be a good starting material for finding a magnetic ZTE material operative at room temperature. In this paper, we study the effect of Cr-substitution on the NTE and the magnetic behavior of a R_2Fe_{17}-type compound, Ho_2Fe_{17}. Our study suggests that $Ho_2Fe_{16}Cr$, with a high T_C, is a ZTE material having a low coefficient of thermal expansion ($\alpha_v = 1.3 \times 10^{-6}$ K^{-1}) over a wide range of temperature (13–330 K).

2 Experimental procedure

$Ho_2Fe_{17-x}Cr_x$ (x = 0, 1, 2) compounds were prepared by the method of arc-melting (in an argon atmosphere) with at least 99.9% pure starting materials. The ingots were re-melted five to six times to ensure homogeneity. The samples were annealed in a vacuum sealed quartz tube at 1173 K for 7 days, followed by quenching in ice water. The room temperature powder X-ray diffraction (XRD) patterns of the samples were taken using CuK_α radiation in a TTRAX III diffractometer (M/S Rigaku Corp., Japan). The XRD patterns at different temperatures (13–515 K) were recorded using the same instrument, with a very low scan speed (0.01° steps, and 0.4° min^{-1}) for a better statistical average. This is necessary in our case as our sample contains more than 85% Fe and the Cu K_α radiation is in the absorption edge of Fe. The magnetization was measured using SQUID VSM and PPMS evercool-II (M/S Quantum Design, Inc., USA) from 4–380 K. High temperature VSM (Model EV9, M/S MicroSense, LLC Corp., USA) was employed to measure the magnetization from 300–550 K.

3 Results and discussion

Fig. 1 [left panel] shows the room temperature XRD data of the $Ho_2Fe_{17-x}Cr_x$ compounds. The data show that all the samples

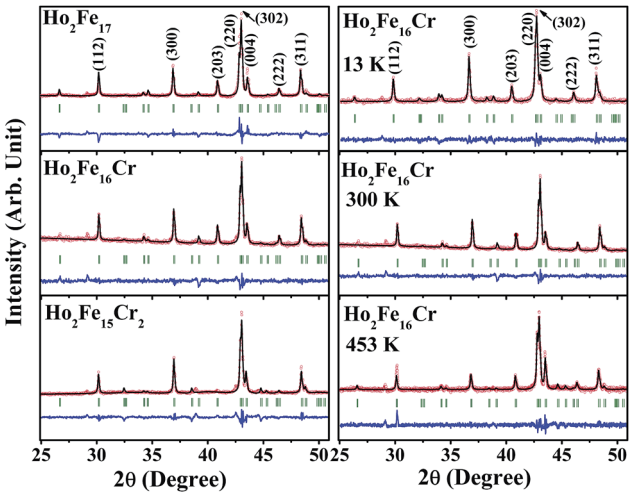

Fig. 1 [Left panel] Room temperature XRD pattern of $Ho_2Fe_{17-x}Cr_x$ (x = 0, 1, 2) compounds. [Right panel] XRD patterns of $Ho_2Fe_{16}Cr$ at T = 13 K, 300 K and 453 K. Red circles depict the experimentally observed data points, the black lines are data generated using FullProf software, and the blue lines are the differences between the estimated and experimentally observed data points. The olive bars are the Bragg positions allowed by the space group.

form in a single phase with a hexagonal Th_2Ni_{17}-type structure (space group: $P6_3/mmc$). Miller indices (hkl) for the major set of crystallographic planes have been shown in the figure. Fig. 1 [right panel] shows the XRD pattern of $Ho_2Fe_{16}Cr$ at three temperatures, namely, 13 K, 300 K, and 453 K. The XRD data suggest that the compound remains in a single phase with the Th_2Ni_{17}-type structure in the temperature range of measurement. This is consistent for other $Ho_2Fe_{17-x}Cr_x$ compounds (x = 0, 2). Lattice parameters (a, c) of each sample at different temperatures have been estimated by analyzing XRD patterns.

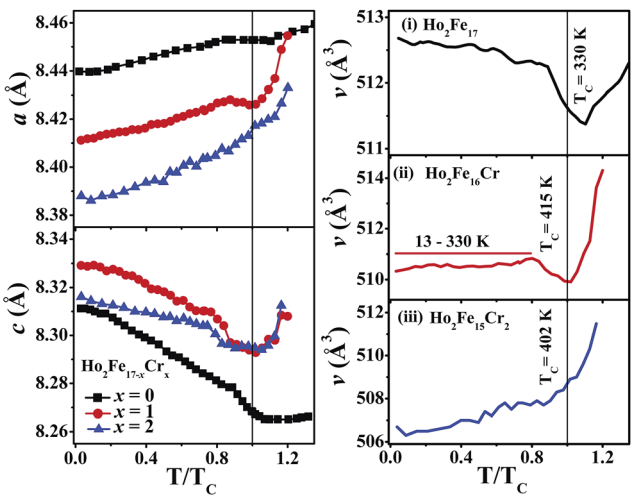

Fig. 2 [Left panel] Lattice parameters a and c and [Right panel] unit cell volume v of $Ho_2Fe_{17-x}Cr_x$ (x = 0, 1, 2) compounds (vertical line in both left and right panel corresponds to T/T_C = 1). Data for the parent compound (x = 0) has been taken from ref. 41.

Fig. 2 [left panel] shows the effect of Cr substitution on the lattice parameters (a, c) and [right panel] the lattice volume v of the $Ho_2Fe_{17-x}Cr_x$ (x = 0, 1, 2) compounds. We observe that the thermal expansion of any of the $Ho_2Fe_{17-x}Cr_x$ compounds is anisotropic like the parent R_2Fe_{17} compounds[33] and their derivatives,[34–36] *i.e.*, a increases while c decreases with increasing temperature. The decrease in c with increasing temperature results from MVE. In R_2Fe_{17} compounds, with a hexagonal Th_2Ni_{17} structure for heavy rare earths (rhombohedral Th_2Zn_{17} structure for light rare earths), the crystallographic sites for the Fe atoms are 4f(6c), 6g(9d), 12j(18f), and 12k(18h) sites.[39] As the distance between the Fe atoms at 4f(6c) sites is very short (<0.244 nm)[36] (Fig. 3), the direct exchange between these atoms gives rise to antiferromagnetic (AFM) coupling, while the rest of the atoms are coupled ferromagnetically. Therefore, a large amount of magnetic energy is stored along the Fe–Fe distance between the atoms at 4f(6c) sites, and this magnetic energy can be reduced by increasing said distance, which is dependent only on the parameter c.[40] Finally, a compromise is obtained between the magnetic energy and the elastic energy by increasing the lattice volume for the magnetic state at a lower temperature. If Cr atoms are substituted for Fe atoms in R_2Fe_{17} compounds, Cr atoms prefer to occupy 4f(6c) sites.[36] As the magnetic moment of a Cr atom is less than that of an Fe atom, such substitution will reduce the effective MVE, and consequently weaken the NTE below T_C.

The Curie temperature (T_C) for each of the $Ho_2Fe_{17-x}Cr_x$ (x = 0, 1, 2) compounds has been determined from the magnetization (M) curve plotted as a function of temperature at a magnetic field of H = 0.05 T (Fig. 4 [left panel]). The data shows that the T_C of $Ho_2Fe_{16}Cr$ is 415 K, higher than that (326 K) of the parent compound, whereas the T_C (402 K) of $Ho_2Fe_{15}Cr_2$ is lower than that of $Ho_2Fe_{16}Cr$. The Cr-substitution enhances T_C substantially for a lower concentration of Cr, and then T_C decreases at higher concentrations. Similar behavior has also been observed for other Cr-substituted R_2Fe_{17} compounds.[34–36]

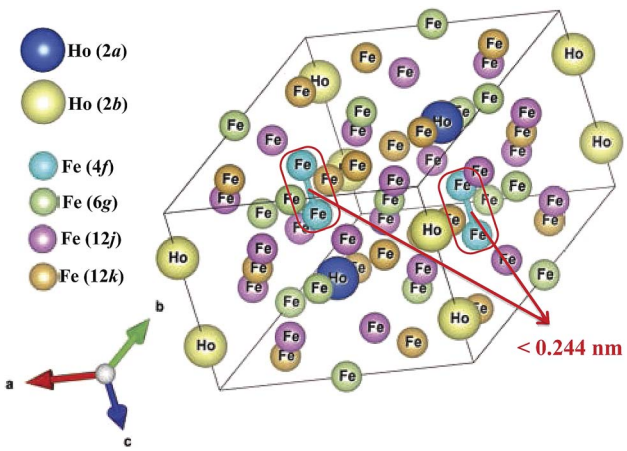

Fig. 3 Th_2Ni_{17} – type crystal structure (space group: $P6_3/mmc$) of Ho_2Fe_{17} compound. Short distances between Fe atoms at 4f sites (highlighted by red boxes) are responsible for the magneto-volume effect.

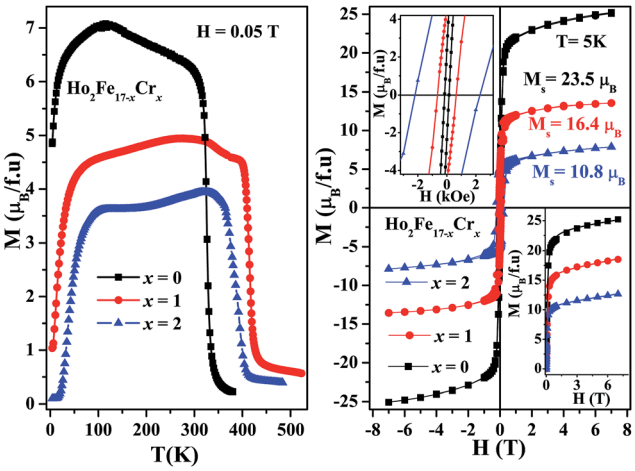

Fig. 4 [Left panel] Magnetization as a function of temperature at a magnetic field of H = 0.05 T, [Right panel] magnetization as a function of magnetic field at T = 5 K for $Ho_2Fe_{17-x}Cr_x$ (x = 0, 1, 2) compounds. The lower inset of [Right panel] shows the virgin curves with the fit of eqn (3), and the upper inset of [Right panel] shows the central part of each M–H curve.

The modification of T_C due to Cr substitution has been explained by the preference of the magnetically weaker Cr atoms to replace Fe atoms at 4f(6c) sites.[36] The strength of the Fe(Cr)–Fe(Cr) interactions in the 3d-sublattice determines the value of T_C in the $R_2Fe_{17-x}Cr_x$ compounds.[36] In the parent compound R_2Fe_{17}, the Fe atoms at the 4f(6c) sites are coupled antiferromagnetically, while the rest of the atoms are coupled ferromagnetically. The Cr atoms at 4f(6c) sites reduce the interactions between 4f(6c) and other crystal sites (4f(6c), 6g(9d), 12j(18f), and 12k(18h)). At lower concentrations of Cr, the strength of the AFM interactions between 4f(6c)–4f(6c) sites reduces much more strongly than the ferromagnetic (FM) interactions between 4f(6c)-other sites.[36] This results in an enhancement in the total FM interactions in the 3d-sublattice and a subsequent increase in T_C. For higher concentrations of Cr, the reduction of FM interactions has been argued to surpass that of AFM interactions causing a decrease in total FM strength of the 3d-sublattice, and an associated lowering of T_C. A similar feature of T_C dependence on the Cr-concentration has also been observed in Fe–Cr alloys,[42] where through experimental as well as computational studies, it was shown that the T_C of the Fe–Cr alloy (up to 6 at% Cr-substitution) is higher than that of pure Fe. The coercive field (H_c) also increases with increasing Cr concentration. Materials with a high coercive field possess a high value of maximum energy product (BH_{max}), a necessary

Table 1 T_C, M_S and H_c of $Ho_2Fe_{17-x}Cr_x$ (x = 0, 1, 2)

Sample name	T_C (in K)	M_S (in μ_B per f.u)	H_c (in Oe)
Ho_2Fe_{17}	330	23.5	175
$Ho_2Fe_{16}Cr$	415	16.4	720
$Ho_2Fe_{15}Cr_2$	402	10.8	2300

criterion for permanent magnetic materials. The values of T_C, M_S and H_c of $Ho_2Fe_{17-x}Cr_x$ ($x = 0, 1, 2$) are shown in Table 1.

According to the Stoner–Edwards–Wohlfarth (SEW) theory,[43] in the absence of any external magnetic field, the volume strain (ω_S) arising from MVE at a temperature T is

$$\omega_S = \frac{\kappa C}{v} {M_0}^2 \quad (1)$$

where M_0 is the spontaneous magnetic moment, κ is the compressibility, and C is the magneto-volume coupling constant. Moriya and Usami modified eqn (1) by including the contribution of spin fluctuations to the free energy as[43]

$$\omega_S = \frac{\kappa C}{v}\left[{M_0}^2 + \xi^2(T)\right] \quad (2)$$

where $\xi^2(T)$ represents the average of the squared thermal spin fluctuation amplitude. The volume strain due to MVE is proportional to the square of M_0. The Cr-substitution reduces the value of M_0. This is evident from Fig. 4 [right panel], where we observe that the saturation magnetization (M_S), which is a measure of M_0, decreases with increasing Cr-concentration. M_S has been estimated by fitting the virgin M–H curve of each sample with the expression[44]

$$M = M_S\left(1 - \frac{A}{H} - \frac{B}{H^2}\right) + \chi H \quad (3)$$

that describes the law of approach to saturation (where A, B and χ are constants). As M_0 decreases with increasing Cr-concentration, so also ω_S decreases.

Fig. 2 [left panel] shows that $a(T)$ is lower for a higher concentration (x) of Cr. This observation can be explained by the smaller ionic size of Cr than Fe,[36] and the fact that MVE does not alter a much. However, Cr is positioned in the left side of the same row of Fe in the periodic table, and it suggests that Cr possesses a larger crystal or ionic radius than that of Fe.[45] It may be pointed out that such understanding holds well when both the ions possess the same valence as well as identical spin state (high-spin or low-spin).[45] Moreover, in two different crystal environments, if the site coordination numbers differ, the same element in a particular valence state may assume two different ionic radii.[45] Reduction of the lattice parameter a has also been found for other members of the $R_2Fe_{17-x}Cr_x$ series.[34–36,46–48] Even for Mn, placed also like Cr on the left side of Fe in the periodic table, similar reduction in a has been found with increasing x, in $R_2Fe_{17-x}Mn_x$.[49,50] A better understanding of the fact can be obtained from the neutron diffraction study of $Nd_2Fe_{17-\delta}Cr_\delta$ ($\delta = 0, 0.5, 1, 1.9$).[47] The study suggests that Cr prefers to occupy 6c, and with the introduction of Cr, 6c–6c, 6c–18h, and 6c–18f bond lengths reduce continuously with increasing δ, while 6c–9d bond length remains almost constant. Considering such reduction in different bond lengths with the introduction of Cr, one may conclude that the ionic size of Cr is less than Fe in the same site of the $R_2Fe_{17-x}Cr_x$ lattice. The reduction of the mentioned bond lengths is an experimental observation, but the underlying reason lies within the valence as well as the spin states of two (Fe, Cr) ions and finally the crystalline environment. Here, MVE does not alter a much. The lattice parameter $c(T)$ for $Ho_2Fe_{16}Cr$ is higher than that of the parent compound even above T_C. This occurs because the strain along the c-axis arising from MVE is not only higher in the parent compound than $Ho_2Fe_{16}Cr$, but also more than the change in the c parameter obtained by just replacing one Fe atom by a Cr atom in Ho_2Fe_{17}. The higher value of $c(T)$ for $Ho_2Fe_{16}Cr$, even above T_C, suggests that the effect of spin fluctuation is important in this system. A similar conclusion can also be drawn from the observation of NTE in the parent compound below 365 K,[41] which is higher than T_C = 330 K (Fig. 2 [right panel]). For $Ho_2Fe_{15}Cr_2$, the reduction of $c(T)$ due to further replacement of one more Fe atom by a Cr atom overcompensates the change in the same due to reduction of MVE, and therefore, $c(T)$ reduces compared to $Ho_2Fe_{16}Cr$.

Fig. 2 [right panel] shows the unit cell volume $v(T)$ of $Ho_2Fe_{17-x}Cr_x$ ($x = 0, 1, 2$). The parent compound Ho_2Fe_{17} shows NTE in the temperature range 295–365 K with α_v lying in the range $(1.3–3.7) \times 10^{-5}$ K^{-1}.[41] The parent compound appears to be a strong magnetostrictive material. In comparison with the parent compound, in $Ho_2Fe_{16}Cr$, Cr-substitution increases T_C and weakens NTE. For $Ho_2Fe_{16}Cr$, NTE is observed in the range T = 330–425 K with $\alpha_v = -4.3 \times 10^{-6}$ K^{-1}. However, the most interesting feature of $Ho_2Fe_{16}Cr$ is the negligible thermal expansion of the unit cell over a wide range of temperature (13–330 K) including room temperature. In this temperature range, the magneto-volume strain compensates for the lattice volume strain, and $Ho_2Fe_{16}Cr$ behaves as a single component ZTE material with $\alpha_v = 1.3 \times 10^{-6}$ K^{-1}. By further increasing the Cr concentration NTE disappears, *i.e.*, we do not observe any NTE for $Ho_2Fe_{15}Cr_2$.

The temperature dependence of the spontaneous linear magnetostrictive deformation in the basal plane, $\lambda_a = (a_m - a_p)/a_p$, that along the c-axis $\lambda_c = (c_m - c_p)/c_p$, and the spontaneous volume magnetostrictive deformation $\omega_S = (v_m - v_p)/v_p$[36] are important parameters for identifying the strength and the nature of magnetoelastic coupling. a_m, c_m, and v_m are the experimentally measured values of a, c and v, whereas a_p, c_p, and v_p are the corresponding values obtained by extrapolation[36] from the paramagnetic state using the Grüneisen relation, $\alpha = \frac{1}{v}\frac{\gamma C_v}{\kappa}$, $C_v(T) = \mathscr{R}(T/\theta_D)^3 \int_0^{\theta_D/T} x^4 e^x/(e^x - 1)^2 dx$, where θ_D is the Debye temperature and $\mathscr{R}$ is the molar gas constant. The value of θ_D has been taken as 400 K, estimated earlier[51] for R_2Fe_{17} compounds other than Y_2Fe_{17}. The parameters a_m, c_m, and v_m along with a_p, c_p, and v_p are presented in Fig. 5 for the compound $Ho_2Fe_{16}Cr$. λ_a, λ_c and ω_S have been plotted as a function of temperature in Fig. 6(a)–(c) respectively.

Although it has been suggested that the free energy in the magnetic state can be reduced by changing the dimension along the c-axis only,[52] our experimental data show a finite λ_a for both the samples $Ho_2Fe_{17-x}Cr_x$ (x = 1 or 2) *i.e.*, the magneto-elastic effect also changes a. Moreover, the larger value of λ_c than λ_a in each case suggests that the magnetoelastic effect along the c-axis is stronger than that in the basal plane. As evident from Fig. 6(c), the value of ω_S is considerably high at low temperatures, and it is non-zero above T_C. Thus $Ho_2Fe_{17-x}Cr_x$ is a strong magnetostrictive

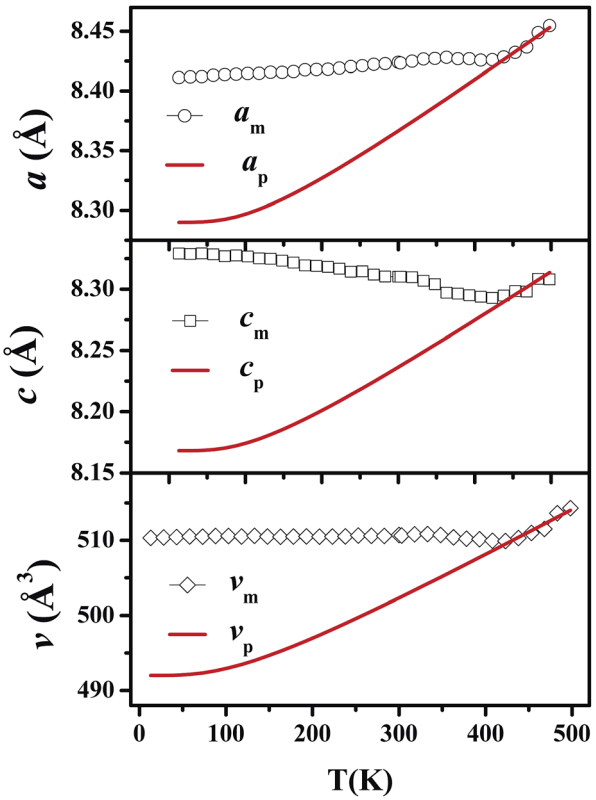

Fig. 5 Temperature dependent lattice parameters *a*, *c* and unit cell volume *v* of the compound $Ho_2Fe_{16}Cr$, extracted from the fitted temperature dependent XRD patterns (denoted by suffix m), and the same parameters extrapolated from the paramagnetic region (denoted by suffix p).

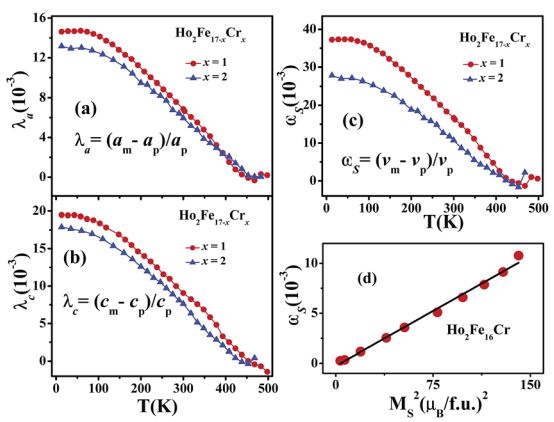

Fig. 6 (a and b) Linear magnetostrictive deformations λ_a, and λ_c, (c) spontaneous volume magnetostrictive deformation ω_S as a function of temperature (*T*) for the $Ho_2Fe_{17-x}Cr_x$ ($x = 1, 2$) compounds. (d) ω_S as a function of M_S^2 for the compound $Ho_2Fe_{16}Cr$.

material in which spin fluctuation plays an important role. Fig. 6(d) shows that ω_S varies linearly with the square of M_S. This is in accordance with eqn (1) and (2), and has been suggested to be a direct experimental proof of the fact that ω_S is related to the MVE.[53]

4 Conclusion

In the search for magnetic ZTE materials, our study shows that Cr-substitution for Fe atoms in Ho_2Fe_{17} weakens the NTE of the parent compound and alters the T_C. $Ho_2Fe_{16}Cr$ behaves as a single component ZTE material in the temperature range 13–330 K. Moreover, the T_C of $Ho_2Fe_{16}Cr$ is 415 K, considerably higher than room temperature. Cr-substitution also increases the coercivity compared to that of the parent compound. Therefore, $Ho_2Fe_{16}Cr$ with a high T_C, moderate coercivity and very low thermal expansion is a potential material for a permanent magnet.

Acknowledgements

Shovan Dan and S. Mukherjee thank UGC for financial support in the form of major project (MRP-MAJOR-PHYS-2013-16282). The work at SINP was carried out under CMPID-DAE Project.

References

1 J. R. Salvador, F. Guo, T. Hogan and M. G. Kanatzidis, *Nature*, 2003, **425**, 702–705.
2 S. Margadonna, K. Prassides and A. N. Fitch, *J. Am. Chem. Soc.*, 2004, **126**, 15390–15391.
3 K. J. Miller, C. P. Romao, M. Bieringer, B. A. Marinkovic, L. Prisco and M. A. White, *J. Am. Ceram. Soc.*, 2013, **96**, 561–566.
4 P. Hu, J. Chen, J. Deng and X. Xing, *J. Am. Chem. Soc.*, 2010, **132**, 1925–1928.
5 K. Takenaka and H. Takagi, *Appl. Phys. Lett.*, 2009, **94**, 131904.
6 T. Suzuki and A. Omote, *J. Am. Ceram. Soc.*, 2006, **89**, 691–693.
7 M. van Schilfgaarde, I. A. Abrikosov and B. Johansson, *Nature*, 1999, **400**, 46–49.
8 M. Shiga, *Curr. Opin. Solid State Mater. Sci.*, 1996, **1**, 340–348.
9 L. Hu, J. Chen, L. Fan, Y. Ren, Y. Rong, Z. Pan, J. Deng, R. Yu and X. Xing, *J. Am. Chem. Soc.*, 2014, **136**, 13566–13569.
10 W. Wang, R. Huang, W. Li, J. Tan, Y. Zhao, S. Li, C. Huang and L. Li, *Phys. Chem. Chem. Phys.*, 2015, **17**, 2352–2356.
11 W. Li, R. Huang, W. Wang, Y. Zhao, S. Li, C. Huanga and L. Li, *Phys. Chem. Chem. Phys.*, 2015, **17**, 5556–5560.
12 S. Li, R. Huang, Y. Zhao, W. Wanga and L. Li, *Phys. Chem. Chem. Phys.*, 2015, **17**, 30999–31003.
13 K. Takenaka, *Sci. Technol. Adv. Mater.*, 2012, **13**, 013001–013012.
14 H. Li, S. Liu, L. Chen, J. Zhao, B. Chen, Z. Wang, J. Meng and X. Liu, *RSC Adv.*, 2015, **5**, 1801–1807.
15 C. Verdon and D. C. Dunand, *Scr. Mater.*, 1997, **36**, 1075–1080.
16 A. Matsumoto, K. Kobayashi, T. Nishio and K. Ozaki, *Mater. Sci. Forum*, 2003, **426–432**, 2279–2284.
17 L. Ding, C. Wang, Y. Na, L. Chu and J. Yan, *Scr. Mater.*, 2011, **65**, 687–690.
18 X. Yan, J. Miao, J. Liu, X. Wu, H. Zou, D. Sha, J. Ren, Y. Dai, J. Wang and X. Cheng, *J. Alloys Compd.*, 2016, **677**, 52–56.

19 X. Shan, R. Huang, Y. Han, C. Huang, X. Liu, Z. Lu and L. Li, *J. Alloys Compd.*, 2016, **662**, 505–509.
20 G. D. Barrera, J. A. O. Bruno, T. H. K. Barron and N. L. Allan, *J. Phys.: Condens. Matter*, 2005, **17**, R217–R252.
21 T. A. Mary, J. S. O. Evans, T. Vogt and A. W. Sleight, *Science*, 1996, **272**, 90–92.
22 F. H. Gillery and E. A. Bush, *J. Am. Ceram. Soc.*, 1959, **42**, 175–177.
23 A. E. Phillips, A. L. Goodwin, G. J. Halder, P. D. Southon and C. J. Kepert, *Angew. Chem., Int. Ed.*, 2008, **47**, 1396–1399.
24 T. Chatterji, T. C. Hansen, M. Brunelli and P. F. Henry, *Appl. Phys. Lett.*, 2009, **94**, 241902.
25 M. P. Attfield, M. Feygenson, J. C. Neuefeind, T. E. Proffen, T. C. A. Lucas and J. A. Hriljac, *RSC Adv.*, 2016, **6**, 19903–19909.
26 T. Matsuda, J. Kimb and Y. Moritomo, *RSC Adv.*, 2011, **1**, 1716–1720.
27 Y. Cheng, Y. Liang, X. Ge, X. Liu, B. Yuan, J. Guo, M. Chao and E. Lianga, *RSC Adv.*, 2016, **6**, 53657–53661.
28 M. Azuma, W. Chen, H. Seki, M. Czapski, S. Olga, K. Oka, M. Mizumaki, T. Watanuki, N. Ishimatsu, N. Kawamura, S. Ishiwata, M. G. Tucker, Y. Shimakawa and J. P. Attfield, *Nat. Commun.*, 2011, **2**, 347.
29 A. Pandey, C. Mazumdar, R. Ranganathan, S. Tripathi, D. Pandey and S. Dattagupta, *Appl. Phys. Lett.*, 2008, **92**, 261913.
30 M. Hayase, M. Shiga and Y. Nakamura, *J. Phys. Soc. Jpn.*, 1973, **34**, 925–933.
31 K. Sumiyama, M. Shiga, M. Morioka and Y. Nakamura, *J. Phys. F: Met. Phys.*, 1979, **9**, 1665–1677.
32 H. Nakamura, H. Wada, K. Yoshimura, M. Shiga, Y. Nakamura, J. Sakurai and Y. Komura, *J. Phys. F: Met. Phys.*, 1988, **18**, 981–991.
33 P. A. Alanso, *Doctoral Thesis*, University of Oviedo, Spain, 2011.
34 H. Yan-Ming, T. Ming, W. Wei and W. Fang, *Chin. Phys. B*, 2010, **19**, 067502.
35 Y. Hao, M. Zhao, Y. Zhou and J. Hu, *Scr. Mater.*, 2005, **53**, 357–360.
36 Y. Hao, X. Zhang, B. Wang, Y. Yuang and F. Wang, *J. Appl. Phys.*, 2010, **108**, 023915.
37 K. Takenaka and H. Takagi, *Appl. Phys. Lett.*, 2005, **87**, 261902.
38 X. Peng, J. Chen, K. Lin, L. Fan, Y. Rong, J. Deng and X. Xing, *RSC Adv.*, 2016, **6**, 32979–32982.
39 J. L. Wang, S. J. Campbell, O. Tegus, C. Marquina and M. R. Ibarra, *Phys. Rev. B: Condens. Matter Mater. Phys.*, 2007, **75**, 174423.
40 D. Givord and R. Lemaire, *IEEE Trans. Magn.*, 1974, **10**, 109–113.
41 J. L. Wang, A. J. Studer, S. J. Kennedy, R. Zeng, S. X. Dou and S. J. Campbell, *J. Appl. Phys.*, 2012, **111**, 07A911.
42 M. Y. Lavrentiev, K. Mergia, M. Gjoka, D. Nguyen-Manh, G. Apostolopoulos and S. L. Dudarev, *J. Phys.: Condens. Matter*, 2012, **24**, 326001.
43 Y. Takahashi, Spin Fluctuation Theory of Itinerant Electron Magnetism, *Springer Tracts in Modern Physics*, Springer-Verlag, Berlin Heidelberg, 2013, p. 253.
44 B. D. Cullity and C. D. Graham, *Introduction to Magnetic Materials*, IEEE Press, Wiley, 2008.
45 R. D. Shannon, *Acta Crystallogr., Sect. A: Cryst. Phys., Diffr., Theor. Gen. Crystallogr.*, 1976, **32**, 751–767.
46 X. C. Kou, F. R. de Boer, R. Grssinger, G. Wiesinger, H. Suzuki, H. Kitazawa, T. Takamasu and G. Kido, *J. Magn. Magn. Mater.*, 1998, **177–181**, 1002–1007.
47 E. Girt, Z. Altounian and J. Yang, *J. Appl. Phys.*, 1997, **81**, 5118–5120.
48 I. Nehdi, L. Bessais, C. D. -Mariadassou, M. Abdellaoui and H. Zarrouk, *J. Alloys Compd.*, 2003, **351**, 24–30.
49 P. C. Ezekwenna, G. K. Marasinghe, W. J. James, O. A. Pringle, G. J. Long, H. Luo, Z. Hu, W. B. Yelon and P. I. Hritier, *J. Appl. Phys.*, 1997, **81**, 4533.
50 Y. Wang, F. Yang, C. Chen, N. Tang, P. Lin and Q. Wang, *J. Appl. Phys.*, 1998, **84**, 6229–6232.
51 A. V. Andreev, A. V. Deryagin, S. M. Zadvorkin, N. V. Kudrevatykh, R. H. Levitin, V. N. Moskalev, Y. F. Popov and R. Y. Yumaguzhin, *Fizika Magnitnykh Materialov, Physics of Magnetic Materials*, ed. D. D. Mishin, Kalinin University, Kalinin, USSR, 1985, p. 21, in Russian.
52 D. Givord, R. Lemaire, W. J. James, J.-M. Moreau and J. S. Shah, *IEEE Trans. Magn.*, 1971, **7**, 657–659.
53 J. Chen, L. Hu, J. Deng and X. Xing, *Chem. Soc. Rev.*, 2015, **44**, 3522–3567.

Journal of Physics and Chemistry of Solids 115 (2018) 92–96

Contents lists available at ScienceDirect

Journal of Physics and Chemistry of Solids

journal homepage: www.elsevier.com/locate/jpcs

Thermal expansion properties of $Ho_2Fe_{16.5}Cr_{0.5}$

Shovan Dan [a], S. Mukherjee [a,*], Chandan Mazumdar [b], R. Ranganathan [b]

[a] Department of Physics, The University of Burdwan, Burdwan, 713104, India
[b] Condensed Matter Physics Division, Saha Institute of Nuclear Physics, 1/AF, Bidhannagar, Kolkata, 700064, India

ARTICLE INFO

Keywords:
A: intermetallic compounds
C: X-ray diffraction
D: Crystal structure
Magnetic properties
Thermal expansion

ABSTRACT

We report the thermal expansion behavior of $Ho_2Fe_{16.5}Cr_{0.5}$ compound in the range of temperature 13–483 K, using structural parameters obtained by analyzing temperature dependent x-ray diffraction (XRD) patterns. From 13 K to 300 K, the compound shows negligible thermal expansion having the coefficient of volume expansion (α_V) $\sim 10^{-6}\,K^{-1}$. The thermal expansion behavior of the studied compound can be explained by the role of magnetovolume effect (MVE) below ferrimagnetic ordering temperature (394 K), in addition to normal phononic contribution. Fe sublattice contribute to MVE, whereas both the rare earth and Fe sublattice determine the value of saturation magnetization.

1. Introduction

Our common experience says that most of the materials expand on heating. Such positive thermal expansion (PTE) is related to the crystal structure and can be explained by the anharmonic vibration of crystal lattice [1]. Moreover, the electronic structure [2], microstructure and defect also play an important role to determine the thermal expansion property of a material [3]. The usage of PTE materials as components causes inconvenience in various fields of application, namely, gigantic buildings, bridges, railway tracks, standard rulers, precision instruments, electronic devices, power cables, thin films *etc.* [1] In such cases, we require zero thermal expansion (ZTE) materials with a very low coefficient of thermal expansion. Due to extensive research in the recent past, a number of materials have been identified as ZTE materials [4–14]. Although rare, there are a few materials which contract on heating on a particular range of temperature, and these negative thermal expansion (NTE) materials are often used as starting materials of the ZTE one [1,15,16]. In fact the property or mechanism responsible for NTE is tuned to achieve ZTE. The mechanism responsible for diverse categories of NTE materials like, tungstates [17], silicates [18], cyanides [19], invar materials [7,8], oxide perovskites [20,21], intermetallic anti-perovskites [22,23] *etc.* are not unique. As an example, tetragonal structure of $PbTiO_3$ is responsible for NTE, and ZTE compound $0.8PbTiO_3$-$0.2BiNi_{0.5}Ti_{0.5}O_3$ is derived from the parent compound by weakening the tetragonality using dopant $BiNi_{0.5}Ti_{0.5}O_3$ [20]. Magnetic NTE materilas are rare, and their NTE behavior originates from the magnetovolume effect (MVE). R_2Fe_{17} compounds (R - rare earth elements) [24,25] and some of its substituted derivatives [26–29] are such NTE materials.

The crystal structure of the R_2Fe_{17} compounds is hexagonal Th_2Ni_{17} type for heavier rare earths (and rhomohedral Th_2Zn_{17} for lighter rare earths) [25,30]. The crystallographic sites for the Fe atoms are 4*f* (6*c*), 6*g*(9*d*), 12*j*(18*f*), and 12*k*(18*h*) [30]. All the Fe atoms in the compound are coupled ferromagnetically except the atoms at 4*f*(6*c*) site due to short Fe-Fe distance [24–29,31–36]. Below the Curie temperature (T_C) the magnetic energy is reduced by increasing the Fe(4*f*/6*c*)-Fe(4*f*/6*c*) distance with a subsequent increase in the lattice parameter *c*, and such reduction in magnetic energy surpasses the increase in elastic energy [37,38]. Cr substitution at the Fe site reduces the effective MVE and subsequently weakens the NTE below T_C [29]. The effect of Cr substitution on the thermal expansion behavior in Tb_2Fe_{17} [27], Tm_2Fe_{17} [28], Gd_2Fe_{17}, [26] and Ho_2Fe_{17} [29] has been reported. Ho_2Fe_{17} is a NTE material with high negative coefficient of volume expansion (α_V) [$-(1.3–3.7)\times 10^{-5}\,K^{-1}$] in the range T = 265–365 K [31]. $Ho_2Fe_{16}Cr$ behaves as a ZTE material with $\alpha_V = 1.3\times 10^{-6}\,K^{-1}$ in the range T = 13–330 K, whereas the same material shows NTE behavior with small $\alpha_V = -4.3\times 10^{-6}\,K^{-1}$ in the range 330–425 K [29]. By substituting two Fe atoms by Cr atoms, we observe that the NTE behavior of the parent compound disappears completely. Therefore, we observe that by tuning the Cr concentration, one can modify the thermal expansion properties of $Ho_2Fe_{17-x}Cr_x$ compounds considerably. This motivates us to study the thermal expansion property of $Ho_2Fe_{16.5}Cr_{0.5}$ compound to find out whether one can have a ZTE material better than $Ho_2Fe_{16}Cr$. In order to correlate our data related to thermal expansion with the existing theoretical picture, we have also carried out the requisite structural and magnetic studies.

* Corresponding author.
E-mail address: sanseb68@yahoo.co.in (S. Mukherjee).

https://doi.org/10.1016/j.jpcs.2017.12.017
Received 6 November 2017; Received in revised form 2 December 2017; Accepted 10 December 2017
Available online 13 December 2017

2. Experimental

$Ho_2Fe_{16.5}Cr_{0.5}$ was prepared using a water cooled copper hearth in an arc-furnace with flowing argon atmosphere. Starting materials were taken with at least 99.9% purity. The ingots were re-melted several times, flipping after every melting to ensure homogeneity. The sample was annealed in a vacuum sealed quartz tube at 1173 K for 7 days, followed by quenching in ice-water. The room temperature powder x-ray diffraction (XRD) pattern of the sample was taken using CuK_α radiation in a 9 kW TTRAX III diffractometer (M/S Rigaku Corp., Japan). The XRD patterns at different temperatures in the temperature range 13–483 K were recorded using the same instrument, with a very low scan speed (0.01° steps, and 0.4° min^{-1}) to ensure a better statistical average. This is necessary in our case as the material contains more than 85% Fe and the CuK_α radiation lies close to the absorption edge of iron. The magnetization (M) was measured using Evercool-II PPMS system (M/S Quantum Design, Inc., USA) in the temperature range T = 4–350 K. High temperature VSM (model: EV9, M/S MicroSense, LLC Corp., USA) was employed to measure M(T) above 300 K. In PPMS one can measure M(T) under both zero field cooled (ZFC) and field cooled (FC) protocol, whereas high temperature VSM can measure M(T) using ZFC protocol only.

3. Results and discussion

3.1. Structure

The XRD data taken at different temperatures in the range of T = 13–483 K have been analyzed through full Rietveld method using FullProf software package [39]. Fig. 1 shows the XRD patterns of $Ho_2Fe_{16.5}Cr_{0.5}$ at three representative temperatures, *viz.*, 13 K, 300 K and 453 K. The patterns suggest that the material forms in hexagonal Th_2Ni_{17} type structure (space group: $P6_3/mmc$, # 194) and remains in single phase without altering the space group throughout the temperature range of measurement. **Although some of the peaks of rather weak intensities, *e.g.*, the (212) Bragg peak appear to have diminishing intensities with the raising of temperature** (Fig. 1), **most likely it is an effect of peak-broadening with the increase in temperature.** Detailed structural parameters with reliability factors of the Rietveld refined XRD pattern taken at 300 K have been listed in Table 1. The deduced parameters are found to be in conformity with those reported in the literature for Ho_2Fe_{17}.

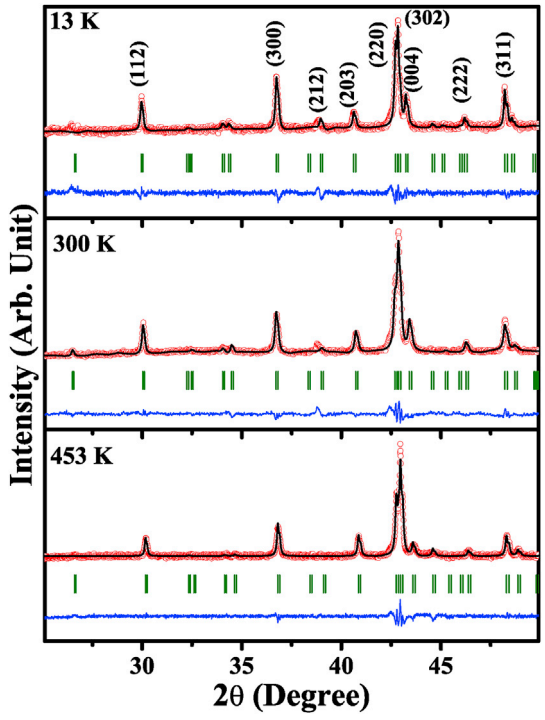

Fig. 1. XRD patterns of $Ho_2Fe_{16.5}Cr_{0.5}$ compound at T = 13 K, 300 K and 453 K. Red circles depict the experimentally observed data points, the black lines are the data generated using FullProf software, and the blue lines are the differences between the estimated and experimentally observed data points. The olive bars are the Bragg Positions allowed by the space group. (For interpretation of the references to color in this figure legend, the reader is referred to the Web version of this article.)

Table 1
Structural parameters and reliability factors obtained after Rietveld refinement of the room-temperature XRD data for the compound $Ho_2Fe_{16.5}Cr_{0.5}$.

Atom site	x	y	z
Ho (2*a*)	0	0	0.25
Ho (2*b*)	1/3	2/3	0.75
Fe/Cr (4*f*)	1/3	2/3	0.106 (7)
Fe/Cr (6*g*)	0.5	0	0
Fe/Cr (12*j*)	0.322 (3)	0.974 (2)	0.25
Fe/Cr (12*k*)	0.169 (5)	0.329 (6)	0.989 (5)
$a = b$ (Å)	8.440 (2)		
c (Å)	8.305 (9)		
R_B: 10.4, R_f: 7.67			

3.2. Magnetization

Fig. 2 shows M(T) measured under ZFC protocol at H = 500 Oe. The sharp rise in M(T) at T_C = 394 K, is associated with a ferrimagnetic transition. Ho_2Fe_{17} is a co-linear ferrimagnetic system in which Ho sublattice is coupled antiferromagnetically with Fe sublattice below T_C = 330 K [29,31]. The fact that T_C increases initially with the substitution of Cr in Ho_2Fe_{17} compound has been discussed in detail in our previous work [29]. The plot showing the increment in T_C with Cr concentration for $Ho_2Fe_{17-x}Cr_x$ system has been shown in Fig. 2 (a). The curve follows the usual nature observed in Cr substituted R_2Fe_{17} compounds, *i.e.* T_C increases with increasing x initially, but decreases finally at higher values of x after reaching a maximum. Fig. 2 (b) shows the behavior of M(T) measured at 500 Oe under both ZFC and FC protocol, although due to the instrumental limitations the upper limit of the temperature remains restricted to 350 K which is slightly below T_C (394 K). The difference between ZFC and FC behavior can be ascribed to magnetohistory effect [40]. Fig. 3 shows the M(H) curves in the range T = 5–350 K, measured upto H = 7 T. Isothermal M(H) curve depicts the presence of spontaneous magnetization below 350 K. The saturation magnetization (M_S), which is

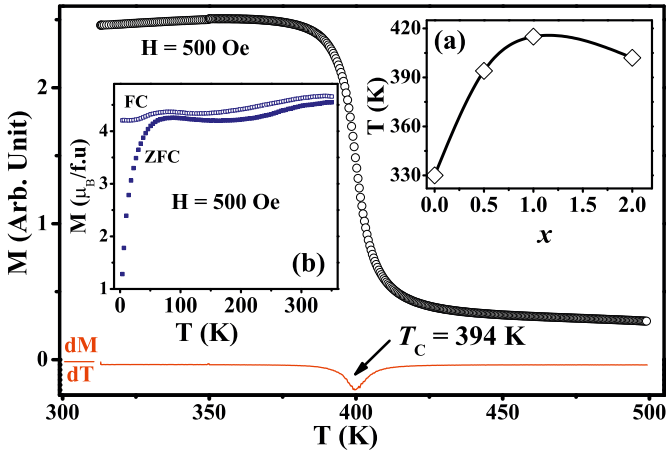

Fig. 2. Magnetization as a function of temperature at a magnetic field of H = 500 Oe for $Ho_2Fe_{16.5}Cr_{0.5}$ under ZFC protocol using the high temperature VSM. Inset (a) shows the variation of T_C with x for $Ho_2Fe_{17-x}Cr_x$ (x = 0, 0.5, 1, 2) (data for x = 0, 1, 2 are taken from Ref. [29]). Inset (b) shows M(T), measured under ZFC and FC protocol of the compound $Ho_2Fe_{16.5}Cr_{0.5}$ at H = 500 Oe, upto T = 350 K using PPMS.

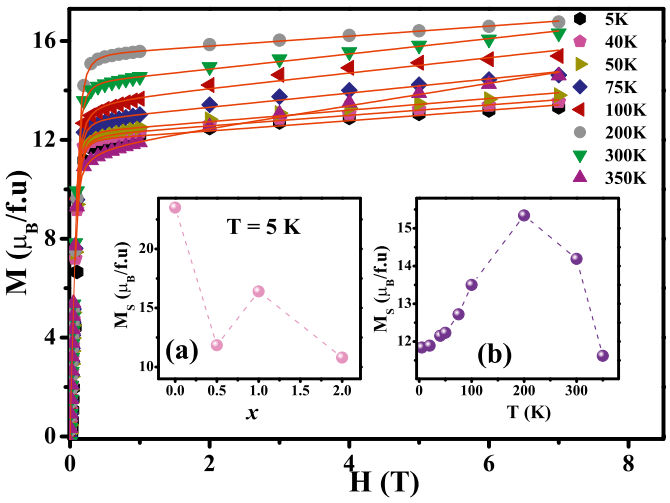

Fig. 3. Virgin magnetization curves as a function of H at different T values for $Ho_2Fe_{16.5}Cr_{0.5}$. Fitted magnetization curves for each temperature using eqn. (1) are shown with red lines. Inset (a) shows the variation of M_S with x for $Ho_2Fe_{17-x}Cr_x$ ($x = 0, 0.5, 1, 2$) (data for $x = 0, 1, 2$ is taken from Ref. [29]). Inset (b) shows M_S as a function of T. Dashed line is guide to the eye. (For interpretation of the references to color in this figure legend, the reader is referred to the Web version of this article.)

a measure of spontaneous magnetization has been determined by using the expression [41]

$$M(H) = M_S\left(1 + \frac{A}{H} + \frac{B}{H^2}\right) - \chi H \quad (1)$$

where A, B and χ are constants. The value of M_S increases with the lowering of temperature and attains a maximum value 16.8 $\mu_B/f.u$ around T = 200 K. Below 200 K, it decreases with the lowering of temperature and reaches 11.8 $\mu_B/f{\cdot}u$at 5 K. The variation of M_S with x is shown in Fig. 3 (a). As the magnetic moment of Cr atom is smaller than that of Fe atom, M_S values should decrease with increasing x. However, our measurement shows an anomalous decrease of M_S at $x = 0.5$. A similar kind of behavior has also been reported in the case of Mn substituted Ho_2Fe_{17} system [31,42]. The anomaly can be attributed to the differences of spontaneous magnetization and saturation magnetization in presence of magnetohistory effect [40].

3.3. Thermal expansion

Fig. 4 shows the temperature dependent behavior of the lattice parameters a, c and unit cell volume v. a_m, c_m and v_m represent respectively the values of a, c and v deduced from the Reitveld refined XRD patterns; and a_p, c_p and v_p are the respective a, c and v data extrapolated from the paramagnetic region. To avoid the precursor effect, we have considered the paramagnetic region slightly above T_C for extrapolation. a_p, c_p and v_p have been obtained by fitting the measured data in the paramagnetic region with Grüneisen relation [1,43] $\alpha_V = \frac{\gamma C_V}{3K_T V}$, γ = Grüneisen parameter, K_T = bulk modulus of elasticity, V = volume of the sample and the specific heat at constant volume $C_V(T) = \mathscr{R}(T/\theta_D)^3 \int_0^{\theta_D/T} x^4 e^x/(e^x - 1)^2 dx$, ($\theta_D$ - Debye temperature, $\mathscr{R}$ - molar gas constant). The value of θ_D has been taken as 400 K as estimated for many members of R_2Fe_{17} compounds except Y_2Fe_{17} [44]. a_m shows a monotonous increase with the increase of temperature, but below T_C, it follows a curve different from a_p. Actually, a_p, c_p and v_p are the values of a, c, v in the absence of MVE. It has been suggested [37] that the MVE affects only the parameter c. However, our measurement shows the effect of MVE in the ab-basal plane also. The same kind of behavior has already been observed in $Ho_2Fe_{17-x}Cr_x$ ($x = 1$ and 2) [29] and other $R_2Fe_{17-x}Cr_x$compounds [26–28]. The effect of MVE is stronger along c-axis, as a result of which c_m continuously decreases with

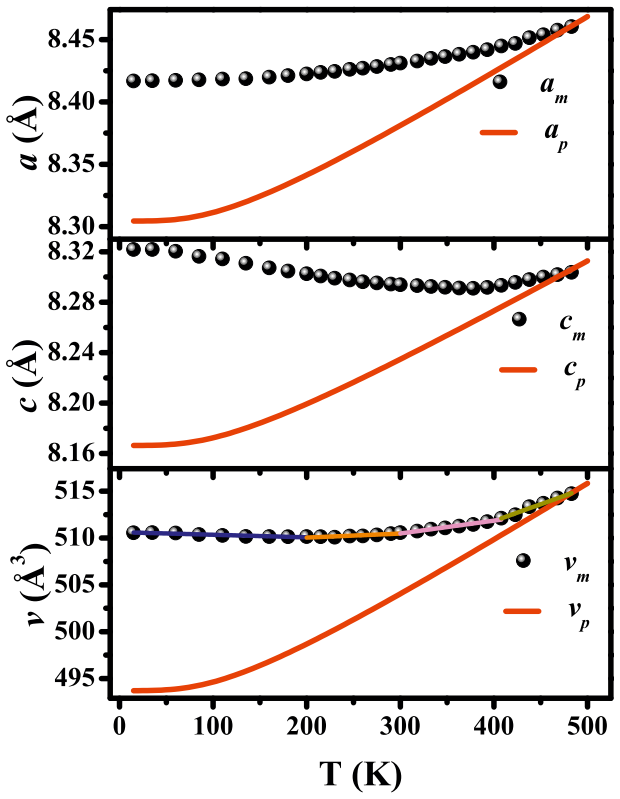

Fig. 4. a_m, c_m and v_m as a function of T, a_p, c_p and v_p as a function of T for $Ho_2Fe_{16.5}Cr_{0.5}$. Solid lines of different colors indicate linear fits of v_m for different temperature regions. (For interpretation of the references to color in this figure legend, the reader is referred to the Web version of this article.)

temperature below T_C. The combined effect on v_m shows a complicated behavior. The temperature dependence of $v_m(T)$ suggest NTE in the range T = 13–200 K and PTE for temperature above 200 K. The average coefficient of thermal expansion (CTE) in different ranges of temperature have been estimated from the linear fit of v_m in those ranges. Average CTEs in different ranges of temperature are shown in Table 2. In the temperature range T = 13–300 K, CTE is found to be of relatively low value. Fig. 5 shows the thermal expansion behavior of $Ho_2Fe_{17-x}Cr_x$ ($x = 0, 0.5, 1, 2$) compounds in a reduced temperature scale. The parent compound shows a prominent NTE behavior in the range T = 265–365 K [31]. For $x = 0.5$, we observe NTE in the range of T = 13–200 K with small α_V. α_V becomes positive above 200 K, but still remains low up to 300 K. For $x = 1$, the compound shows ZTE behavior in the range T = 13–330 K and NTE behavior in the range 330–425 K [29]. The same system for $x = 2$ shows usual PTE behavior in the whole temperature range of measurement [29]. Therefore as a ZTE material, $Ho_2Fe_{16}Cr$ appears to be better than $Ho_2Fe_{16.5}Cr_{0.5}$, considering the operative temperature range and the value of CTE. Thus, Cr substitution weakens NTE of the parent compound, and by tuning the Cr concentration close to 1, one can have a good ZTE material.

λ_a, λ_c and ω_S, defined as $\lambda_a = (a_m - a_p)/a_p$, $\lambda_c = (c_m - c_p)/c_p$ and $\omega_S = (v_m - v_p)/v_p$ are the important parameters related to magnetostrictive deformation [24,25,28]. λ_a and λ_c are the spontaneous linear

Table 2
CTE in different ranges of temperature.

Temperature range	CTE
(in K)	(in K^{-1})
13–200	-5.0×10^{-6}
201–300	8.4×10^{-6}
301–400	2.7×10^{-5}
401–480	7×10^{-5}

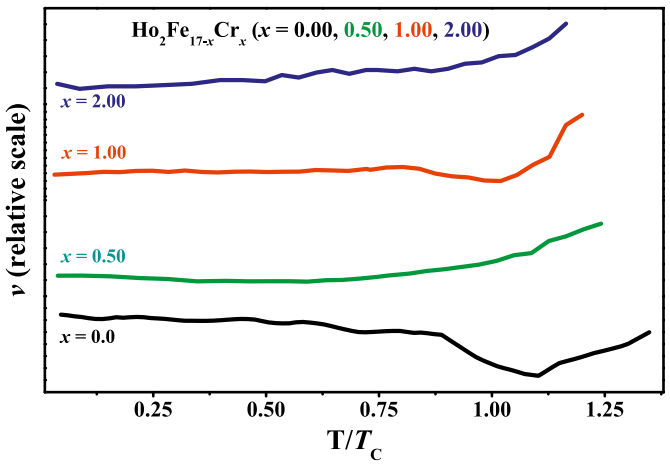

Fig. 5. v_m as a function of reduced temperature for $Ho_2Fe_{17-x}Cr_x$, $x = 0$, 0.5, 1, 2. Data for $x = 0$ has been taken from Ref. [31] and $x = 1$, 2 are taken from Ref. [29].

magnetostrictive deformation parameters along the *ab*-basal plane and along the *c*-axis respectively. ω_S is the volume magnetostrictive deformation. Such parameters indicate the nature and the strength of magnetoelastic coupling in a compound. Our data for $x = 0.5$ compound shows that all the three parameters *viz.*, λ_a, λ_c and ω_S increase with the lowering of temperature, below T_C. For $Ho_2Fe_{17-x}Cr_x$ system, we observe, λ_a, λ_c and ω_S are of the order of 10^{-2} [29]. This is comparable with the permanent magnetic material $R_2Fe_{14}B$ [45]and other R_2Fe_{17} compounds [24,25,46], and suggests a huge spontaneous magnetostriction in the compound. It has been pointed out that the spontaneous magnetostriction in R_2Fe_{17} compounds is determined by Fe sublattice only [25,37,46]. Actually, such magnetostriction originates from the strong dependence of magnetic exchange coupling upon the Fe(4*f*/6*c*)--Fe(4*f*/6*c*) distance [24–29]. Stoner-Edward-Wolfrath (SEW) theory have been employed to explain the thermal expansion property of different

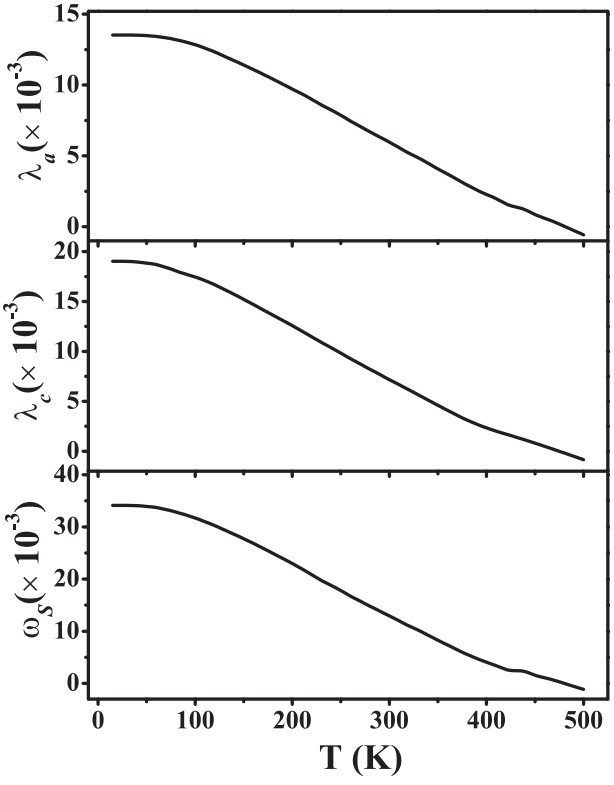

Fig. 6. λ_a, λ_c and ω_S as a function of T.

metallic alloys [47]. According to the SEW theory [48], ω_S due to MVE, in the absence of H, at temperature T, can be expressed as

$$\omega_S = \frac{\kappa C}{v} M_S^2 \quad (2)$$

where κ is the compressibility and C is the magnetovolume coupling constant. In our case, we observe that ω_S increases with lowering of temperature down to the lowest temperature of measurement. However, M_S value decreases below 200 K. The reason behind such anomaly is as follows. The decrease in the value of M_S below 200 K is related to the increase of magnetic moment of the rare earth atom with the lowering of temperature, and the rare earth sublattice is coupled to the Fe sublattice antiferromagnetically suggesting $\mu_{Total} = \sum_{i=1}^{17}\mu_{Fe} - \sum_{i=1}^{2}\mu_{Ho}$. However, the Fe sublattice only contributes to the MVE and μ_{Fe} increases with lowering of temperature [25,37]. According to Fig. 6, ω_S does not become zero at T = T_C, but falls down to zero at T = 478 K = 1.2 T_C. Similar behavior has also been observed for ferrimagnetic Dy_2Fe_{17} system for which ω_S decreases to zero at T = 1.4T_C [45], and ferrimagnetic Er_2Fe_{17} system for which ω_S decreases to zero at T = 1.5T_C [25]. The reason behind such behavior has been pointed out as the existence of short range magnetic correlation above T_C [25,46].

4. Conclusion

We have studied the thermal expansion properties of $Ho_2Fe_{16.5}Cr_{0.5}$ compound as a function of temperature. The compound shows NTE in the temperature range T = 13–200 K with small α_V (-5×10^{-6} K^{-1}). α_V is positive for temperatures above 200 K, although it remains small upto 300 K. Above 300 K, it behaves like a normal PTE material. Below T_C = 394 K, $Ho_2Fe_{16.5}Cr_{0.5}$ orders ferrimagnetically and MVE causes a strong spontaneous magnetostriction in the compound resulting from the dependence of magnetic exchange coupling on the Fe (4*f*) - Fe (4*f*) distance. Both rare earth and Fe sublattice contribute to M_S, but Fe sublattice only responsible for MVE. As a functional material $Ho_2Fe_{16}Cr$ appears to be better than $Ho_2Fe_{16.5}Cr_{0.5}$.

Acknowledgment

Shovan Dan and S. Mukherjee thank UGC, India for financial support in the form of major project (F.No-43-519/2014(SR)). The work at SINP was carried out under CMPID-DAE Project.

Appendix A. Supplementary data

Supplementary data related to this article can be found at https://doi.org/10.1016/j.jpcs.2017.12.017.

References

[1] K. Takenaka, Sci. Technol. Adv. Mater. 13 (2012) 013001–013012.
[2] N. Yaozhuang, X. Youqing, L. Xiaobo, P. Hongjian, J. Phys. Chem. Solid. 69 (2008) 852–858.
[3] W. Miller, C.W. Smith, D.S. Mackenzie, K.E. Evans, J. Mater. Sci. 44 (2009) 5441–5451.
[4] J.R. Salvador, F. Guo, T. Hogan, M.G. Kanatzidis, Nature 425 (2003) 702–705.
[5] S. Margadonna, K. Prassides, A.N. Fitch, J. Am. Chem. Soc. 126 (2004) 15390–15391.
[6] K.J. Miller, C.P. Romao, M. Bieringer, B.A. Marinkovic, L. Prisco, M.A. White, J. Am. Ceram. Soc. 96 (2013) 561–566.
[7] M. van Schilfgaarde, I.A. Abrikosov, B. Johansson, Nature 400 (1999) 46–49.
[8] M. Shiga, Curr. Opin. Solid State Mater. Sci. 1 (1996) 340–348.
[9] T. Suzuki, A. Omote, J. Am. Ceram. Soc. 89 (2006) 691–693.
[10] L. Hu, J. Chen, L. Fan, Y. Ren, Y. Rong, Z. Pan, J. Deng, R. Yu, X. Xing, J. Am. Chem. Soc. 136 (2014) 13566–13569.
[11] W. Wang, R. Huang, W. Li, J. Tan, Y. Zhao, S. Li, C. Huang, L. Li, Phys. Chem. Chem. Phys. 17 (2015) 2352–2356.
[12] W. Li, R. Huang, W. Wang, Y. Zhao, S. Li, C. Huanga, L. Li, Phys. Chem. Chem. Phys. 17 (2015) 5556–5560.
[13] S. Li, R. Huang, Y. Zhao, W. Wanga, L. Li, Phys. Chem. Chem. Phys. 17 (2015) 30999–31003.

[14] X. Jiang, M.S. Molokeev, P. Gong, Y. Yang, W. Wang, S. Wang, S. Wu, Y. Wang, R. Huang, L. Li, Y. Wu, X. Xing, Z. Lin, Adv. Mater. 28 (2016) 7936–7940.
[15] G.D. Barrera, J.A.O. Bruno, T.H.K. Barron, N.L. Allan, J. Phys. Condens. Matter 17 (2005) R217–R252.
[16] J. Chen, L. Hu, J. Deng, X. Xing, Chem. Soc. Rev. 44 (2015) 3522–3567.
[17] T.A. Mary, J.S.O. Evans, T. Vogt, A.W. Sleight, Science 272 (1996) 90–92.
[18] F.H. Gillery, E.A. Bush, J. Am. Ceram. Soc. 42 (1959) 175–177.
[19] A.E. Phillips, A.L. Goodwin, G.J. Halder, P.D. Southon, C.J. Kepert, Angew. Chem. Int. Ed. 47 (2008) 1396–1399.
[20] M. Azuma, W. Chen, H. Seki, M. Czapski, S. Olga, K. Oka, M. Mizumaki, T. Watanuki, N. Ishimatsu, N. Kawamura, S. Ishiwata, M.G. Tucker, Y. Shimakawa, J.P. Attfield, Nat. Commun. 2 (2011) 347.
[21] P. Hu, J. Chen, J. Deng, X. Xing, J. Am. Chem. Soc. 132 (2010) 1925–1928.
[22] K. Takenaka, H. Takagi, Appl. Phys. Lett. 87 (2005), 261902.
[23] A. Pandey, C. Mazumdar, R. Ranganathan, S. Tripathi, D. Pandey, S. Dattagupta, Appl. Phys. Lett. 92 (2008), 261913.
[24] P.A. Alonso, Doctoral Thesis, University of Oviedo, Spain, 2011.
[25] P.A. Alonso, P. Gorria, J.A. Blanco, J.S. Marcos, G.J. Cuello, I.P. Orench, J.A.R. Velamazan, G. Garbarino, I. de Pedro, J.R. Fernandez, J.L.S. Llamazares, Phys. Rev. B 86 (2012), 184411.
[26] H. Yan-Ming, T. Ming, W. Wei, W. Fang, Chin. Phys. B 19 (2010), 067502.
[27] Y. Hao, M. Zhao, Y. Zhou, J. Hu, Scripta Mater. 53 (2005) 357–360.
[28] Y. Hao, X. Zhang, B. Wang, Y. Yuang, F. Wang, J. Appl. Phys. 108 (2010), 023915.
[29] S. Dan, S. Mukherjee, C. Mazumdar, R. Ranganathan, RSC Adv. 6 (2016) 94809–94814.
[30] J.L. Wang, S.J. Campbell, O. Tegus, C. Marquina, M.R. Ibarra, Phys. Rev. B 75 (2007), 174423.
[31] J.L. Wang, A.J. Studer, S.J. Kennedy, R. Zeng, S.X. Dou, S.J. Campbell, J. Appl. Phys. 111 (2012), 07A911.
[32] X.C. Kou, F.R. de Boer, R. Grössinger, G. Wiesinger, H. Suzuki, H. Kitazawa, T. Takamasu, G. Kido, J. Magn. Magn Mater. 177–181 (1998) 1002–1007.
[33] E. Girt, Z. Altounian, J. Yang, J. Appl. Phys. 81 (1997) 5118–5120.
[34] I. Nehdi, L. Bessais, C.D. Mariadassou, M. Abdellaoui, H. Zarrouk, J. Alloy. Comp. 351 (2003) 24–30.
[35] P.C. Ezekwenna, G.K. Marasinghe, W.J. James, O.A. Pringle, G.J. Long, H. Luo, Z. Hu, W.B. Yelon, P.I. Héritier, J. Appl. Phys. 81 (1997) 4533.
[36] Y. Wang, F. Yang, C. Chen, N. Tang, P. Lin, Q. Wang, J. Appl. Phys. 84 (1998) 6229–6232.
[37] D. Givord, R. Lemaire, W.J. James, J.-M. Moreau, J.S. Shah, IEEE Trans. Magn. 7 (1971) 657–659.
[38] D. Givord, R. Lemaire, IEEE Trans. Magn. 10 (1974) 109–113.
[39] J. Rodriguez-Carvajal, Physica B 192 (1993) 55–69.
[40] Z.-g. Sun, S.-y. Zhang, H.-w. Zhang, B.-g. Shen, J. Alloy. Comp. 349 (2003) 1–5.
[41] B.D. Cullity, C.D. Graham, Introduction to Magnetic Materials, IEEE Press, Wiley, 2008.
[42] J. Wang, S.J. Campbell, A.J. Studer, S.J. Kennedy, R. Zeng, J. Phys. Conf. 200 (Section 8) (2010) 1–4.
[43] L. Glasser, J. Phys. Chem. Solid. 73 (2012) 139–141.
[44] A.V. Andreev, A.V. Deryagin, S.M. Zadvorkin, N.V. Kudrevatykh, R.H. Levitin, V.N. Moskalev, Y.F. Popov, R.Y. Yumaguzhin, Fizika Magnitnykh Materialov, (Physics of Magnetic Materials), in: D.D. Mishin (Ed.), Kalinin University, Kalinin, USSR, 1985, p. 21 (in Russian).
[45] N. Yang, Doctoral Thesis, Iowa State University, Ames, Iowa, 2004.
[46] P.A. Alonso, P. Gorria, J.L.S. Llamazares, G.J. Cuello, I.P. Orench, J.S. Marcos, G. Garbarino, M. Reiffers, J.A. Blanco, Acta Mater. 61 (2013) 7931–7937.
[47] H.J. Van Rign, H.L. Alberts, J.A.J. Lourens, J. Phys. Chem. Solid. 48 (1987) 283–288.
[48] Y. Takahashi, Spin Fluctuation Theory of Itinerant Electron Magnetism, Springer Tracts in Modern Physics, Springer-Verlag Berlin Heidelberg, 2013, p. 253.

ISSN: 2277-9655
Impact Factor: 5.164
CODEN: IJESS7

IJESRT
INTERNATIONAL JOURNAL OF ENGINEERING SCIENCES & RESEARCH TECHNOLOGY

TEMPERATURE DEPENDENT MAGNETIC BEHAVIOR Of $Ho_2Fe_{17-x}Cr_x$ (x = 0.5, 1, 2)

S. Mukherjee
Department of Physics, The University of Burdwan, Burdwan-713104, West Bengal, India

DOI: 10.5281/zenodo.1184036

ABSTRACT
$Ho_2Fe_{17-x}Cr_x$ (x = 0.5, 1, 2) is a ferrimagnetic system with T_C lying in the temperature range T = 394 – 415 K. The magnetization of the compounds at different values of H (0.05 T – 7T) in the temperature range T = 4 – 380 K have been reported. The overall behavior has been explained by the temperature and field dependent magnitude of the rare earth moment in addition to the Fe-sublattice. The lower temperature (<<T_C) behavior is more complex and needs farther studies for a clear picture.

KEYWORDS: Permanent magnetic material, Intermetallic compounds, Ferrimagnaetism

I. INTRODUCTION
The early research work in the R_2Fe_{17} (R-rare earth) compounds mainly encompassed on the utility of this compound as a permanent magnetic material (PMM). A PMM should possess high Curie temperature (T_C), high saturation magnetization (M_S) and easy-axis anisotropy. The commonly used PMM are $R_2Fe_{14}B$ (R = Nd), $SmCo_5$ *etc*. Compared to these materials, R_2Fe_{17} series of compounds contain low rare earth concentration, and hence would be economically cheaper. However, the main hindrance in using R_2Fe_{17} compounds as PMM comes from their comparatively lower T_C (although close to room temperature) [1,2] and their easy-plane anisotropy.[2] The early research work mainly focused on to increase the T_C and change the anisotropic direction from easy plane to easy axis of these compounds, by substituting other elements (magnetic: Cr, Mn, non-magnetic: Ga, Al, Si) on the Fe site as well as inserting elements like C, B, H and N in the interstices.[2,3,4,5,6,7] For the substituted compounds, $Gd_2Fe_{16}Cr$ shows the highest T_C ~ 575 K,[3] whereas the nitrogen inserted compound $Gd_2Fe_{17}C_yN_x$ shows the maximum T_C ~ 764 K.[4] However, uni-axial anisotropy has only been observed in C/N filled Sm_2Fe_{17} with a lower value of M_S.[5] So, the prospect of R_2Fe_{17} compound and their derivatives appear to be bleak as a PMM.
However, the interest in the R_2Fe_{17} compounds/its derivatives did not decay with time, rather it increased due to observation of interesting phenomena like spin reorientation, first-order magnetic phase transitions, magnetocaloric effect and negative thermal expansion (NTE) below T_C. [6,7,1,3,9,10,11,12,13] Such observations indicated the richness of the system from the fundamental as well as application point of view. The most interesting contribution of the recent study is the discovery of $Ho_2Fe_{16}Cr$, performing as a single component ZTE material in the temperature range T = 13 – 330 K. [10]
R_2Fe_{17} compounds show various types of magnetic ordering. Compounds containing lighter rare earth atoms show a collinear ferromagnetism, and those having heavier rare earth atoms show mainly ferrimagnetism.[1] Ho_2Fe_{17} compound is a ferrimagnet with T_C = 326 K.[10] The Cr- substitution increases the T_C for lower concentration, and then it decreases for higher concentration of Cr. Table 1 shows the ordering temperature of the three compounds, already reported.[10,11] In this article we want to study the magnetic field (H) and temperature (T) dependent behavior of magnetization(M) of $Ho_2Fe_{17-x}Cr_x$ (x = 0.5, 1, 2).

ISSN: 2277-9655
Impact Factor: 5.164
CODEN: IJESS7

Table 1 Curie temperature of the compounds $Ho_2Fe_{17-x}Cr_x$ (x = 0.5, 1, 2)

Sample name	T_C (in K)
$Ho_2Fe_{16.5}Cr_{0.5}$	394
$Ho_2Fe_{16}Cr$	415
$Ho_2Fe_{15}Cr_2$	402

II. MATERIALS AND METHODS

$Ho_2Fe_{17-x}Cr_x$ (x = 0.5, 1, 2) compounds were prepared in arc-furnace. The details of the procedure were described elsewhere.[10,11] The magnetization was measured in a SQUID VSM (M/S Quantum Design, Inc., USA) from 4–380 K.

III. RESULTS AND DISCUSSION

The $Ho_2Fe_{17-x}Cr_x$ (x = 0.5, 1, 2) samples used here are taken from the same batch used in reference [10]. The samples are in single phase having hexagonal Th_2Ni_{17} structure with space group: $P6_3/mmc$ (#194). The crystal structure of $Ho_2Fe_{17-x}Cr_x$ is shown in figure 1. Here, Fe/Cr atoms occupy four atomic positions 4f, 6g, 12j and 12k, whereas Ho occupies 2a and 2b atomic positions.

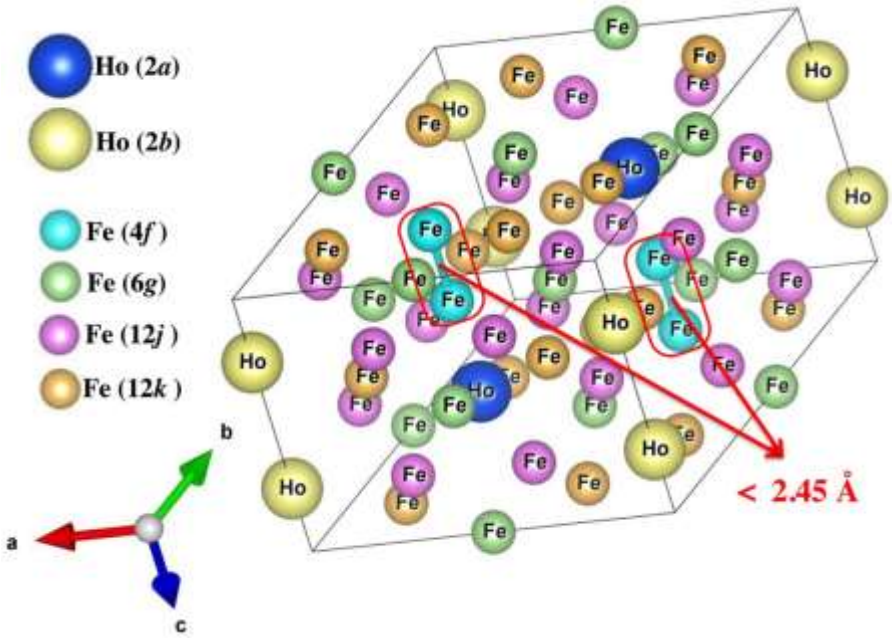

Figure 1. Crystal Structure of $Ho_2Fe_{17-x}Cr_x$

Figure 2, 3 and 4 show the behaviour of M as a function of T for the compounds $Ho_2Fe_{17-x}Cr_x$ (x = 0.5, 1, 2) at different H, measured under both zero field cooled protocol (ZFC) and field cooled (FC) protocol. With the lowering of temperature, M (T) increases suddenly near the ferrimagnetic transition temperature T_C. The magnetism of R_2Fe_{17} compound can be explained with the help of two sublattice model, namely, rare earth sublattice and Fe sublattice. For the ferromagnetic system spins of both the sublattice orders in the same direction, whereas it is opposite for the ferrimagnetic system.[8,10] Above T_C, in Ho_2Fe_{17}, the Fe atoms at the 4f sites are coupled antiferromagnetically, while the rest of the atoms (6g, 12j and 12k) are coupled ferromagnetically.[8] Below T_C, the 4f-4f bond length increases resulting into a ferromagnetic interaction.[10].

ISSN: 2277-9655
Impact Factor: 5.164
CODEN: IJESS7

The rare earth sublattice is coupled anti-parallel to the Fe- sublattice. The effect of substitution of magnetically weaker atom Cr at the Fe site has been discussed earlier.[10,11]

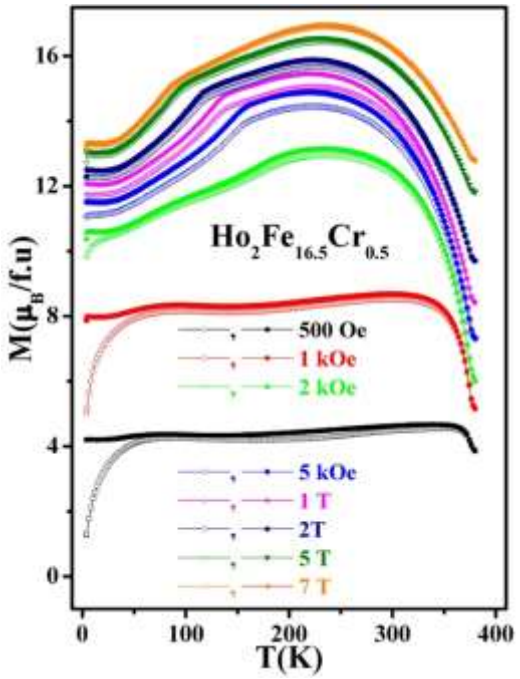

Figure 2. Magnetization (M) of $Ho_2Fe_{16.5}Cr_{0.5}$ as a function of temperature (T) at different magnetic fields (H = 0.05 T – 7 T)

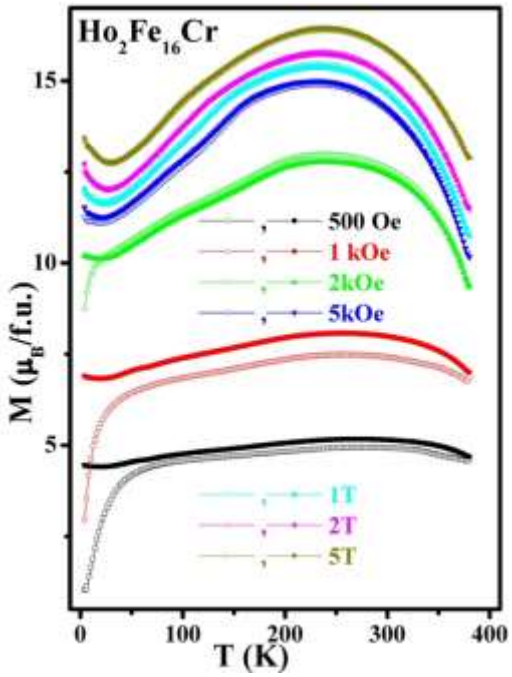

Figure 3. Magnetization (M) of $Ho_2Fe_{16}Cr$ as a function of temperature (T) at different magnetic fields (H = 0.05 T – 5 T)

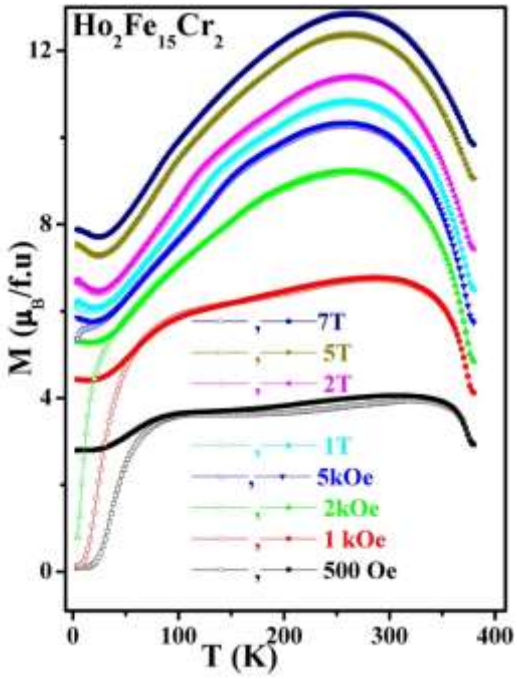

Figure 4. Magnetization (M) of $Ho_2Fe_{15}Cr_2$ as a function of temperature (T) at different magnetic fields (H = 0.05 T – 7 T)

The salient feature of the M(T) curve at different H values are the sudden rise in the value of M(T) near T_C. This rise may be associated with ferromagnetic transition of the Fe-sublattice. At a lower value of H, ZFC and FC curves starts decreasing at temperatures much lower than T_C, whereas at higher measuring field M(T) starts decreasing at temperatures just below T_C. Such lowering of M (T) may be due to either of the two reasons: (a) the competition between the rare earth and Fe sublattice, (b) thermomagnetic history effect.[6] The thermomagnetic history effect can be explained as follows. Below T_C, in the 3d sublattice ferromagnetic domains are formed. At comparatively higher temperature, the domain walls remain free and easily respond to the magnetic field. For strongly anisotropic system, the crystalline anisotropy causes narrow domain wall with high domain wall energy per unit area. As we lower the temperature, the thermal activation cannot provide the energy for domain wall motion. This causes to decrease M with lowering T. In such cases we should observe a decrease in M (T) just below T_C even at a lower value of H. On the other hand, we observe such behaviour only at high H. The reason lies in the increasing rare earth moment at high H, and the rare earth moment is antiparallel to Fe moment.

As we increase the measuring field H more and more, the ZFC curve approaches FC curve. Moreover, the maximum shifts to the lower temperature with increasing H. Such behaviour can be compared with the cooperative freezing of the spin glass system. Such behaviour can be related to the competing interaction of the Fe-sublattice and rare earth sublattice.

An upturn in M(T) is observed at low temperatures particularly for x = 1, 2 compounds. Such upturn is associated with increasing magnetic moment of rare earth atom with the lowering of temperature.

IV. CONCLUSION

The behaviour of magnetization of $Ho_2Fe_{17-x}Cr_x$ (x = 0.5, 1, 2) as a function of temperature at different values of the applied magnetic field, both under ZFC and FC conditions have been studied. The study establishes that the changing magnitude of the rare earth moment with increasing field and temperature plays a crucial role in determining the magnetic behaviour of the studied compounds, in addition to the Fe-sublattice. The cusp around T_C reminds us of the spin glass freezing phenomenon. The lower temperature behaviour ($<<T_C$) of magnetization is more complex and requires farther studies.

V. ACKNOWLEDGEMENTS

S. Mukherjee thanks UGC, India for financial support in the form of major project (F.No-43-519/2014(SR))

VI. REFERENCES

[1] P.A. Alonso, Doctoral Thesis, University of Oviedo, Spain, 2011.
[2] X.C. Kou, F.R. de Boer, R. Grössinger, G. Wiesinger, H. Suzuki, H. Kitazawa, T. Takamasu, G. Kido, J. Magn. Magn Mater. 177–181 (1998) 1002–1007.
[3] H. Yan-Ming, T. Ming, W. Wei, W. Fang, Chin. Phys. B 19 (2010), 067502.
[4] K. Machida, G. Adachi, Magnetic properties of rare earth-iron compounds containing carbon and/or nitrogen. In: Oyama S.T. (eds) The Chemistry of Transition Metal Carbides and Nitrides. Springer, Dordrecht (1996).
[5] K.H. Müller , L. Cao , N. M. Dempsey , P. A. P. Wendhausen , J. Appl. Phys. 79, (1996),5045-5050
[6] Z.-g. Sun, S.-y. Zhang, H.-w. Zhang, B.-g. Shen, J. Alloy. Comp. 349 (2003) 1–5.
[7] Y. Hao, M. Zhao, Y. Zhou, J. Hu, Scripta Mater. 53 (2005) 357–360.
[8] Y. Hao, X. Zhang, B. Wang, Y. Yuang, F. Wang, J. Appl. Phys. 108 (2010), 023915.
[9] S. Dan, S. Mukherjee, C. Mazumdar, R. Ranganathan, RSC Adv. 6 (2016), 94809–94814
[10] S. Dan, S. Mukherjee, C. Mazumdar, R. Ranganathan , J. Phys. Chem. Solid. 115 (2018), 92–96.
[11] P.A. Alonso, P. Gorria, J.A. Blanco, J.S. Marcos, G.J. Cuello, I.P. Orench, J.A.R. Velamazan, G. Garbarino, I. de Pedro, J.R. Fernandez, J.L.S. Llamazares, Phys. Rev. B 86 (2012), 184411.
[12] J.L. Wang, S.J. Campbell, O. Tegus, C. Marquina, M.R. Ibarra, Phys. Rev. B 75, (2007), 174423.
[13] J.L. Wang, A.J. Studer, S.J. Kennedy, R. Zeng, S.X. Dou, S.J. Campbell, J. Appl. Phys. 111 (2012), 07A911.

CITE AN ARTICLE

Mukherjee, S. (n.d.). TEMPERATURE DEPENDENT MAGNETIC BEHAVIOR Of Ho2Fe17-xCrx (x = 0.5, 1, 2). *INTERNATIONAL JOURNAL OF ENGINEERING SCIENCES & RESEARCH TECHNOLOGY*, *7*(2), 642-645.

Journal Name

ARTICLE TYPE

Cite this: DOI: 10.1039/xxxxxxxxxx

Effect of Si substitution in ferromagnetic Pr_2Fe_{17}: a magnetocaloric material with zero thermal expansion operative at high temperature

Shovan Dan[a], S. Mukherjee[a*], Chandan Mazumdar[b] and R. Ranganathan[b]

Received Date
Accepted Date

DOI: 10.1039/xxxxxxxxxx

www.rsc.org/journalname

The article deals with the magnetic and thermal expansion properties of $Pr_2Fe_{16}Si$. The compound has been well characterized from the structural point of view by analysing X-ray diffraction (XRD) pattern. The temperature dependent behaviour of magnetization (M) and the structural parameters (lattice parameters, unit cell volume) suggest that the compound undergoes a second order phase transition from a paramagnetic to a ferromagnetic state at T_C = 390 K, driven by an increase in bond length between iron atoms at 6*c* sites. The field-dependent behaviour of M below T_C, and comparatively lower value of coercivity (H_c) have been explained by the role of Si atoms as pinning centres. In the ferromagnetic phase, the system is found to behave like an in-homogenous mean field system. The study of thermal expansion properties establishes that the compound is a zero thermal expansion material ($\alpha_v = 5.3\times10^{-6}$ K^{-1}) operative in the temperature range T = 200 - 340 K. As a magnetocaloric material, $Pr_2Fe_{16}Si$ possesses high RCP (87 JKg^{-1} at H = 1.5 T), high operating temperature (390 K) and moderate $|\Delta S_M|^{max}$.

1 Introduction

In the past, the detailed study on the crystallographic structure, magnetic and thermodynamic properties of the R_2Fe_{17} series of compounds (R = rare earth, Y)[1–11] were carried out from the motivation to find a permanent magnetic material (PMM) like $Nd_2Fe_{14}B$, $SmCo_5$ *etc.* Although R_2Fe_{17} compounds possess high saturation magnetization (M_S), the prospect of these compounds as PMM appeared to be dim because of their lower Curie temperature (T_C) (maximum value of 479 K for R = Gd)[7] and presence of basal plane anisotropy at room temperature.[7,12] In order to increase the value of T_C and to have room temperature uniaxial anisotropy, various research groups focused on either substitution of other elements into the Fe sites[13–18] or insertion of elements like C, N, H *etc.* in the interstitial positions.[19–23] However, all the favorable conditions (high magnetization (M), high T_C and a large uniaxial anisotropy) of a PMM is not satisfied in any of the parent, substituted or inserted R_2Fe_{17} compounds. Later on, the observation of interesting phenomena like spin reorientation, first-order magnetic phase transitions *etc.*, revives the fundamental research interest in the R_2Fe_{17} compounds.[24–29] In addition, these compounds have also become the subject of practical interest as some of these compounds show moderate magnetocaloric effect (MCE) and negative thermal expansion (NTE) below T_C.[1,8]

Magnetocaloric materials with appreciable magnitude of adiabatic entropy change (ΔS_{mag}), large adiabatic temperature change (ΔT_{ad}) and high relative cooling power (RCP) are suitable for a green energy refrigerating system. Although R_2Fe_{17} compounds do not possess a large ΔS_{mag},[8] they possess comparatively higher values of RCP, ΔT_{ad} and the highest magnitude of ΔS_{mag} around the room temperature.[1,8,10,11,30] Hence, these compounds appear to be advantageous from the point of view of application.[31] Moreover,among the R_2Fe_{17} compounds $|\Delta S_{max}|$ is maximum for Pr_2Fe_{17} around T_C = 286 K.[11] R_2Fe_{17} compounds also show NTE below T_C due to magnetovolume effect (MVE).[32] Substitution at the Fe site reduces the value of NTE coefficient by weakening the MVE with a simultaneous increase in T_C. So judicious substitution of proper element with appropriate concentration at the Fe site may give a zero thermal expansion (ZTE) material operative at a high temperature region including room temperature. Such a single component ZTE material $Ho_2Fe_{16}Cr$, in the temperature range T = 13 − 330 K, has already been reported.[5] As Pr_2Fe_{17} shows the most systematic NTE behavior among the R_2Fe_{17} compounds, there is a good possibility to find a ZTE derivative. From the point of view of practical importance, ZTE materials or materials with tailored thermal expansion has been the topic of recent research interest.[33]

[a] *Department of Physics, The University of Burdwan, Burdwan - 713104, India*
[b] *Condensed Matter Physics Division, Saha Institute of Nuclear Physics, 1/AF, Bidhannagar, Kolkata - 700064, India.*
∗ *sanseb68@yahoo.co.in*

In this article, the structural, magnetic and thermal expansion properties of $Pr_2Fe_{16}Si$ have been studied. The present study attempts to focus on both the fundamental aspect as well as the practical one. The study deals with the basic underlying physics of the system like: the role of domain wall pinning and Si atoms in determing the coercivity (H_C), the correlation between the structural parameters and the magnetic phase transition. We have also estimated the critical exponents from the MCE data. Such critical analysis from MCE data is useful for identifying the nature of the phase transition.[34] Moreover, the study of MCE and thermal expansion will help in identifying the suitability of $Pr_2Fe_{16}Si$ as a refrigerating material and a ZTE material.

2 Experimental procedure

$Pr_2Fe_{16}Si$ compound was prepared by the method of arc-melting (in inert argon atmosphere) with at least 99.9% pure starting materials. The ingot was re-melted several times to ensure homogeneity. The sample was annealed in a vacuum sealed quartz tube at a temperature 1173 K for one week, followed by quenching in water. The room temperature powder x-ray diffraction (XRD) patterns of the compound were taken using CuK_α (λ = 1.54056 Å) radiation (model: TTRAX III, M/S Rigaku Corp., Japan). The XRD at different temperatures (13 - 483 K), were recorded using the same instrument, with a very low scan speed (0.01° steps, and 0.4° per min) for better statistical average. 13 K is the lower limit of our measurement system (x-ray diffractometer). Slow scanning speed is necessary as the sample contains more than 85% Fe and the CuK_α radiation is in the range of absorption edge of Fe. FullProf software package[35] was used for analyzing the XRD patterns. Magnetization was measured using SQUID VSM (model: MPMS3,M/S Quantum Design, Inc., USA) from 4 - 380 K. High temperature VSM (model: EV9, M/S MicroSense, LLC Corp., USA) was employed to measure the magnetization at 300K <T < 550 K.

3 Results and discussion

3.1 Structural characterization

Fig. 1 shows the XRD patterns of the compound $Pr_2Fe_{16}Si$ taken at 13 K, 300 K, and 453K. The experimental patterns are analyzed assuming that the compound crystallizes in a rhombohedral Th_2Zn_{17} type crystal structure (space group: $R\bar{3}m$, # 166). Fig. 1 indicates that the system remains in single phase throughout the experimental range of temperature (T = 13 – 483 K). The parameters extracted from the XRD patterns at each temperature are unique. Structural parameters, lattice parameters and reliability factors of the compound obtained from the Rietveld refinement of the XRD data taken at 300 K have been listed in table 1. The lattice parameters are comparable to those of the parent compound.[11] A qualitative discussion of other temperature dependent structural parameters have been done later.

3.2 Magnetization

Fig. 2[left] shows the behavior of magnetization (M) and its first derivative ($\frac{\partial M}{\partial T}$) as a function of temperature (T). The data shows that $Pr_2Fe_{16}Si$ undergoes a paramagnetic to ferromagnetic transition around T_C = 390 K. The T_C of the parent compound Pr_2Fe_{17} has been reported earlier as 286 K.[11] Therefore the substitution of one Fe atom by an Si atom increases the T_C by 105 K. The cause of enhancement of T_C due to substitution of weaker/non-magnetic element at Fe site has been discussed in reference 5.

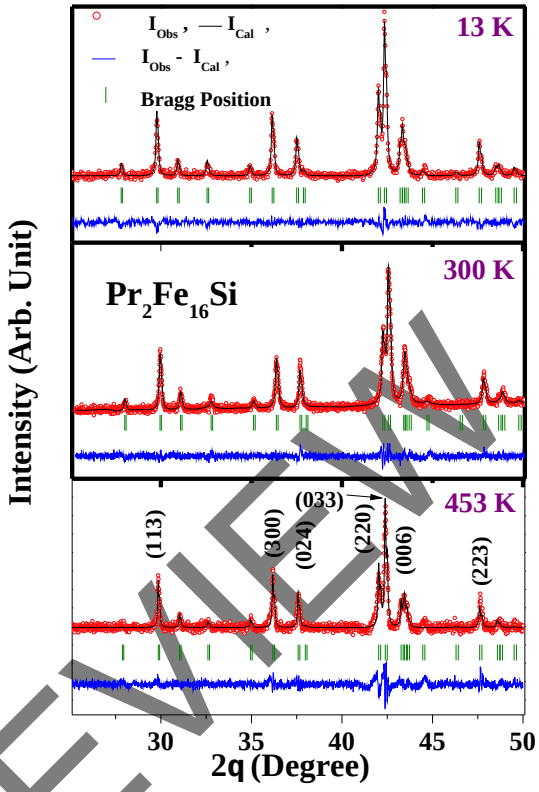

Fig. 1 XRD patterns of $Pr_2Fe_{16}Si$ compound at T = 13 K, 300 K and 453 K. Red circles depict the experimentally observed data points, the black lines are data generated using FullProf software, and the blue lines are the differences between the estimated and experimentally observed data points. The olive bars are the Bragg Positions allowed by the space group.

Fig. 2 [right] shows the lower temperature part (T = 4 - 380 K) of the M(T) curve measured at different magnetic fields (H = 0.5 T, 1 T, 2 T, 5 T) under zero field cooled (ZFC) and field cooled (FC) conditions. M_{ZFC}(T) decreases with the lowering of temperature below a characteristic temperature T_P ($< T_C$). Difference between the ZFC and the FC curve indicates thermo-magnetic irreversibility in the system. With increasing H, the ZFC curve approaches the FC one. T_P decreases with increasing H. For a ferromagnetic sample, similar decrease of M with the lowering of T has been associated with the pinning of domain wall motion.[36] An idea of the height of the pinning potential can be obtained from the field dependence of T_P (inset of fig. 2[right]). The inset shows that T_P decreases linearly with H, and the height of the pinning potential is of the order of $k_B T_P$ (H = 0) $\sim 2.69\times 10^{-21} J$. Such a potential barrier may be related to either the magnetocrystalline anisotropy or the presence of substituted Si atoms, lowering the exchange energy. If the magnetocrystalline anisotropy is the cause of the reduction of M(T), then the crystalline anisotropy constant K of such system is of the order of $4.3\times 10^6 J.m^{-3}$, esti-

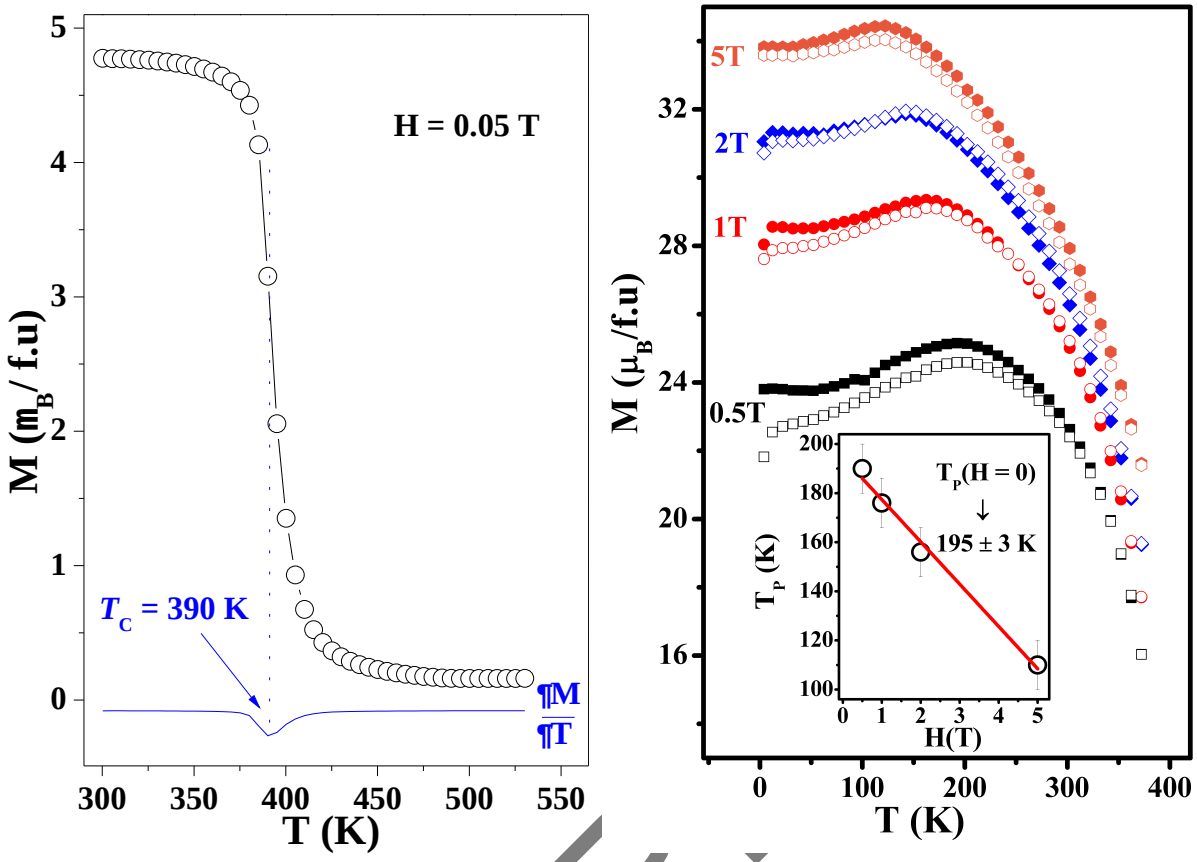

Fig. 2 [left] M (T) at H = 0.05 T, blue line shows $\frac{\partial M}{\partial T}$ as a function of T. [right] M (T) for H = 0.5 T - 5 T. Filled and open symbols corresponds to the FC and ZFC magnetization curves respectively. Inset shows the variation of T_P with H, red line shows the linear fit.

Table 1 Lattice parameters, structural parameters and reliability factors obtained during Rietveld refinement of the compound $Pr_2Fe_{16}Si$ at T = 300 K.

Atom site	x	y	z
Pr (6*c*)	0	0	0.3438(2)
Fe/Si (6*c*)	0	0	0.0895(1)
Fe/Si (9*d*)	0.5	0	0.5
Fe/Si (18*f*)	0.2901(3)	0	0
Fe/Si (18*h*)	0.1703(4)	0.8296(6)	0.4923(0)
$a = b$ (Å)	8.564(7)		
c (Å)	12.471(2)		
R_p:1.80, R_{wp}: 2.29			
Bragg R-factor: 7.97, Rf-factor: 7.82, χ^2: 10.2			

mated from the relation $K.a^3 \sim k_B T_P$ (H = 0).[37] Such a strong anisotropic system with narrow domain walls should show a high value of coercivity (H_c).[36,37] However, M-H curve at the lowest measuring temperature (4 K) shows only a small value of H_c = 545 Oe. So the role of Si atoms appears to be important. In order to conclude, let us concentrate on the M - H curve at 4 K (fig. 3 [left]). The central portion is shown separately in fig. 3 [left]. The initial part of the M-H curve represents a reversible domain wall motion. At an H comparable to H_c, we get a certain jump in M value. This happens in the case of systems with point defects having relatively high pinning potential and low domain wall energy.[36] In this case, initially the applied magnetic field will bend the domain wall. This corresponds to a reversible process. At a certain critical value of H ($\sim H_c$ in our case), the radius of curvature attains a critical value, the wall expands discontinuously and irreversibly accompanied by a jump in the value of M (shown by an arrow in the fig. 3 [left]). The higher field portion of the M-H curve appears to be reversible and is due to coherent rotation of domains. In such case, the coercivity depends upon the number density of the pinning sites, and low for low number density. Therefore, in $Pr_2Fe_{16}Si$ with low H_c, the domain wall pinning reflected in the M(T) curve below T_C, is related to Si atoms substituted at lower concentration compared to Fe atoms. So substitution of Si atoms to a higher concentration may increase H_c, favorable for PMM, but there will be a consequent decrease in M_S value. The characteristic parameters of the M-H curve, namely, remanent magnetization M_r, coercivity H_c and M_S are shown in table 2 along with T_C. M_S has been determined using approach to saturation law[38].

$$M = M_S(1 - \frac{A}{H} - \frac{B}{H^2}) - \chi H \quad (1)$$

where A, B and χ are constants. The estimated M_S is 36.3 μ_B/f.u.(fig. 3[right]). The same for the parent compound is 37.9 μ_B/f.u.[11] This suggests that the Fe site carries an average moment of 1.8 μ_B/f.u.

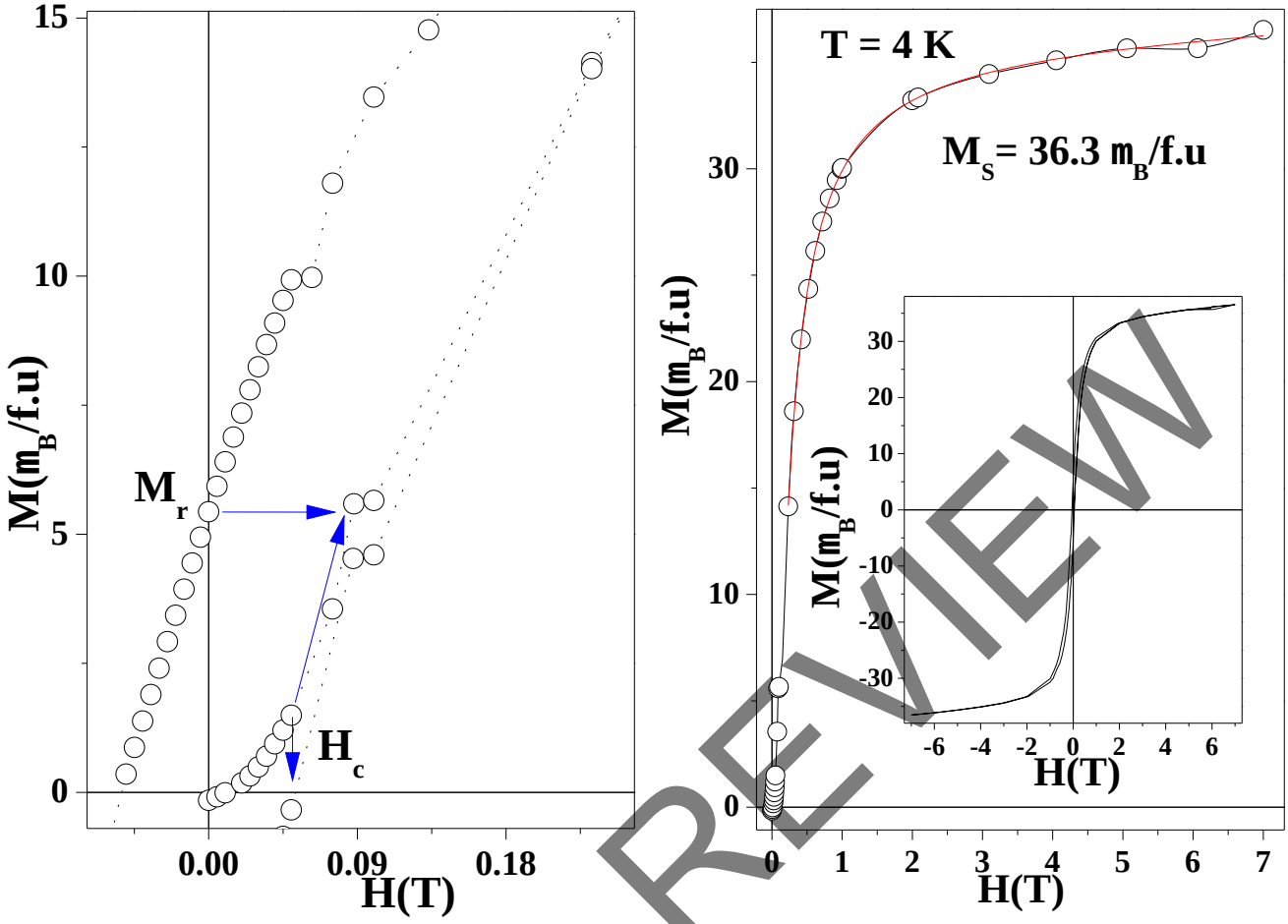

Fig. 3 [left] Enlarged central part of the M(H) curve showing M_r and H_c (T = 4 K). [right] Virgin magnetization curve as a function of applied magnetic field at T = 4 K, red line shows the fit of virgin curve with eqn. 1. Inset shows the magnetization curve with a magnetic field cycle -7T → +7T.

Table 2 T_C, M_S, H_c and M_r.

T_C (K)	M_S (4K) (μ_B/f.u)	H_c(4K) (Oe)	M_r(4K) (μ_B/f.u)
390	36.3	545	5.45

3.3 Correlation between Structure and Magnetism

For Pr_2Fe_{17} (rhombohedral), there are one Pr site (6*c*) and four Fe sites (6*c*, 9*d*, 18*f*, 18*h*) as shown in fig. 4 (a). In R_2Fe_{17} compounds, Fe(6*c*) - Fe(6*c*) bond length is the shortest and the coupling between the Fe(6*c*) atoms is AFM.[9] The strength of the coupling depends upon the bond-length. In this system the lattice parameter *c* and the Fe(6*c*)-Fe(6*c*) bond length increases with the lowering of temperature. Therefore, the strength of the AFM coupling between two Fe(6*c*) atoms as well as the magnetic energy of the system reduces with the lowering of temperature. However, such increase in bond length increases the elastic energy of the system. Below T_C, the reduction in magnetic energy overpowers the increase in the elastic energy, and as a result a ferromagnetic (FM) ground state is obtained.[9] In Er_2Fe_{17}, it has been reported that, with the lowering of temperature below T_C, the average Fe moment increases with a continuous increase in *c*.[1]. The change in 6*c*-6*c* bond length pushes Fe atoms at 6*c* sites towards (006) plane around T_C (fig. 4 (b)) The 6*c*-6*c* bond length (*d*) at different temperatures for $Pr_2Fe_{16}Si$ has been estimated by refining the XRD data by Rietveld method. It has been observed that *d* increases by almost 0.26 Å on lowering below T_C (fig. 5[left]). However, in the region surrounding T_C, the estimated *d* values appear to be unphysical. This is expected and associated with the fluctuation in the parameter *d* in the critical region around T_C. Such fluctuation is reflected in the sudden rise in intensity of the X-ray beam diffracted from (006) plane (fig. 5 [right]) at 393 K (close to T_C). The intensities at different temperatures have been normalized, considering the peak height corresponding to the plane (033) at a particular temperature as 100. For a better visualization, the variation of normalized intensity of different peaks (corresponding to different values of 2θ /reflecting planes) of the XRD pattern has been plotted as a function of temperature in fig. 6[left]). We observe an increase in intensity reflected from (006) plane at the vicinity of T_C (fig. 6[left] and [right]). The immediate conclusion is, the electron density at the (006) plane have been increased around T_C. The change in electron density at the (006) plane around T_C is associated with the change in 6*c*-6*c* bond length.

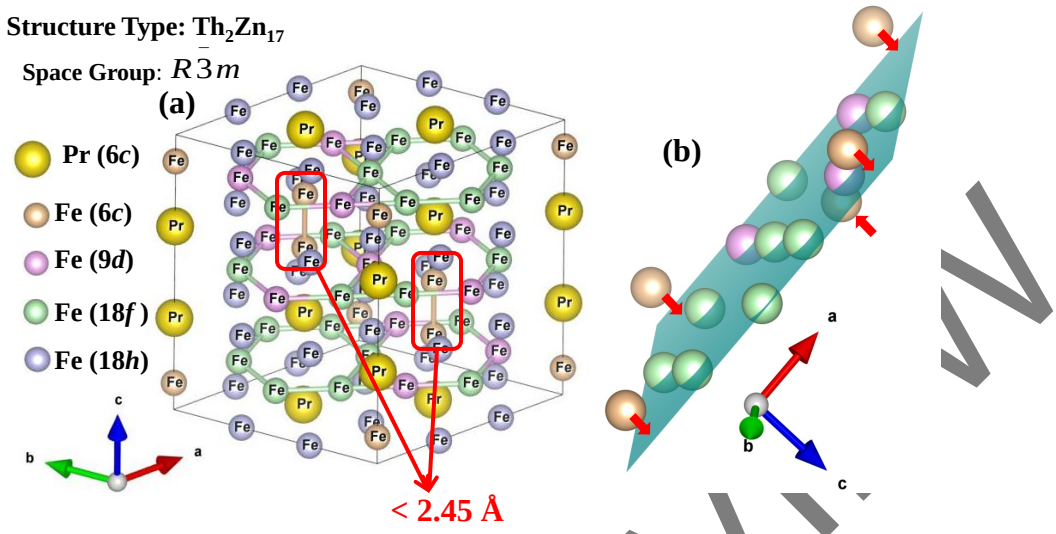

Fig. 4 (a)Crystal structure of the compound $Pr_2Fe_{16}Si$, Fe 6*c*-6*c* bonds are shown by red boxes. (b) Slice of (006) plane, only the atoms on the plane and very close to the plane are shown. The arrow indicates the movement of the Fe (6*c*) atoms towards (006) plane around T_C.

3.4 Thermal Expansion

The lattice parameters (a, c) and the unit cell volume (v) for the studied compound at different temperatures have been estimated from the analysis of XRD data of the corresponding temperatures. The variation of these structural parameters a, c and v (a_m, c_m and v_m) and the extrapolated paramagnetic lattice parameters (a_p, c_p and v_p) with temperature have been shown in fig. 7. The paramagnetic data have been extrapolated using the Grüneisen relation[5]

$$\alpha_v = \frac{1}{v}\frac{\gamma C_V}{\kappa} \quad (2)$$

where $C_V = R(T/\theta_D)^3 \int_0^{\theta_D} x^4 e^x (e^x - 1)^2 dx$, γ = Grüneisen parameter, θ_D = Debye temperature and R is the molar gas constant. The value of θ_D has been taken as 400 K following the estimation by A.V. Andreev *et. al*[39]. The strong MVE and its consequence NTE is observed in all the R_2Fe_{17} compounds below T_C.[8] The relatively weaker MVE can result into ZTE.[40] Attempt has been made to synthesize single component ZTE materials which are of practical use by substituting weaker magnetic elements like Cr at the Fe site.[3–6] Moreover, not particularly focusing on the application aspect, several thermal expansion studies have been performed for Cr and Mn substituted R_2Fe_{17} compounds.[7,13,14] The role of substitution of non-magnetic element Si at Fe site appears to be important and such a role of Si in controlling thermal expansion behaviour in $LaFe_{13}$ compound has already been reported.[41] The present thermal expansion study on Si (non-magnetic) substituted Pr_2Fe_{17} shows that v_m remains almost constant in the temperature range 200 - 340 K (fig. 8[top]). The temperature range of negligible thermal expansion and the value of CTE of the previously studied substituted R_2Fe_{17} compounds and $Pr_2Fe_{16}Si$ have been summarized in table 3. In addition, table 3 shows the same parameters of some well known ZTE materials for comparison. Interestingly, $Pr_2Fe_{16}Si$ shows negligible thermal expansion in a temperature region centered about the room temperature.

The volume magnetostriction coefficient $\omega_S = (v_m - v_p)/v_p$ gives a measure of MVE in the material, and also its dependence on M_S can identify the presence of fluctuation in the system. The plot of ω_S as a function of temperature (fig. 8 [bottom]) shows that $Pr_2Fe_{16}Si$ is a strong magnetostrictive material below T_C, like the parent compound. The linear relation between ω_S and M_S^2 (fig. 9) suggests the absence of spin fluctuation in this system. The similar phenomenon was also observed earlier in the R_2Fe_{17} system.[50]

3.5 Magnetocaloric Effect

Isothermal M (H) data collected for H = 0 - 1.5 T, in a temperature region T = 360 - 450 K, centered around T_C = 390 K (in steps of 5 K) are shown in fig. 10 [left]. Using the Maxwell relation[51], the isothermal magnetic entropy change, ΔS_M (T, H), due to the change of the applied magnetic field from an initial value of zero to a final value of H can be expressed as

$$\Delta S_M(T,H) = \int_0^H [\frac{\partial M}{\partial T}] dH \quad (3)$$

ΔS_M (T,H) have been estimated from our M(H) data by replacing the partial derivative $\frac{\partial M}{\partial T}$ by $\frac{\Delta M}{\Delta T}$, the ratio of finite differences, and finally integrating by numerical approximation. $|\Delta S_M|$ (T, H) have been shown in fig. 10[right].

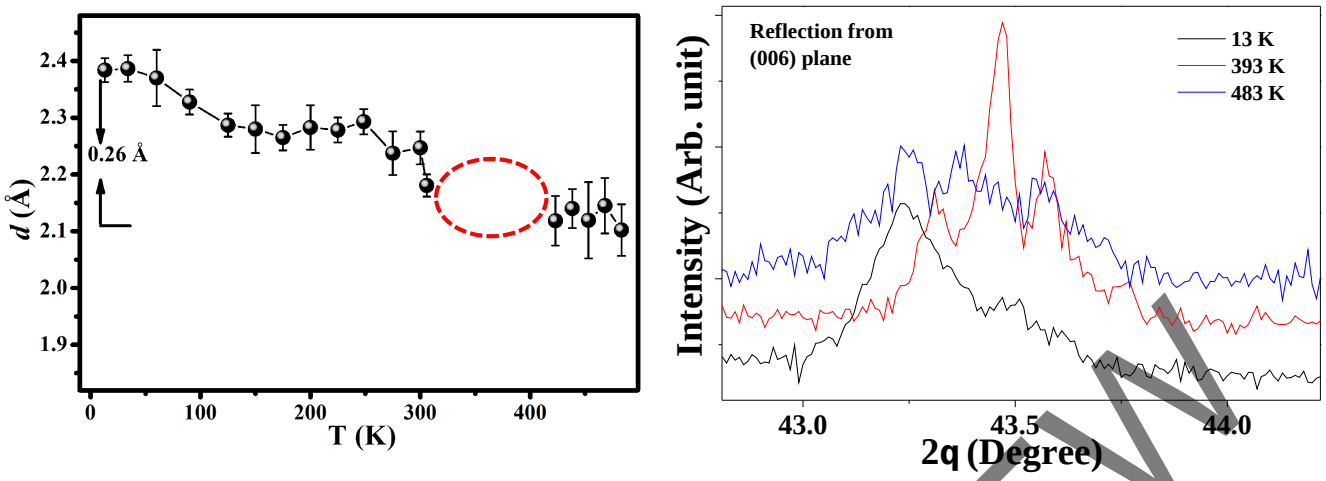

Fig. 5 [left] Variation of Fe 6*c*-6*c* bond length (d) with temperature. Value of the same bond length appears to be unphysical in the region marked with dashed oval. [right] Relative intensities of the reflections from the (006) plane at temperatures 13K, 300 K and 483 K.

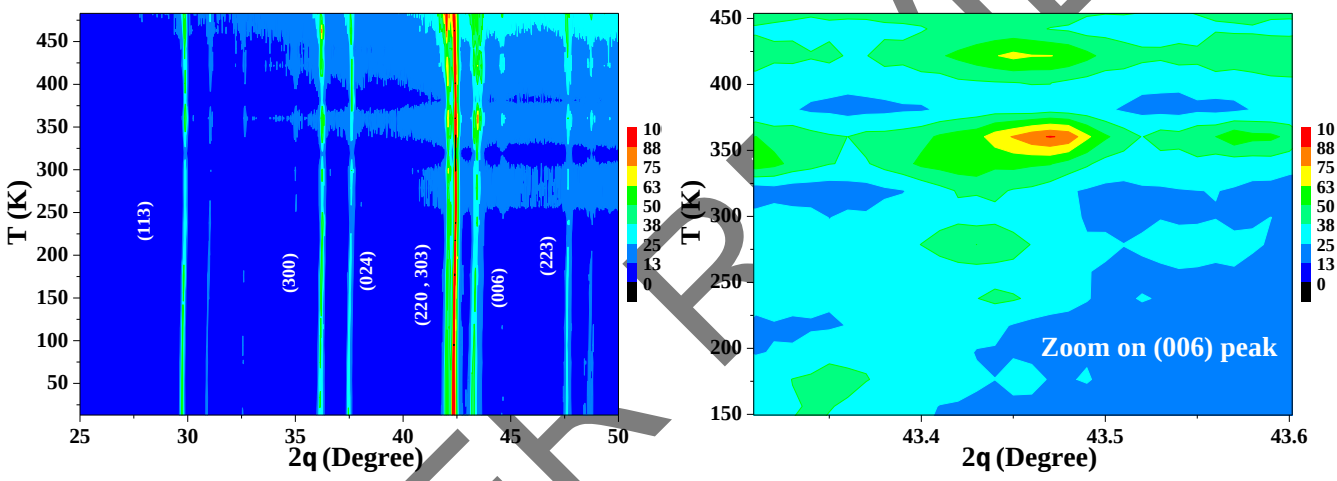

Fig. 6 [left] The variation of normalized intensity of different peaks (corresponding to different values of 2θ) of the XRD pattern as a function of temperature. [right] Enlarged color map of reflections from (006) plane in the vicinity of T_C.

ΔS_M reaches its maximum value $|\Delta S_M|^{max} = 1.61\ J.kg^{-1}.K^{-1}$, around $T_C = 390$ K, whereas for the parent compound Pr_2Fe_{17}, for the field sweep of 1 T, $|\Delta S_M|^{max}$ is $\sim 2\ J.kg^{-1}.K^{-1}$ [11] at T = 286 K (T_C of the parent compound). Since Si substitution increases the T_C, the operating temperature, namely, the one corresponds to $|\Delta S_M|^{max}$ is higher for $Pr_2Fe_{16}Si$ compared to the parent compound. This is a practical advantage. However,the associated disadvantage lies in lowering the value of $|\Delta S_M|^{max}$ due to reduction in average magnetic moment of Fe atoms. Although a large number of materials have been reported to show large MCE at low temperatures, there are only a few which show large MCE above 300 K.[52–57] Among them, Gd_7Pd_3 [52] (T_C = 323 K, ΔH = 5.0 T, ΔT_{ad} = 8.5 K), MnAs [53] (T_C = 318 K, ΔH = 5.0 T, $|\Delta S_M|^{max}$ = 30 $J.kg^{-1}.K^{-1}$), $La_{0.75}Ca_{0.15}Sr_{0.1}MnO_3$ [54] (T_C = 327 K, ΔH = 1.5 T, $|\Delta S_M|^{max} = 2.8\ J.kg^{-1}.K^{-1}$), $LaFe_{11.5}Si_{1.5}H_{1.8}$ [55] (T_C = 341 K, ΔH =5 T, $|\Delta S_M|^{max} = 20.5\ J.kg^{-1}.K^{-1}$) *etc.* are noteworthy. For $Pr_2Fe_{16}Si$, the operating temperature is really high and $|\Delta S_M|^{max}$ is moderate for ΔH = 1.5 T.

Relative cooling power (RCP) for a particular H, defined as the product of $|\Delta S_M|^{max}$ and δT_{FWHM} (full width at half-maxima of ΔS_M versus T curve) [58], gives a measure of both the working temperature range and the cooling efficiency. This is an important parameter for magnetocaloric materials. RCP for $Pr_2Fe_{16}Si$ is high (87 $J.kg^{-1}$). Several materials like GdSiGe,[59] LaFeSi,[60] MnAsSb,[53] Fe-Rh [61] *etc.* undergoing first order magnetic transition show high $|\Delta S_M|^{max}$, but possess low RCP. High RCP of $Pr_2Fe_{16}Si$ originates from high δ_{TFWHM}, and high δ_{TFWHM} is associated with a second order transition. Therefore, $Pr_2Fe_{16}Si$ with moderate $|\Delta S_M|^{max}$ is a better magnetocaloric material as it undergoes a second order Paramagnetic- Ferromagnetic transition.

The second-order magnetic phase transition near the critical point is characterized by a set of critical exponents, β, γ, δ and α. They are defined as [62]

Table 3 Thermal expansion coefficient and temperature ranges of some compounds

Compound	CTE ($\times 10^{-6}$ K^{-1})	Temperature Range(K)	Ref.
$Pr_2Fe_{16}Si$	α_v = 5.26	200 - 340	This report
$Ho_2Fe_{16}Cr$	α_v = 1.3	13 - 330	5
$Ho_2Fe_{16.5}Cr_{0.5}$	α_v = -5	13 - 200	6
$Tm_2Fe_{16.5}Cr_{0.5}$	α_v = -9.15	340 - 400	3
$Gd_2Fe_{16.5}Cr_{0.5}$	α_v = 9.2	294 - 472	42
$(1-x)PbTiO_3$-$xBi(Ni_{1/2}Ti_{1/2})O_3$ (x=0.2)	α_v = 1.21	25 - 525	43
$Mn_3(Ga_{0.5}Ge_{0.4}Mn_{0.1})\times(N_{0.9}C_{0.1})$	α_l = 0.5	190 - 272	44
$Mn_3Cu_{0.5}Ge_{0.5}N$	α_l = 0.11	12 - 230	45
$In_{2-x}Cr_xMo_3O_{12}$ (x=0.7)	α_l = -0.761	400 - 750	46
$LaFe_{13-x}Si_x$ (x = 2.4)	α_v = -0.8	15 - 150	47
$(Al_{2x}(HfMg)_{1-x})(WO_4)_3$ (x=0.15)	Nearly zero (value not given)	273 - 1073	48
$(Sc_{0.85}Ga_{0.05}Fe_{0.1})F_3$	α_l = 0.234	300 - 900	49

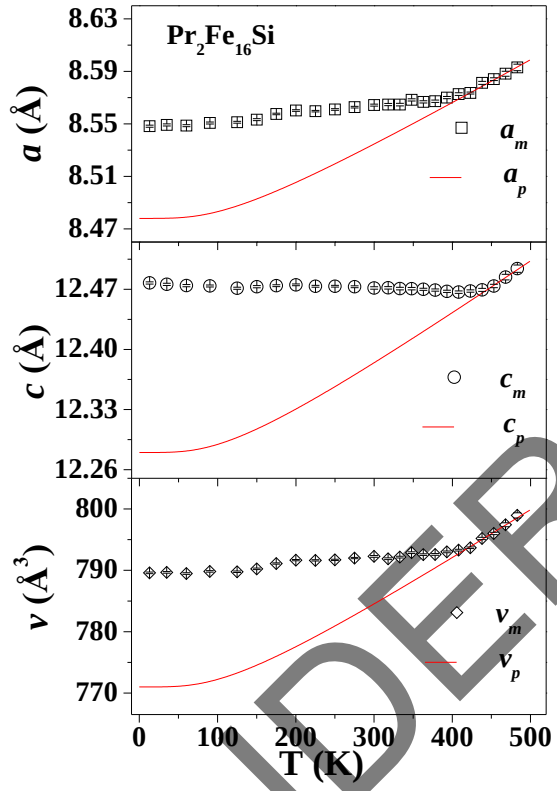

Fig. 7 Lattice parameter a, c and unit cell volume v as a function of temperature. Scattered black symbols refers the experimentally obtained values and the continuous red lines refers the simulated values extrapolated from paramagnetic region.

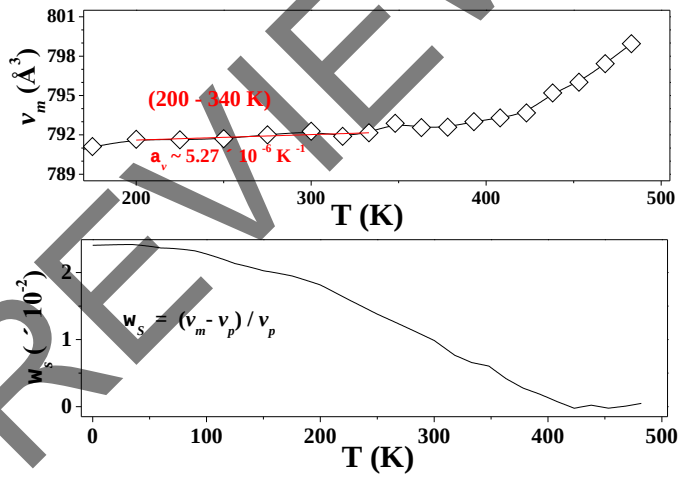

Fig. 8 [top] Coefficient of thermal expansion of the unit cell volume in ZTE region. [bottom] Variation of volume magnetostriction parameter ω_S with temperature.

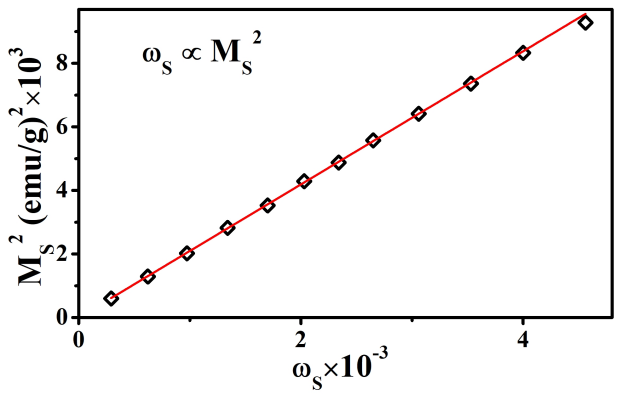

Fig. 9 Volume magnetostriction parameter ω_S with the square saturation magnetization in the vicinity of T_C (360 K ≤ T ≤ 415 K).

$$M_S(T) = M_0(-\varepsilon)^{\beta}, \qquad \varepsilon < 0 \qquad (4)$$

$$\chi_0^{-1}(T) = (\frac{h_0}{M_0})\varepsilon^{\gamma}, \qquad \varepsilon > 0 \qquad (5)$$

$$M = A_0(H)^{1/\delta}, \qquad \varepsilon = 0 \qquad (6)$$

$$C = C_0\varepsilon^{-\alpha}, \qquad \varepsilon > 0 \qquad (7)$$

where M_S, χ_0, M and C are respectively the spontaneous magnetization, initial susceptibility, magnetization and specific heat. $\varepsilon = (T - T_C)/T_C$, T_C is the critical temperature and M_0 , h_0/ M_0, A_0, C_0 are the critical amplitudes. The mean field approximation gives the value of the critical exponents as: α = 0, β = 0.5, γ = 1, δ = 3.

According to Oesterreicher and Parker[63], within the mean field

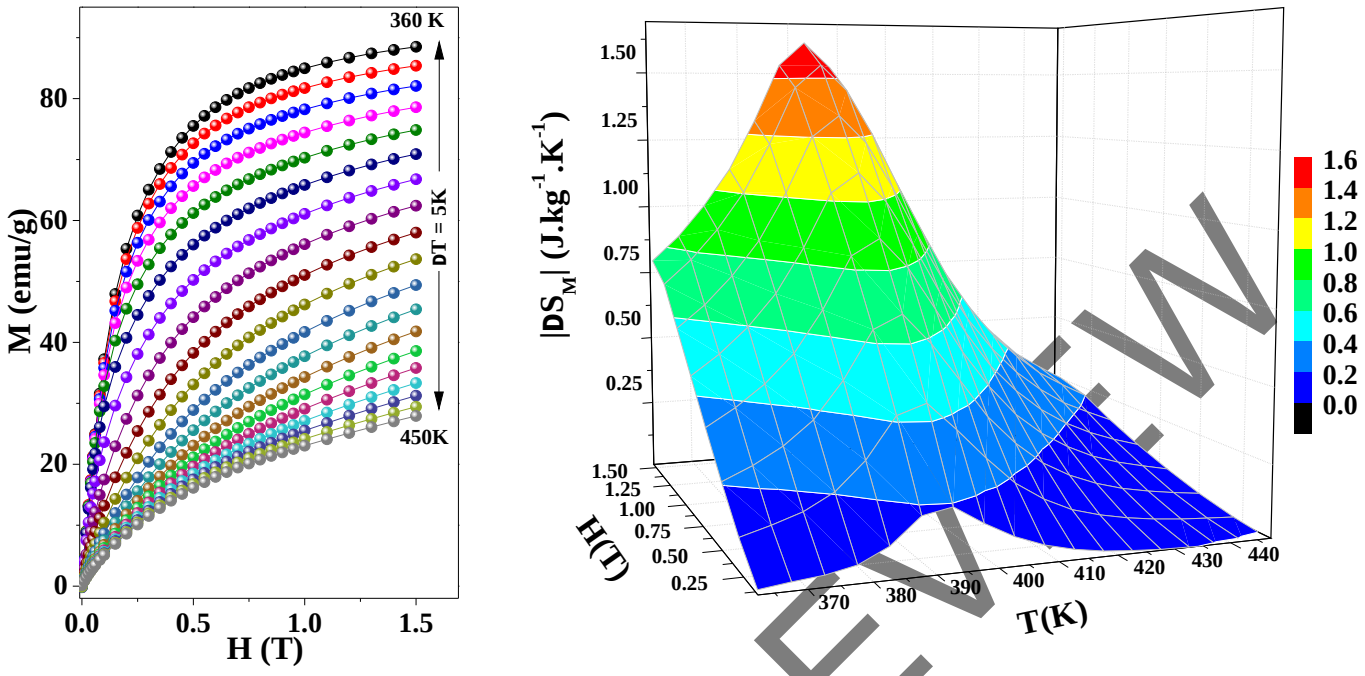

Fig. 10 [left] Magnetization as a function of applied magnetic field upto 1.5 T at different temperatures. [right] $|\Delta S_M|$ as function of temperature and applied magnetic field.

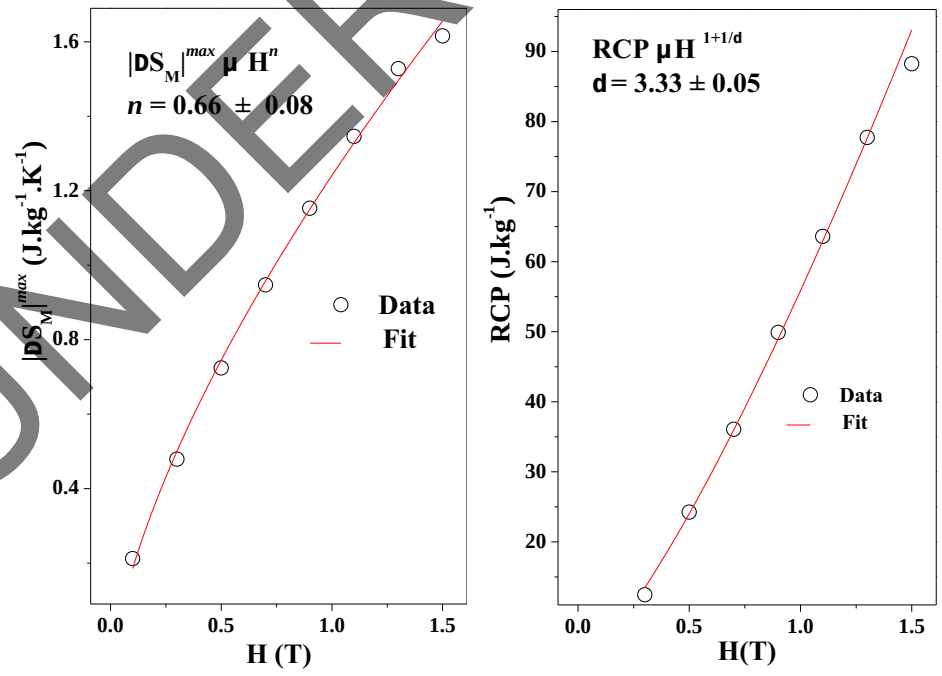

Fig. 11 [left] Variation of $|\Delta S_M|^{max}$ with applied magnetic field H. Fitting of $|\Delta S_M|^{max}$ was done using eqn. 8. [right] Variation of RCP with applied magnetic field H. Fitting of RCP was done using eqn.9.

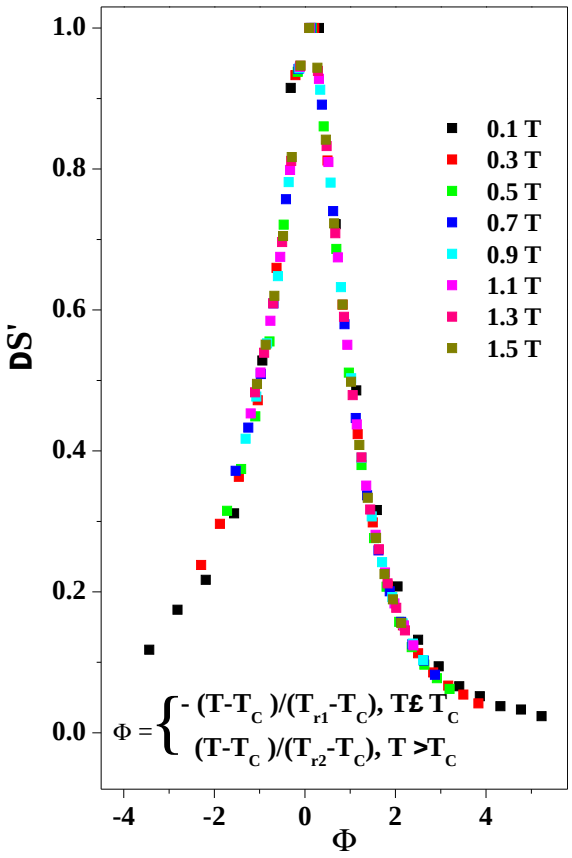

Fig. 12 Universal curve of magnetocaloric effect with reduced temperature Φ(using eqn. 14)

approximation (MFA), the field dependence of the magnetic entropy change at the critical temperature associated with a second order magnetic phase transition follows the relation

$$|\Delta S_M|^{max} \propto H^n \tag{8}$$

and n is equal to $\frac{2}{3}$ for a crystalline material.[63,64] Fig. 11[left] shows the plot of $|\Delta S_M|^{max}$ as a function of H for $Pr_2Fe_{16}Si$. The power law fit of eqn. 8 suggests $n = 0.66$.

Within the MFA, the RCP varies as a function of H as[65]

$$RCP \propto H^{1+1/\delta} \tag{9}$$

Fig. 11[right] shows the plot of RCP as a function of H for $Pr_2Fe_{16}Si$ compound. The power law fit of eqn.9 gives $\delta = 3.33$. We have the following two relations: one suggested by Franco *et al.*[64],

$$n = 1 + \frac{(\beta - 1)}{(\beta + \gamma)} \tag{10}$$

and another from Widom scaling relation[62]

$$\delta = 1 + \frac{\gamma}{\beta} \tag{11}$$

From equations 10 and 11) we can write:

$$\beta = \frac{1}{\delta(1-n)+1}, \quad \gamma = \frac{(\delta - 1)}{\delta(1-n)+1} \tag{12}$$

Using eqn. 12, we have estimated the values of γ and β. The value of critical exponents $\beta = 0.476$ and $\gamma = 1.095$ are closer to the mean field values $\beta = 0.5$ and $\gamma = 1$.[62,63] Therefore, according to a renormalization group analysis by Fisher *et. al.*[66] the exchange interaction in $Pr_2Fe_{16}Si$ is of long range order.

It has been pointed out that for materials undergoing second order magnetic phase transitions, a universal curve can be obtained for normalized parameter $\Delta S' = |\Delta S_M|/|\Delta S_M|^{max}$, as a function of the rescaled temperature[58,64]

$$\Phi = \frac{(T - T_C)}{(T_r - T_C)} \tag{13}$$

with T_r is the temperature at which $|\Delta S_M| = a \times |\Delta S_M|^{max}$ (a is an adjustable parameter with value lying between 0 and 1). According to Franco *et al.*[58,64], if the sample is not magnetically homogeneous or the measuring field is too low, then it requires two scaling parameters T_{r1} and T_{r2} instead of a single one (T_r). Then Φ is defined as

$$\Phi = \begin{cases} -\frac{(T-T_C)}{(T_{r1}-T_C)}, & T \leq T_C \\ \frac{(T-T_C)}{(T_{r2}-T_C)}, & T > T_C \end{cases} \tag{14}$$

For $Pr_2Fe_{16}Si$, after rescaling the temperature using eqn.14 and choosing $a = \frac{1}{2}$, we find that $\Delta S'(\Phi)$ for all the applied fields collapse in a single curve (fig. 12). This suggests that $Pr_2Fe_{16}Si$ undergoes a second order paramagnetic - ferromagnetic transition around $T_C = 390$ K and the system below T_C is an inhomogeneous mean field one.

4 Conclusion

$Pr_2Fe_{16}Si$ crystallizes in a rhombohedral, Th_2Zn_{17} - type crystal structure (Space Group $R\bar{3}m$, # 166) like the parent compound. The compound remains in the same structural phase in the temperature range of our measurement (T = 13 - 483 K). The compound undergoes a paramagnetic to a ferromagnetic transition around $T_C = 390$ K, with $M_S = 36.3$ μ_B/f.u at T = 4 K. Si substitution increases the value of T_C and reduces the value of M_S. The coercivity and the remanent magnetization of the compound at T = 4 K are relatively low ($H_c = 545$ Oe , $M_r = 5.45$ μ_B/f.u). The lower value of coercivity is associated with the lower concentration of Si atoms. The behavior of M (H, T) suggests that the Si atoms act as pinning centers lowering the exchange energy. The magnetic phase transition occurs in tandem with a change in Fe(6*c*) − Fe(6*c*) bond length. This results in a change in electron density at the (006) plane, supported by an observation in the sudden increase in XRD intensity from (006) plane at the vicinity of T_C. The study of thermal expansion shows that $Pr_2Fe_{16}Si$ behaves like a ZTE material in the temperature range T = 200 - 340 K. The study of MCE establishes that $Pr_2Fe_{16}Si$ is a magnetocaloric material with high RCP (87 $J.kg^{-1}$, at H = 1.5 T), high operating temperature and moderate $|\Delta S_M|^{max}$. The critical exponents (β, γ) estimated from the MCE data suggests the system to be mean field like with $\beta = 0.476$ and $\gamma = 1.095$.

Acknowledgement

Shovan Dan and S. Mukherjee thank UGC for financial support in the form of major project (F.No-43-519/2014(SR)). The work at SINP was carried out under CMPID-DAE Project.

References

1 P. A. -Alonso, P. Gorria, J.A. Blanco, J.S. -Marcos, G.J. Cuello, I.P. -Orench, J.A.R -Velamazán, G. Garbarino, I.de Pedro, J.R. Fernández, and J.L.S. Llamazares, *Phys. Rev. B*, 2012, **86**, 184411.

2 H. Yan-Ming, T. Ming, W. Wei and W. Fang, *Chin. Phys. B*, 2010, **19**, 067502.

3 Y. Hao, M. Zhao, Y. Zhou and J. Hu, *Scripta Mater.*, 2005, **53**, 357–360.

4 Y. Hao, X. Zhang, B. Wang, Y. Yuang and F.Wang, *J. Appl. Phys.*, 2010, **108**, 023915.

5 S. Dan, S. Mukherjee, C. Mazumdar and R. Ranganathan, *RSC Adv.*, 2016, **6**, 94809–94814.

6 S. Dan, S. Mukherjee, C. Mazumdar and R. Ranganathan, *J. Phys. Chem. Solid.*, 2018, **115**, 92–96.

7 X.C. Kou, F.R. de Boer, R. Grössinger, G. Wiesinger, H. Suzuki, H. Kitazawa, T. Takamasu and G. Kido, *J. Magn. Magn. Mater.*, 1998, **177-181**, 1002–1007.

8 P.A. -Alonso, Doctoral Thesis, University of Oviedo, Spain, 2011.

9 D. Givord, R. Lemaire, W. J. James, J.-M. Moreau and J. S. Shah, *IEEE Trans. Magn.*, 1971, **7**, 657–659.

10 P. A. -Alonso, P. Gorria, J.L.S. Llamazares, G.J. Cuello, I.P. -Orench, J.S. -Marcos, G. Garbarino, M. Reiffers, and J. A. Blanco, *Acta Mater.*, 2013, **61**, 7931–7937.

11 P. Gorria, P. Alvarez, J.S. Marcos, J.L.S. Llamazares, M.J. Pérez, and J.A. Blanco, *Acta Mater.*, 2009, **57**, 1724–1733.

12 B. Shen, Z. Cheng, B. Liang, H. Guo, J. Zhang, H. Gong, F. Wang, Q. Yan, W. Zhan, *Appl. Phys. Lett.*, 1995, **67**, 1621–1623.

13 J.L. Wang, S.J. Campbell, O. Tegus, C. Marquina and M.R. Ibarra, *Phys. Rev. B*, 2007, **75**, 174423.

14 J.L. Wang, A.J. Studer, S.J. Kennedy, R. Zeng, S.X. Dou and S.J. Campbell, *J. Appl. Phys.*, 2012, **111**, 07A911.

15 E. Girt, Z. Altounian, and J. Yang, *J. Appl. Phys.*, 1997, **81**, 5118–5120.

16 I. Nehdi, L. Bessais, C.D. -Mariadassou, M. Abdellaoui and H. Zarrouk, *J. Alloys Compd.*, 2003, **351**, 24–30.

17 P.C. Ezekwenna, G.K. Marasinghe, W.J. James, O.A. Pringle, G.J. Long, H. Luo, Z. Hu, W.B. Yelon, and P. I·Héritier, *J. Appl. Phys.*, 1997, **81**, 4533.

18 Y. Wang, F. Yang, C. Chen, N. Tang, P. Lin and Q. Wang, *J. Appl. Phys.*, 1998, **84**, 6229–6232.

19 L. X. Liao, X. Chen, Z. Altounian, and D. H. Ryan, *Appl. Phys. Lett.*, 1992, **60**, 129–131.

20 J. M. D. Coey, J. F. Lawler, Hong Sun, and J. E. M. Allan, *J. Appl. Phys.*,1991, **69**, 3007–3010.

21 X.-P. Zhong, R.J. Radwaiiski, F.R. de Boer, T.H. Jacobs and K.H.J. Buschow, *J. Magn. Magn. Mater.*, 1990, **86**, 333–340.

22 O. Isnard, S. Miraglia and D. Fruchart, *J. Magn. Magn. Mater.*, 1995, **140–144**, 981–982.

23 Z. Altounian, X. Chen, L.X. Liao, D.H. Ryan, J.O. S.-Olsen, *J. Appl. Phys.*, 1993, **73**, 6017–6022.

24 T.H. Jacobs, K.H.J. Buschow, G.F. Zhou, X. Li, F.R. de Boer, *J. Magn. Magn. Mater.*, 1992, **116**, 220–230.

25 Z. Cheng, B. Shen, Q. Yan, H. Guo, D. Chen, C. Gou, K. Sun, F. de Boer, K. Buschow, *Phys. Rev. B*, 1998, **57**, 14299–14309.

26 X.C. Kou, E.H.C.P. Sinneckery and R. Grössinger, *J. Phys.: Condens. Matter.*, 1996, **8**, 1557–1565.

27 B. Shen, H. Gong, B. Liang, Z. Cheng, J. Zhang, *J. Alloys Compd.*, 1995, **229**, 257–261.

28 D.M. Zhang, Y.H. Gao, B.M. Yu, C.Q. Tang, N. Tang, X.P. Zhong, W.G. Lin, F.M. Yang, F.R. de Boer, *J. Appl. Phys.*, 1994, **76**, 7452–7544.

29 F. Albertini, F. Bolzoni, A. Paoluzi, L. Pareti, E. Zannoni, *Physica B*, 2001, **294–295**, 172–176.

30 P. Alvarez, P. Gorria, J.L.S. Llamazares, M.J. Pérez, V. Franco, M. Reiffers, I. Čurlik, E. Gažo, J. Kováč, J.A. Blanco, *Intermetallics*, 2011, **19**, 982–987.

31 Z.-L. Zhang, D.-M. Liu, W.-Q. Xiao, H. Li, S.-B. Wang, Y.-T. Liang, H.-G. Zhang, S.-L. Li, J.-J. Fu and M. Yue, *Phys. Chem. Chem. Phys.*, 2018, **20**, 18117–18126.

32 D. Givord and R. Lemaire, *IEEE Trans. Magn.*, 1974, **10**, 109–113.

33 J.A. Monroe, D. Gehring, I. Karaman, R. Arroyave, D.W. Brown, B. Clausen, *Acta Mater.*, 2016, **102**, 333–341.

34 C. Romero-Muiz, V. Franco and A. Conde, *Phys. Chem. Chem. Phys.*, 2017, **19**, 3582–3595.

35 J. Rodriguez-Carvajal, *Physica B*, 1993, **192**, 55–69.

36 D. Jiles, Introduction to Magnetism and Magnetic Materials, 2nd Ed., CRC Press, 1998.

37 S. Blundell, Magnetism in Condensed Matter (Oxford Master Series in Physics), 1st Ed., Oxford University Press, 2001.

38 B.D. Cullity and C.D. Graham, *Introduction to Magnetic Materials*, IEEE Press, Wiley, 2008.

39 A.V. Andreev, A.V. Deryagin, S.M. Zadvorkin, N.V. Kudrevatykh, R.H. Levitin, V.N. Moskalev, Y.F. Popov and R.Y. Yumaguzhin, *Fizika Magnitnykh Materialov*, (*Physics of Magnetic Materials*) edited by D. D. Mishin (Kalinin University, Kalinin, USSR),1985, pp. 21 (in Russian).

40 W. Li, R. Huang, W. Wang, Y. Zhao, S. Li, C. Huanga and L. Li, *Phys. Chem. Chem. Phys.*, 2015, **17**, 5556–5560.

41 W. Wang, R. Huang, W. Li, J. Tan, Y. Zhao, S. Li, C. Huang and L. Li, *Phys. Chem. Chem. Phys.*, 2015, **17**, 2352–2356.

42 Y. Hao, F. Liang, X. He, Y.Z. Wu, Y. Qin, F. Wang, *Adv. Mater. Res.*, 2011, **299-300**, 4750.

43 L. Hu, J. Chen, L. Fan, Y. Ren, Y. Rong, Z. Pan, J. Deng, R. Yu and X. Xing, *J. Am. Chem. Soc.*, 2014, **136**, 13566–13569.

44 K. Takenaka and H. Takagi, *Appl. Phys. Lett.*, 2009, **94** , 131904.

45 X. Song, Z. Sun, Q. Huang, M. Rettenmayr, X. Liu, M. Seyring, G. Li, G. Rao and F. Yin, *Adv. Mater.*, 2011, **23**, 4690–4694.

46 K.J. Miller, C.P. Romao, M. Bieringer, B.A. Marinkovic, L. Prisco and M.A. White, *J. Am. Chem. Soc.*, 2013, **566**, 561−566.
47 W. Wang, R. Huang, W. Li, J. Tan, Y. Zhao, S. Li, C. Huanga and L. Li, *Phys.Chem.Chem.Phys.*,2015, **17**, 2352−2356
48 T. Suzuki and A. Omote, *J. Am. Ceram. Soc.*, 2006, **89**, 691−693.
49 L. Hu, J. Chen, L. Fan, Y. Ren, Y. Rong, Z. Pan, J. Deng, R. Yu, X. Xing, *J. Am. Chem. Soc.*, 2014, **136**, 13566−13569.
50 Y. Takahashi, *Spin Fluctuation Theory of Itinerant Electron Magnetism*, Springer Tracts in Modern Physics, **253**, Springer-Verlag Berlin Heidelberg, 2013.
51 A.M. Tishin, *Handb. Magn. Mater.* 1999, **12**, 395524.
52 K.A. Gschneidner Jr., V.K. Pecharsky, *Mater. Sci. Eng. A.*, 2000, **287**, 301−310.
53 H. Wada, and Y. Tanabe, *Appl. Phys. Lett.*, 2001, **79**, 3302−3304.
54 Z.B. Guo, Y.W. Du, J.S. Zhu, H. Huang, W.P. Ding, and D. Feng, *Phys. Rev. Lett.*, 1997, **78**, 1142−1145.
55 Y.F. Chen, F. Wang, B.G. Shen, F.X. Hu, J.R. Sun, G.J. Wang, Z.H. Cheng, *J. Phys.: Condens. Matter.*, 2003, **15**, L161.
56 D.Y. Cong, L. Huang, V. Hardy, D. Bourgault, X.M. Sun, Z.H. Nie, M.G. Wang, Y. Ren, P. Entel, Y.D. Wang, *Acta Mater.*, 2018, **146**, 142−151.
57 Y.H. Qu, D.Y. Cong, X.M. Sun, Z.H. Nie, W.Y. Gui, R.G. Li, Y. Ren, Y.D. Wang, *Acta Mater.*, 2017, **134**, 236−248.
58 V. Franco, J.S. Blzquez, B. Ingale and A. Conde, *Annu. Rev. Mater. Res.*, 2012, **42**, 305342.
59 K.A. Gschneidner Jr, V.K. Pecharsky, and A.O. Tsokol, *Rep. Prog. Phys.*, 2005, **68**, 1479−1539.
60 A. Fujita, Y. Akamatsu, and K. Fukamichi, *J. Appl. Phys.*, 1999, **85**, 4756−4758.
61 M. Manekar and S.B. Roy, *J. Phys. D: Appl. Phys.*, 2008, **41**, 192004.
62 S. Mukherjee, P. Raychaudhuri, and A.K. Nigam, *Phys. Rev. B*, 2000, **61**, 86518653.
63 H. Oesterreicher and F. T. Parker, *J. Appl. Phys.*, 1984, **55**, 4336.
64 V. Franco, J. S. Blazquez, and A. Conde, *Appl. Phys. Lett.*, 2006, **89**, 222512.
65 Y. Su, Yu Sui, J.-G. Cheng, J.-S. Zhou, X. Wang, Y. Wang, and J. B. Goodenough, *Phys. Rev. B*, 2013, **87**, 195102.
66 M.E. Fisher, S.K. Ma, and B.G. Nickel, *Phys. Rev. Lett.*, 1972, **29**, 917.